

**Regulation of kinetochore and inner-centromere structure
and function by the Chromosome Passenger Complex
during mitosis.**

Prasad Trivedi

Pune, India

M.S., University of Pune, 2010

A Dissertation presented to the Graduate Faculty of the University of Virginia in
Candidacy for the Degree of Doctor of Philosophy.

Department of Cell Biology

University of Virginia,
August 2018

Abstract:

Mitosis is an important stage in the cell cycle when the duplicated chromosomes are segregated to the daughter cells. Errors in segregation of chromosomes can lead to genomic instability that underlies multiple developmental diseases and cancer. Aurora-B, which is a member of the Chromosome Passenger Complex (CPC), is a key mitotic kinase and plays an important role in ensuring high fidelity mitosis by phosphorylating numerous substrates in the mitotic spindle. Most of the CPC is localized to the inner-centromere during pro-metaphase. This localization of the CPC to the inner-centromere is important for the concentration-dependent auto-activation of the CPC during mitosis. The inner-centromeric CPC also regulates localization of multiple proteins to the inner-centromeres, which are important for proper mitotic progression. How the CPC is maintained in the inner-centromere at high concentration during pro-metaphase and the effect of this high concentration of the CPC on the organization and composition of the inner-centromere are unclear. In Chapter 2, I will show that the liquid-liquid phase separation driven by the centromere-targeting region of the CPC is important for its inner-centromere localization and function and may underlie the mesoscale organization of the inner-centromere. Once localized to the inner-centromere the key substrates that Aurora-B phosphorylates to ensure error-free mitosis are often localized 100's of nm away from the site of peak kinase localization. It is unclear how the activity of the Aurora-B kinase reaches its distant substrates. In Chapter 3, I will describe a mechanism that enables the phosphorylation of distant outer kinetochore substrates by the CPC. I will show that inner-centromeric and microtubule-bound non-inner centromeric

CPC cooperate to ensure proper phosphorylation of the outer kinetochore substrates, which is important for correction of improper kinetochore-microtubule attachment. Apart from regulating kinetochore-microtubule attachment Aurora-B also regulates the assembly of the outer kinetochore during mitosis. Aurora-B activity at the kinetochore changes in response to the kinetochore-microtubule attachment status and this change is important for proper mitosis. However, the outer kinetochore organization is thought to remain unchanged before and after kinetochore-microtubule attachment. It is thus unclear if the same interactions underlie the organization of the core outer kinetochore before and after mature kinetochore-microtubule attachment. In Chapter 4, I will present data that suggests that different pathways play a role in the maintenance of the outer kinetochore before and after mature kinetochore-microtubule attachment. I will show that the outer kinetochore maintenance is dependent on the CPC and Plk1 activity before but not after mature kinetochore-microtubule attachment.

Acknowledgements:

My journey towards completion of this degree has been aided by the constant support, encouragement, and guidance from many people. Firstly, I would like to thank Todd Stukenberg for his exceptional mentorship and guidance throughout my graduate studies. I could not have asked for a more understanding and nurturing mentor. I sincerely appreciate his efforts in developing me as an independent scientist. His enthusiasm towards science, the drive to always come up with the right experiment and the ability to embrace new ideas have made my stay in his lab extremely valuable and I hope I can carry these qualities with me in the future.

I would also like to thank my thesis committee members Noelle Dwyer, Yuh-Hwa Wang and Mazhar Adli for their valuable inputs and support throughout my graduate work. I would also like to thank my previous committee members Dan Burke and Dan Foltz for their helpful inputs, which has helped shape my work in various ways. The nurturing and supportive environment that Dan Burke and Dan Foltz created together with Todd Stukenberg has been critical for my growth as a scientist.

My work in Todd's lab would not have been possible without the most wonderful and helpful colleagues that I had the pleasure of working with. I am very thankful to all the past and present members of the Stukenberg lab: Budhaditya Banerjee, Limin Liu, Pawel Janczyk, Ewa Niedzielkowska, Cortney Kestner, Dan Matson, Eliza Zylkiewicz, Arkadi Manukyan, Katherine Pfister and Erin Moran for all the technical and intellectual help. I would especially like to thank Limin Liu for teaching me various aspects of mammalian cell culture; and Pawel Janczyk for all the technical help with the protein purifications and for always being "just a call away" even after leaving Stukenberg Lab. I

would also like to thank the Burke and Foltz lab members for helping me throughout my Ph.D. in various ways.

Being part of both the Cell Biology Department and the Biochemistry and Molecular Genetics Department, I had the opportunity to work and interact with two wonderful communities. I am thankful to all the faculties and students in both these departments for all the stimulating conversations and support through the years. I would like to especially thank Mary Hall for all the help and support throughout my time in UVa.

Finally, I would like to thank all my friends and family for their unconditional love and support. Especially, I would like to thank my parents, sister, brother-in-law, nephew, and Pooja for believing in me and for being there for me all the time.

Index:

(1) Abstract -----2

(2) Acknowledgements -----4

(3) Chapter 1. General introduction -----8

- Kinetochore -----9
- A Centromere Signaling Network (CSN) underlies coordination amongst mitotic events: -----23

(4) Chapter 2. Phase separation by the chromosome passenger complex underlies the biophysical organization of the inner centromere. -----49

(5) Chapter 3. The binding of Borealin to microtubules underlies a tension independent kinetochore-microtubule error correction pathway. -----87

(6) Chapter 4. Outer kinetochore maintenance requires Plk1 and Aurora-B activity before but not after end-on attachment.-----163

(7) Chapter 5. Concluding remarks and future directions.-----184

(8) References. -----195

List of Abbreviations:

CPC: Chromosome Passenger Complex.

CSN: Centromere Signaling Network.

SAC: Spindle Assembly checkpoint.

MCC: Mitotic Checkpoint Complex.

APC/C: Anaphase Promoting Complex/Cyclosome.

CCAN: Constitutive Centromere Associated Network.

KMN: Knl1 complex, Mis12 complex, Ndc80 complex.

ISB: INCENP-Survivin-Borealin complex.

Plk1: Polo like kinase-1.

CENP: Centromere protein (followed by the single alphabet specific protein name.)

Cdk1: Cyclin Dependent Kinase 1.

EM: Electron microscopy.

IF: Immunofluorescence.

FRAP: Fluorescence Recovery After Photo-bleaching.

BRB80: Brinkley Reassembly Buffer 80

DTT: Dithiothreitol.

FBS: Fetal Bovine Serum.

GTP: Guanosine Triphosphate.

kDa: kiloDalton.

K-fiber: Kinetochore associated microtubule fiber.

MTBM: Microtubule Binding mutant.

MTBD: Microtubule Binding domain.

Chapter 1

General Introduction.

Kinetochores:

Kinetochores are multi-protein structures that are assembled on specific loci on mitotic chromosomes called centromeres during mitosis. They enable the movement of the chromosomes by coupling them with either the ends of the depolymerizing microtubules, through a complex structure composed of multiple microtubule binding proteins, or to the walls of the microtubules, through motor proteins. Kinetochores also monitor the progression of mitosis and are the site for initiation of spindle assembly checkpoint, which monitors kinetochore-microtubule attachments and prevents anaphase onset until all the chromosomes are properly attached to the kinetochores. Kinetochores also act as a scaffold on which multiple kinases and phosphatases are dynamically localized to regulate the events of chromosome segregation.

Structure and assembly pathways of kinetochores:

Although kinetochores are thought to be functionally conserved the structural components often show differences in either evolutionary conservation or essentiality in different organisms (Drinnenberg et al., 2016; Musacchio and Desai, 2017). In the interest of simplicity, I will concentrate on describing mammalian kinetochore in this section. Kinetochores are composed of more than 90 proteins some of which are core structural proteins and others localize dynamically to the kinetochores during various steps of mitosis (Stukenberg and Burke, 2015). The kinetochore is assembled on the specific loci on the mitotic chromosomes, which is specified epigenetically through the presence of a histone H3 variant CENP-

A in most eukaryotes, however, some exceptions exist (Drinnenberg et al., 2016; Musacchio and Desai, 2017).

Constitutive Centromere Associated Network (CCAN):

Constitutive Centromere Associated Network (CCAN) forms the inner kinetochore and is the scaffold for the assembly of the outer kinetochore. The CCAN consists of multiple proteins, which connects the outer kinetochore with the centromeric chromatin (Foltz et al., 2006; Okada et al., 2006). CCAN is localized to the CENP-A chromatin throughout the cell cycle. CCAN in mammals is composed of two branches that connect the centromeric DNA with the outer-kinetochore (Musacchio and Desai, 2017) (Fig. 1-1).

The CENP-T branch is comprised of four-proteins, which are thought to form CENP-TWSX complex (Amano et al., 2009; Hori et al., 2008). CENP-T and CENP-W have a histone fold domain and structurally resemble H2A-H2B dimer CENP-S and CENP-X also have DNA binding properties and together CENP-TWSX are thought to wrap DNA in a fashion similar to nucleosomes (Nishino et al., 2012; Takeuchi et al., 2014). However, differences in phenotypes associated with loss of different members of CENP-TWSX complex suggest a more complex organization (Amano et al., 2009; Hori et al., 2008). The CENP-C branch begins with CENP-C protein in the CCAN, which directly interacts with the CENP-A nucleosome through the C-terminus of CENP-A and through its interaction with the middle portion of CENP-A (Falk et al., 2016; Guse et al., 2011; Kato et al., 2013; Westhorpe et al., 2015). CENP-C plays a role in the recruitment of a complex comprised of CENP-L and CENP-N, CENP-N also

directly interacts directly with the CENP-A CATD domain (Carroll et al., 2009; Weir et al., 2016). Together CENP-C and CENP-LN proteins are also important for maintaining the stability of the CENP-A nucleosome (Guo et al., 2017). The CENP-LN complex then recruits the CENP-HIKM complex composed of CENP-H, CENP-I, CENP-K, and CENP-M (McKinley et al., 2015; Weir et al., 2016). CENP-HIKM complex also interacts with CENP-C (Weir et al., 2016). CENP-HIKM interacts and recruits CENP-OPQU complex comprised of CENP-O, CENP-P, CENP-Q, and CENP-U (Foltz et al., 2006; Okada et al., 2006). CENP-U interacts directly with Plk1 kinase and is one of the main recruiters of Plk1 to the kinetochore (Kang et al., 2006). CENP-Q can bind microtubules although the function of this microtubule interaction is unclear (Amaro et al., 2010). The CENP-HIKM complex and the CENP-TWSX complex interact with each other and co-operate for their localization to the centromeres (Basilico et al., 2014). Interactions within the CCAN complex are dynamic during the cell cycle, and the dependencies for their localizations change in different stages of the cell cycle (Nagpal et al., 2015). The conservation and essentiality of these complex members are also varied amongst different organisms (Drinnenberg et al., 2016; Musacchio and Desai, 2017). CENP-B is the only protein at the centromeres that can recognize DNA in a sequence-specific manner and may represent a genetic aspect of centromere specification (Masumoto et al., 1989). It localizes to the centromere through its direct interaction with the α -satellite DNA. CENP-B interacts with N-terminus of CENP-A and also interacts with CENP-C. CENP-B contributes to the phasing of the CENP-A nucleosomes and for its stability (Fachinetti et al., 2015; Hasson et al., 2013).

Outer kinetochore:

KMN network is a 10-protein assembly which comprises of the Knl1 complex (Knl1 and Zwint), Mis12 complex (Mis12, Dsn1, Nnf1 and Nsl1) and Ndc80 complex (Ndc80/Hec1, Nuf2, Spc25, and Spc24) and is the core of the outer kinetochore (Bharadwaj et al., 2004; Cheeseman et al., 2006; 2004; Desai et al., 2003; Kline et al., 2006; McClelland et al., 2003). KMN is assembled during mitosis in a phosphorylation-dependent manner (Emanuele et al., 2008; Huis in 't Veld et al., 2016; Musacchio and Desai, 2017; Rago et al., 2015). CENP-C and CENP-T are the key recruiters of the KMN members to the kinetochore (Musacchio and Desai, 2017) (Fig. 1-1C). KMN is assembled on the CCAN upon nuclear envelope breakdown in presence of CDK1 and Aurora-B activity (Gascoigne and Cheeseman, 2013; Yang et al., 2008). The N-terminus of CENP-C interacts with the Mis12 complex in an Aurora-B phosphorylation-dependent manner (Fig. 1-1B,C). Phosphorylation on S100 and S109 of Dsn1 by Aurora-B kinase allows the interaction of the Mis12 complex with the CENP-C and its subsequent recruitment (Przewloka et al., 2011; Screpanti et al., 2011). The mis12 complex then interacts with Knl1 and Ndc80 complex through their RWD domain and with Zwint through an elongated coiled coil (Petrovic et al., 2014). CENP-C can thus recruit one molecule of KMN assembly to the kinetochore (Fig.1-1B, C).

CENP-T through its N-terminus can interact with two molecules of Ndc80 complex through a CDK1 phosphorylation on T11 and T85 of CENP-T (Huis in 't Veld et al., 2016; Rago et al., 2015) (Fig.1-1A,C). CDK1 also phosphorylates CENP-T on T201 and allows the recruitment of one molecule of KMN to the CENP-T through the

interaction of Mis12 complex with the CENP-T (Huis in 't Veld et al., 2016); Aurora-B activity is also required for this interaction (Rago et al., 2015) (Fig.1-1A,C). Although CENP-T can recruit two molecules of Ndc80 complex and one molecule of KMN assembly and CENP-C can recruit one molecule of KMN *in-vitro* (Huis in 't Veld et al., 2016; Rago et al., 2015). In-vivo measurements of metaphase kinetochore suggest that only ~40% of the CENP-C recruits KMN to the kinetochore and CENP-T is also not functional to its full potential (Suzuki et al., 2015). This discrepancy between in-vitro and in-vivo binding of CENP-T and CENP-C with KMN and Ndc80c indicates that the recruitment of KMN and Ndc80c at the kinetochore is dynamic and regulated. In Chapter 4, I will provide the molecular basis for the dynamic regulation of KMN organization during mitosis.

KMN and CCAN are the scaffolds on which multiple protein complexes that create a structure called *fibrous corona* are assembled. *Fibrous corona* is a term used to describe the fuzzy structure seen outside the outer plate of kinetochore in the electron microscopy images of kinetochores in the absence of microtubules (Musacchio and Desai, 2017; Stukenberg and Burke, 2015). Recruitment of the proteins downstream of KMN is responsive to the attachment status of the kinetochore. Before the kinetochore attachment various proteins like CENP-E, Mad1, Mad2, Bub1, BubR1, Bub3, RZZ complex (Rod, Zw10, and Zwilch), Spindly, Dynein, Ndel1, Nde1, Lis1 etc. are recruited to the kinetochore (Stukenberg and Burke, 2015). Some of the inner and outer kinetochore components and the majority of the Dynein recruitment module undergoes expansion in a phosphorylation-dependent manner, which is seen in *Xenopus levis* egg extracts or

at mammalian kinetochores after long duration in absence of microtubules (Sacristan et al., 2018; Thrower et al., 1996; Wynne and Funabiki, 2015; 2016). These proteins are important for making the motor-dependent attachment with the walls of the microtubules and for initiating spindle assembly checkpoint. After formation of the stable mature kinetochore-microtubule attachment, a combined process of Dynein dependent stripping and changes in kinase and phosphatase levels at the kinetochore removes most of these proteins (Stukenberg and Burke, 2015). Another set of proteins such as SKA complex, Astrin-SKAP, PP1 etc., are recruited to the kinetochore upon mature kinetochore-microtubule attachment, which either function in stabilizing these attachments and coupling the force generated by the depolymerizing microtubules to move chromosomes or are important for silencing the spindle assembly checkpoint (Musacchio and Desai, 2017). Detailed recruitment mechanisms and functions of these proteins are discussed at relevant locations later.

Functions of kinetochores:

Kinetochores can be thought to carry out at least six functions in order to preserve genomic stability (Fig.1-2). The proteins that carry out these functions at kinetochore are not mutually exclusive and often the same protein carries out multiple functions, which may underlie the coordination amongst these processes. First, the kinetochores are a site for the nucleation of microtubules post-nuclear envelope breakdown (Mishra et al., 2010; Sikirzhytski et al., 2018; Tulu et al., 2006). After nuclear envelope breakdown, the kinetochore searches the 3D space and makes initial contact with the spindle microtubules, this process termed as the

search and capture process (Kirschner and Mitchison, 1986). The kinetochore-nucleated microtubules may increase the effective interaction volume of the kinetochore and allow for a quick contact with the spindle microtubules in 3D space (Stukenberg and Burke, 2015). Although the identity of the microtubule nucleator is not known, the nuclear pore complex proteins that localize to the kinetochores are involved in this process (Mishra et al., 2010). Apart from this, the kinetochore volume also expands early on and this has a similar effect of reducing the duration to form initial contact with the spindle microtubules (Magidson et al., 2015). This process is important for completing mitosis in a reasonable amount of time by shortening the search and capture process of microtubules.

Second, after the nuclear envelope breakdown, the kinetochores make the initial attachment with the microtubules through the action of kinetochore localized motor proteins such as CENP-E and Dynein (Stukenberg and Burke, 2015; Tanaka, 2012). These initial attachments are with the wall of the microtubule and enable early movements such as rotation and congression of mitotic chromosomes (Magidson et al., 2015). These initial kinetochore-microtubule attachments are termed as “lateral attachments” (Tanaka, 2012). The rotational and congressional movements may ensure biorientation and allow efficient formation of kinetochore-microtubule attachment with the plus-ends of the microtubule. The lateral attachment may play a central role in prevention of improper kinetochore-microtubule attachments.

Third, the kinetochore, upon establishment of the lateral attachments transition to form stable load-bearing attachments with plus ends of the

microtubules. The Ndc80 complex mediates these attachments to the ends of the microtubules (Cheeseman et al., 2006; DeLuca et al., 2006; Kline et al., 2006; McClelland et al., 2003; Miller et al., 2008). These kinetochore-microtubule attachments are termed as “end-on” attachments (Tanaka, 2012). These are the attachments that drive the movement of the sister chromatids during anaphase. Unlike motor driven movements where ATP hydrolysis is used to power the movements of the chromatid, during anaphase the end-on attached chromatid moves by the force generated by using the potential energy stored in depolymerizing microtubules after GTP hydrolysis. A composite “foot” like structure formed by the oligomeric arrays of Ndc80 complexes and SKA complexes on microtubules is suggested to couple the depolymerizing microtubules with the chromatid movements during anaphase (Janczyk et al., 2017). The mechanism for the transition of lateral attachments to end-on attachments is still mysterious but Aurora-B and kinesin CENP-E and MCAK are known to play a role in this process (Shrestha and Draviam, 2013; Shrestha et al., 2017). End-on attachments are highly regulated to ensure proper bi-orientation and genomic stability. The end-on attachments are prevented during prometaphase by CPC dependent phosphorylation of Ndc80 complex, which reduces its affinity for microtubules and by the RZZ complex (Cheerambathur et al., 2013; DeLuca et al., 2011). The mechanism of how CPC phosphorylates various substrates to allow proper lateral to end-on attachment transition is unclear. In Chapter 3 of this thesis I will describe a mechanisms that will answer these long standing questions. I will show the data that suggest that the CPC localized on the microtubules cooperates with the inner-

centromere localized CPC to phosphorylate the outer kinetochores. This mechanism may underlie the transition of lateral to end-on kinetochore-microtubule attachments.

Fourth, kinetochores are the site of initiation of the regulatory process called the spindle assembly checkpoint (SAC) (Stukenberg and Burke, 2015). Unattached kinetochores prevent anaphase onset by generating a diffusible protein complex called the mitotic checkpoint complex (MCC), which consists of Mad2, BubR1, Bub3, and Cdc20 (Fang et al., 1998a; 1998b; Fraschini et al., 2001; Hardwick et al., 2000; Hwang et al., 1998; Sudakin et al., 2001). The SAC signaling starts by recruitment of the kinase Mps1 to the kinetochore by the key microtubule-binding complex, Ndc80 complex when it is not attached to microtubules (Nijenhuis et al., 2013; Saurin et al., 2011). Mps1 kinase then phosphorylates MELT repeats on the Knl1, which becomes the site where Bub1 and Bub3 localize (London and Biggins, 2014; Overlack et al., 2015; Shepperd et al., 2012; Vleugel et al., 2015; Yamagishi et al., 2012). Kinetochore localized Bub1 and RZZ complex recruits Mad1 to the kinetochore (London and Biggins, 2014; Meraldi and Sorger, 2005; Moyle et al., 2014) (Fig.1-3). Mad1 localization to the kinetochore is sufficient to trigger SAC arrest (Maldonado and Kapoor, 2011). Mad1 is the receptor for closed Mad2, which localizes to the kinetochore and triggers the conformational change in an open Mad2 molecule to allow formation of closed Mad2 and Cdc20 complex (De Antoni et al., 2005; Vink et al., 2006). This Mad3-Cdc20 induces the formation of more diffusible closed Mad3-Cdc20 complexes by a self-propagating prion-like mechanism and thus formation of more MCC (De Antoni et al., 2005; Luo et al., 2000; 2002; 2004). MCC sequesters

Cdc20, an activator of the E3 ubiquitin ligase called Anaphase Promoting Complex or the Cyclosome (APC/C), and keeps it in an inactive state (Luo et al., 2000; 2002; 2004) (Fig.1-3). MCC thus inhibits activation of the APC/C and prevents it from degrading Cyclin B and Securin to prevent anaphase onset (Stukenberg and Burke, 2015). Upon end-on attachment the competitive binding of microtubules to the Ndc80 complex displaces the Mps1 kinase from the kinetochore (Hiruma et al., 2015; Ji et al., 2015). A Dynein dependent process called stripping then physically removes spindle assembly checkpoint proteins from the kinetochores in order to silence the SAC (Howell et al., 2001). A concomitant recruitment of phosphatases PP1 through its interaction with Knl1 and SKA complex then leads to dephosphorylation of multiple substrates at kinetochores including MELT repeats is also required to turn off the SAC (Nijenhuis et al., 2014; Sivakumar et al., 2016).

Although the detailed mechanism of the SAC signaling is known the role key mitosis kinases like Aurora-B and Plk1 play in maintenance of the SAC is unclear. In Chapter 4, I will investigate this question and will show data that suggest that Aurora-B and Plk1 allow maintenance of the SAC arrest by stabilizing the outer-kinetochore structure in absence of microtubules.

Fifth, the inner-kinetochore members such as CENP-I and CENP-C are required to maintain the epigenetic identity of the centromeres through multiple cell cycles (Falk et al., 2016; Okada et al., 2006). The exact mechanism of this function is unclear. Sixth, finally, the kinetochore serves as the site for localization of multiple kinases and phosphatases to allow for the initiation of mitotic signaling networks, which controls the inner-centromere regions and provide unique

properties to these chromosome loci during mitosis. This function of the kinetochore has been discussed in detail in the next section.

Figure 1-1: Two branches of outer kinetochore assembly mediated by the Constitutive Centromere Associated Network (CCAN) in mitosis. (A) Cartoon of CENP-T (T) branch of Knl1 complex, Mis12 complex, and Ndc80 complex (KMN) recruitment. (B) Cartoon of CENP-C (C) branch of KMN recruitment. (C) Current model of the kinetochore organization showing CENP-T and CENP-C branch of KMN recruitment together. Abbreviations used in the figure are: CENP-C (C); CENP-L and CENP-N complex (LN); CENP-H, CENP-I, CENP-K and CENP-M complex (HIKM); CENP-T, CENP-W, CENP-S and CENP-X complex (TWSX); CENP-O, CENP-P, CENP-Q, and CENP-U complex (OPQU); KNL1 complex (KNL1); Ndc80 complex (Ndc80c); Mis12 complex (Mis12c). KMN comprises of 1:1:1 complex of of Knl1, Mis12c and Ndc80c.

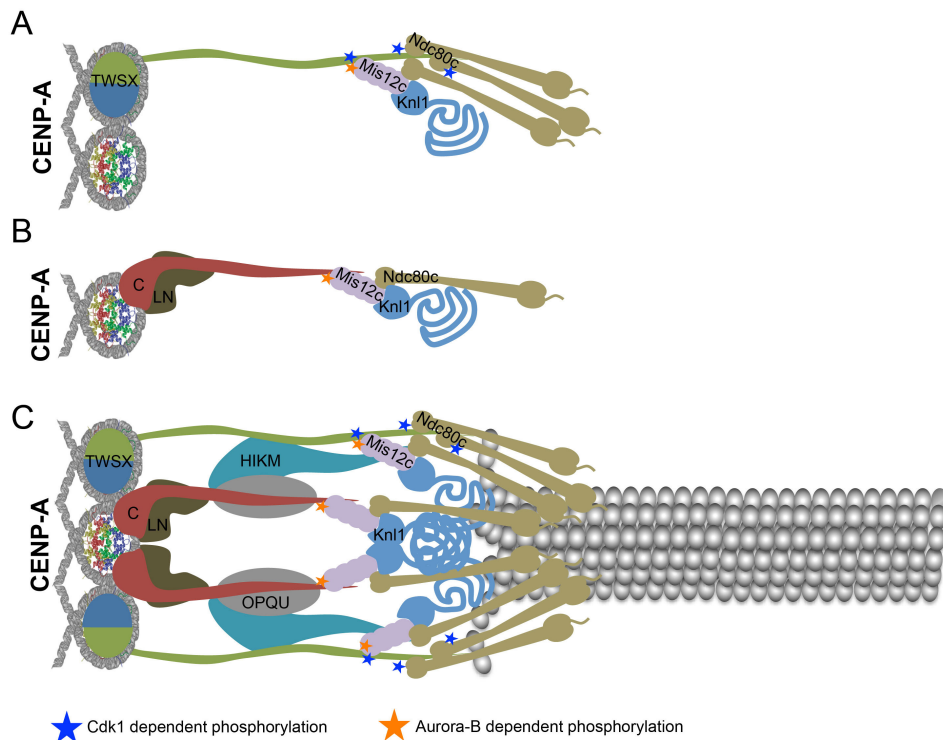


Figure. 1-1

Figure 1-2: Various functions of kinetochore.

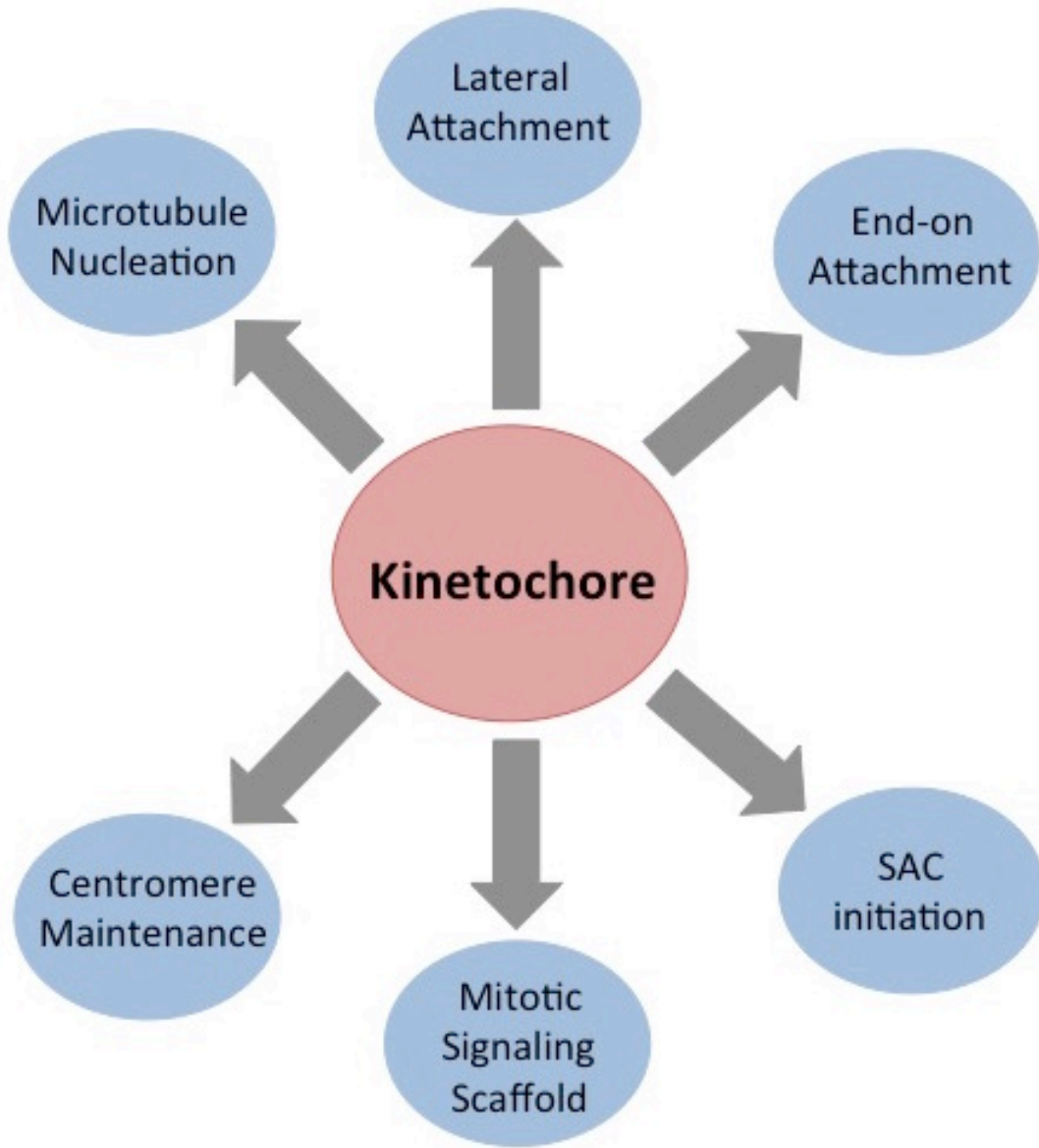


Figure 1-3: Model of Spindle Assembly Checkpoint (SAC) initiation at unattached kinetochore. Cartoon of the kinetochore showing KMN recruited to CENP-C driving localization of spindle assembly checkpoint proteins to allow SAC arrest. Localization of spindle assembly checkpoint proteins Rod, Zw10 and Zwilch complex (RZZ); Bub1; Bub2; BubR1; Mad1 to kinetochore catalyzes the formation of Mitotic Checkpoint Complex (MCC) which inhibits Anaphase Promoting Complex/ Cyclosome (APC/C).

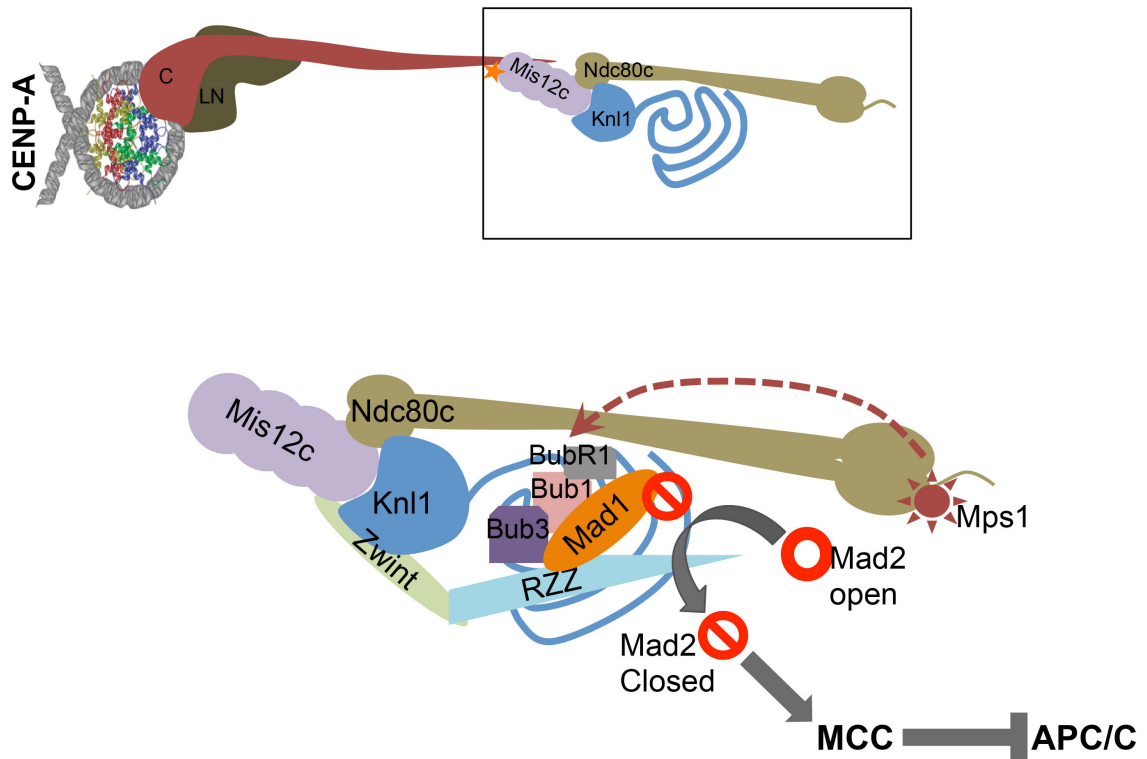


Figure. 1-3

(This section is previously published as “A Centromere-Signaling Network Underlies the Coordination amongst Mitotic Events.”

Trivedi P, Stukenberg PT. Trends Biochem Sci. 2016 Feb;41(2):160-174.)

A Centromere Signaling Network (CSN) underlies coordination amongst mitotic events:

There is increasing evidence that regulators of the spindle assembly checkpoint, kinetochore microtubule attachments and sister chromatid cohesion are part of an interconnected mitotic regulatory circuit with two positive feedback loops and the Chromosome Passenger Complex (CPC) at its center. If true, this conceptual breakthrough needs to be integrated into models of mitosis. In this review, we describe this circuit and point out how the double feedback loops could provide insights into the self-organization of some mitotic processes and the autonomy of every chromosome on the mitotic spindle. We will also provide working models for how mitotic events may be coordinated by this circuit.

Are mitotic events coordinated?

During mitosis the cell is dramatically reorganized and a number of events occur simultaneously (Fig. 1-4). Traditionally, the activation of the spindle checkpoint, sister chromatid cohesion and the generation of kinetochore-microtubule attachments were thought to have distinct regulation. This simplification has been necessary to dissect these very complex cellular processes.

However, these mitotic processes share kinase and phosphatase regulators. A number of recent papers suggest that these regulators also control each other and a regulatory circuit can now be drawn that connects the major regulators of these three seemingly distinct mitotic events. Moreover, employing this circuit can provide answers to paradoxical situations that arise during mitosis such as how the Aurora kinase phosphorylates kinetochores (where the kinase is low), while at the same time Aurora B activity must be kept in check on inner centromere cohesin substrates (where the kinase is high) to protect cohesion. While it is possible that isolated circuits independently regulate these events, we will explore the possibility that these interconnected circuits coordinate mitotic events to provide robust regulation of mitosis.

We propose to name this greater regulatory circuit the Centromere Signaling Network (CSN). The CSN is a kinase phosphatase signaling network that contains four kinases: Aurora B kinase, which is part of the CPC, MPS1 kinase, Bub1 kinase and Haspin kinase, as well as Sgo1, which binds Protein Phosphatase 2a (PP2A). Plk1 kinase is also involved (Espeut et al., 2015; Ghenoiu et al., 2013; Schubert et al., 2015; Zhou et al., 2014), however we have limited our discussion of Plk1 because its kinetochore functions are poorly understood. One major reason to explore the concept that the CSN proteins coordinate mitotic events is that sets of CSN proteins regulate different events in mitosis (Fig.1-5). First, formation of proper kinetochore-microtubule attachments is regulated by Aurora B, Mps1, Sgo1 (Cimini et al., 2006; DeLuca et al., 2011; Hauf et al., 2003; Jelluma et al., 2008b; Knowlton et al., 2006; Liu et al., 2009; Meppelink et al., 2015; Meraldi and Sorger, 2005; Salimian et al., 2011;

Welburn et al., 2010). Second, the activation of the spindle checkpoint, which arrests the cell cycle until kinetochores make mature kinetochore attachments and is regulated by Aurora B, Mps1, Bub1 (Abrieu et al., 2001; Biggins and Murray, 2001; Hauf et al., 2003; Kallio et al., 2002; Matson et al., 2012; Meraldi and Sorger, 2005; Sacristan and Kops, 2015; Santaguida et al., 2011; Stukenberg and Burke, 2015). Third, cohesin is removed from chromosome arms while it is protected at the inner centromere region, which is regulated by Aurora B, Haspin and Sgo1 (Dai et al., 2006; Resnick et al., 2006; Tanno et al., 2010). Fourth, the inner centromere is identified on each chromosome as a chromosome territory for CPC localization by the entire circuit (Boyarchuk et al., 2007; Dai et al., 2005; Kawashima et al., 2010; Kelly et al., 2010; Liu et al., 2015; Niedzialkowska et al., 2012; Ricke et al., 2012; Tsukahara et al., 2010; Wang et al., 2010; 2011b).

Another reason to consider that the CSN may coordinate mitosis is that the four events occur with spatial and temporal regularity (Fig.1-4). For example, the spindle checkpoint is generated on chromosomes that are not aligned at the metaphase plate, while on the same spindle; aligned kinetochores are not generating the signal. Since chromosomes are regulated differently, depending upon their location on the spindle, this is a form of spatial regulation. A second form of spatial regulation is the fact that cohesin is differentially regulated on chromosomes arms and centromeres. There is also temporal regulation. For example, kinetochores first generate “lateral” kinetochore-microtubule attachments, which then mature to “end-on” attachments (Fig.1-4). Finally, there is coordination between events as the

kinetochore-microtubule attachment status is coupled to the generation of the spindle checkpoint signal.

The importance of linking the regulators of distinct events through a common circuit is that the CSN may act as an information processor that integrates information regarding the environment of each chromosome and produces outputs that ensure genomic stability. For example, it was recently shown that the microtubule plus end binding protein EB1 and microtubules regulate the CPC and this also controls Bub1 and Haspin activity to connect spindle status with kinetochore regulation (Banerjee et al., 2014). Because many of these events happen at distinct times on different chromosomes we also highlight how the CSN may underlie chromosome autonomy, wherein each chromosome regulates itself independently of adjacent chromosomes on the same spindle.

The Centromere Signaling Network

Recent work suggests that CSN proteins can regulate each other and pathways can be drawn that are composed of two positive feedback loops that are interdependent because they share the CPC (Fig.1-6A). A central feature of these loops is that they recruit the CPC to inner centromeres through two histone phosphorylation events (Fig.1-6B, C). The haspin kinase phosphorylates histone H3 on Thr-3 (H3-pT3), which is directly bound by the survivin subunit of the CPC (Fig.1-6C) (Kelly et al., 2010; Wang et al., 2010; Yamagishi et al., 2010). A second loop contains the Bub1 kinase, which phosphorylates Histone H2A on T120 (Boyarchuk et al., 2007; Kawashima et al., 2010; Ricke et al., 2012) (Fig.1-6C). H2A-

pT120 recruits Sgo1, which can bind the Borealin subunit of the CPC (Fig.1-6A) (Kawashima et al., 2010; Liu et al., 2015; Ricke et al., 2012). We will describe below the recent data from many groups that allow one to draw the circuit in this manner and the interesting regulatory properties that may be a function of the double positive feedback nature of the circuit.

Signaling network regulating the H3-pT3 histone mark (cohesion sub-network)

The Haspin kinase both recruits the CPC and it is thought to be recruited to chromosomes in a CPC dependent manner. Haspin kinase phosphorylates histone H3 on T3 during mitosis. The Survivin subunit of the CPC directly binds H3-pT3 to recruit the CPC to the inner-centromere (Kelly et al., 2010; Niedzialkowska et al., 2012; Wang et al., 2010; Yamagishi et al., 2010) (Fig.1-6A). The CPC in turn can stimulate haspin recruitment through phosphorylation, generating a positive feedback loop (Wang et al., 2011b). Haspin kinase is auto-inhibited by a domain known as the Haspin basic inhibitory segment (HBIS) and multisite phosphorylation of HBIS by Plk1 and CDK1 during mitosis neutralizes the HBIS to activate Haspin (Ghenoiu et al., 2013). Aurora has been shown to activate Plk1 at kinetochores and thus may also indirectly activate Haspin (Carmena et al., 2012a).

The inner centromere localization of the CPC is highest in the center of the chromosomes between the kinetochores (Fig.1-6C) suggesting that there are mechanisms that allow the CPC to locate the central axis of mitotic chromosomes. The cohesin complex, which physically holds sister chromosomes together, is found in the central axis between the sister chromatids (Giménez-Abián et al., 2004).

Haspin is not abundant and difficult to localize on chromosomes so the localization is implied from H3pT3 patterns and biochemical interactions. Current models suggest that the spatial pattern of H3-T3 phosphorylation on the chromosome is controlled by the localization of Haspin by the Cohesin complex (Yamagishi et al., 2010). Haspin binds to the cohesin regulator Pds5 in yeast (Yamagishi et al., 2010). A similar mechanism is thought to work in mammals, because knockout of the Pds5 homologue Pds5B (but not Pds5A) results in low H3-T3 phosphorylation and low Aurora B at the inner-centromere (Carretero et al., 2013). This suggests that the H3pT3 loop directs the CPC to the central axis of the mitotic chromosome and we will refer to this part of the CSN as the cohesion sub-network (Fig.1-6C).

Signaling network regulating the pH2aT120 mark (kinetochore sub-network)

There must also be mechanisms to localize the CPC to the chromosome region between kinetochores (Fig.1-6C), which may be the function of the second positive-feedback loop of the CSN. The kinase Bub1 recruits the CPC to the centromere by phosphorylating the histone H2A at T120 (Boyarchuk et al., 2007; Kawashima et al., 2010; Ricke et al., 2012). Sgo1 binds this phospho-histone mark and brings the CPC to the inner-centromere through its CDK1-dependent interaction with Bir1 (survivin) in *S. pombe* (Tsukahara et al., 2010) (Fig.1-6A). A similar pathway exists in humans although the domain that binds Sgo1 has been transferred to the Borealin subunit (Tsukahara et al., 2010) (Fig.1-6B). Bub1 is recruited to kinetochores by the MPS1 kinase, and MPS1 in turn is targeted to kinetochores by Aurora B phosphorylation, completing a second positive feedback

loop (Hiruma et al., 2015; Ji et al., 2015; London et al., 2012; Nijenhuis et al., 2013; Saurin et al., 2011; Shepperd et al., 2012; van der Waal et al., 2012; Yamagishi et al., 2012). Because both Bub1 and Mps1 are localized to kinetochores, this pathway will phosphorylate histones between the two kinetochores to direct the CPC to the inner centromere region. We will refer to this part of the CSN as the kinetochore sub-network (Fig.1-6A).

The CSN, as drawn in Figure 1-6A, shows a simple linear relationship between the proteins in the kinetochore sub-network. This model is based on recent experiments that combine cell biological observations and have strong biochemistry as support. However, we note that some older experiments suggest independence of Bub1 and Aurora B (Meraldi and Sorger, 2005) and it is hard to reconcile all data in the literature. Thus, the network may be more of a web with some redundant pathways regulating proteins in the network.

It is unclear how proteins at kinetochores can affect Aurora B in the inner centromeres and vice-versa, which are hundreds of nanometers away from each other. Bub1 was recently shown to activate RNA Polymerase II-dependent transcription at kinetochores and transcription is required for the movement of Sgo1 from kinetochores to inner centromeres where it protects cohesion (Liu et al., 2015). Sgo1 can also bind to cohesin (Liu et al., 2015). Thus, the pool of Sgo1 that binds inner centromere Aurora B may be bound to cohesin and not H2ApT120 (Fig.1-7). Aurora B can bind RNA, which regulates its activity and localization (Jambhekar et al., 2014) and an important area of future research is how transcription regulates the CPC and the entire CSN.

Functions of the CSN

It has been unclear how the CPC could regulate so many mitotic events. During pro-metaphase the CPC prevents or corrects improper kinetochore attachments (Cimini et al., 2006; DeLuca et al., 2011; Hauf et al., 2003; Knowlton et al., 2006; Lan et al., 2004; Welburn et al., 2010), preserves centromeric cohesion (Dai et al., 2006; Resnick et al., 2006; Tanno et al., 2010), and generates the spindle assembly checkpoint (Biggins and Murray, 2001; Hauf et al., 2003; Kallio et al., 2002; Matson et al., 2012; Santaguida et al., 2011). We suggest that the CPC coordinates these events through its role within the CSN. To demonstrate this point we will describe how the network: 1) epigenetically defines the area between kinetochores to become the inner-centromere, 2) regulates centromeric cohesion protection and 3) allows proper coordination of kinetochore-microtubule attachments.

The inner centromere localization of the CPC is an emergent property of the CSN.

Self-organizing systems underlie many biological processes by employing circuits with emergent properties to build resultant structures. Self-organizing systems are based on emergence, where a new property arises from the collective behavior of agents that themselves do not contain that property. Self-organization requires a positive feedback system to elicit dramatic changes to a system (Solé and Bascompte, 2012). We suggest that the CSN provides the emergent properties that drive the formation of the key aspects of inner centromere using self-organization

principles including the localization of the CPC and the maintenance of cohesion (which we will discuss in another section).

In late G2 and early prophase the CPC is located throughout the nucleus. During prophase there is a dynamic reorganization of the CPC as it dissociates from the chromosome arms and then accumulates at the inner centromere (Fig.1-4) (Carmena et al., 2012b). Histone H3 phosphorylation on T3 follows a similar pattern, providing a positive signal for these movements, but how H3T3 phosphorylation is spatially and temporally controlled is unclear. The CSN network may drive these dynamics to provide spatial information for CPC localization. To do this, the CSN must identify chromatin region between the kinetochores. However, if the signal was only derived from kinetochores then one would predict that the CPC would decrease as a function of distance from the kinetochores. This is not true; rather, it is highest in the center of chromosomes between the kinetochores, suggesting that there must be another mechanism to identify the central region.

The interaction between haspin and cohesin may identify the central axis of the chromosome. Like the CPC, cohesin is found throughout interphase chromatin (through its recruitment by CTCF) (Wendt et al., 2008). The bulk of cohesin is removed from chromatin during prophase by phosphorylation by mitotic kinases including CDK1, Plk1 and the CPC kinase Aurora B (Nishiyama et al., 2013; Sumara et al., 2002), and since the sisters remained cohesed along the central axis of chromosomes it is reasonable the cohesin remains high in this location (Fig.1-6D) (Waizenegger et al., 2000). The maintenance of cohesion in the central axis engages the cohesion loop of the CSN to spatially locate H3pT3 and the CPC to the central

zone between the two sisters (Carretero et al., 2013; Kelly et al., 2010; Niedzialkowska et al., 2012; Wang et al., 2010; Yamagishi et al., 2010).

Mitotic chromosomes are bisected by a second axis of histone phosphorylation that is established by the second positive feedback loop (Fig.1-6D) (Boyarchuk et al., 2007; Hiruma et al., 2015; Ji et al., 2015; Kawashima et al., 2010; London et al., 2012; Nijenhuis et al., 2013; Ricke et al., 2012; Saurin et al., 2011; Shepperd et al., 2012; Tsukahara et al., 2010; van der Waal et al., 2012; Yamagishi et al., 2010; 2012). Bub1 phosphorylates chromatin near kinetochores (Liu et al., 2015; Yamagishi et al., 2010). This targets Sgo1 to chromatin between kinetochores, where it binds the CPC. Thus the CPC, which binds both H3pT3 and Sgo1, is localized by two orthogonal axes that are established on mitotic chromosomes: one axis between the sister chromosomes and one axis between the kinetochores (Fig.1-6 C, D) (Yamagishi et al., 2010). The positive feedback nature of the two independent loops may reinforce the inner centromere location after initial recruitment of the CPC and the inner centromere chromosome region emerges as a function of the centromere-signaling network.

There is abundant evidence that the CSN may drive this rapid change of mitotic chromosomes and we will highlight the key findings that show that the inner centromere localization of the CPC is an emergent property of the two-loop circuit. In a pioneering paper the Dasso group showed that the CPC was distributed throughout chromatin after depletion of Bub1, even though kinetochores could form (Boyarchuk et al., 2007). Similarly, Aurora B remains localized to chromosome arms in cells depleted of haspin (Yamagishi et al., 2010). In early prophase the CPC can

localize along the inner chromatid axis as if this is an intermediate of the CPC moving to inner centromere (Yamagishi et al., 2010). Thus the localization pattern of the CPC when one disrupts either loop suggests a dynamic process involving two feedback loops.

The network as written is dominated by kinases, although the Sgo1 protein can bind PP2A. Positive feedback systems must be limited to prevent them from dominating a system and there are likely additional phosphatase networks that need to be included to build robust models for mitotic regulation. For example, the protein Repo-Man recruits PP1 to dephosphorylate Histone H3 on T3 and limit Haspin activity. This may allow CPC to be released from chromosome arms so that it can be concentrated at the inner centromere during early mitosis (Qian et al., 2011). Repo-Man-PP1 must be displaced from inner centromeres to allow the accumulation of the CPC during early mitosis. This may be achieved by Aurora B itself, which inhibits chromosome binding of PP1-Repo-Man by direct phosphorylation (Qian et al., 2013) and we suggest that there is only enough Aurora B to counter Repo-Man activity within the regions between kinetochores. However, there may be additional mechanisms to reverse Haspin phosphorylations on chromosome arms in prometaphase and metaphase when CDK inhibits PP1-Repo-Man interaction and Repo-Man binding to the chromatin (Trinkle-Mulcahy et al., 2006; Vagnarelli et al., 2006; 2011). This may be through local reactivation of Repo-Man, which can bind PP2A to reactivate it (Qian et al., 2013).

On chromosomes that have neocentromeres, which are ectopic centromeres that occasionally arise at the non-centromeric location of a chromosome, the CPC is

found at the neocentromere. The CPC is not found on the original centromere that got inactivated but still has alpha satellite repeat DNA, that define the centromere, arguing that it is localized by epigenetic mechanisms (Bassett et al., 2010). Centromeres are epigenetically identified by presence of a histone H3 variant CENP-A, yet how this translates to epigenetic identification of the inner centromere is less well understood. Note that the CSN dependent mechanisms that we just discussed link the epigenetic mechanisms of CENP-A specification that localize kinetochores to specification of the inner centromere.

Regulation of sister chromatid cohesion by the CSN

Sister chromatids must be held together until anaphase in order to faithfully segregate the genetic material to the daughter cells. This is accomplished by the ring-shaped cohesin complex, which physically pairs the sister chromatids. Cohesion is established coincident with DNA replication, to enable faithful pairing of the two sister DNA strands (Nasmyth and Haering, 2009; Peters et al., 2008). Cohesin is removed from the chromatin in two steps during mitosis in higher eukaryotes (Waizenegger et al., 2000). The prophase pathway removes most of the cohesin from chromosome arms, but centromeric cohesin is protected from this pathway (Fig.1-8A) (Waizenegger et al., 2000). This generates a new state where mitotic chromosomes are paired by centromeric cohesin that is maintained until every chromosome obtains bipolar microtubule attachment (Fig.1-8A). At that point, centromeric cohesion is released by activation of the protease Separase, which cleaves chromatin-bound centromeric cohesin to drive the metaphase-to-

anaphase transition (Fig.1-8A) (Buonomo et al., 2000; Hauf et al., 2001; Uhlmann et al., 1999; 2000).

The release of cohesin from chromosome arms in prophase is controlled by three factors: Pds5 (Pds5 A/B in mammals), which directly binds cohesin; Wapl, which can release chromatin-bound cohesin (Gandhi et al., 2006; Kueng et al., 2006), presumably by opening the ring; and Sororin, which competes for the Wapl binding site on Pds5 and therefore protects chromatin-bound cohesin (Dreier et al., 2011; Hara et al., 2014; Nishiyama et al., 2010). The spatial segregation of cohesin on mitotic chromosomes is thus determined by the recruitment of Wapl: Wapl is recruited to cohesin on the chromosome arms, whereas cohesin at the centromere is protected from Wapl binding (Gandhi et al., 2006; Hara et al., 2014; Hauf et al., 2001; Kueng et al., 2006; Nishiyama et al., 2010). Proteins in the CSN control these events and we suggest that these dynamics can be explained by one branch of the CSN acting at chromosome arms in prophase, while both positive feedback loops are engaged at centromeres. Aurora B and Cdk1 phosphorylate Sororin on multiple sites and reduce its interaction with Pds5, allowing Wapl to bind and remove cohesin from the chromosome arms (Fig.1-8A, B) (Hara et al., 2014). In addition, Plk1 can directly phosphorylate and release cohesin (Fig.1-8A, B) (Tang et al., 2006). However, we are left with a paradox: how is it that the CPC removes cohesin from chromosome arms, yet cohesin is protected in the centromere where the CPC is highest? We suggest the answer lies in the feedback loops, which can be redrawn as a spatially segregated negative feedback system (Fig.1-8B, C). That Pds5 recruits haspin suggests the cohesin complex indirectly recruits the CPC, which drives the

dissociation of cohesin (Carretero et al., 2013; Yamagishi et al., 2010). This simple feedback system allows the CPC, via the cohesion sub-network of the CSN, to quickly bind and remove cohesin from the arms. However, the CPC recruits the Bub1 kinase to the region between kinetochores (Hauf et al., 2003; Santaguida et al., 2011; Saurin et al., 2011; van der Waal et al., 2012), driving the association of Sgo1 preserves centromeric cohesion by recruiting the phosphatase PP2A, which removes the Aurora B and Plk1 phosphorylations to preserve cohesion (Kitajima et al., 2006; McGuinness et al., 2005; Shintomi and Hirano, 2009). Thus, on chromosome arms there is a simple feedback loop where cohesin recruits the CPC to release cohesin. However, between kinetochores the negative feedback system is negated because the CPC can also recruit the inhibitor of cohesion release. This is a spatially segregated negative feedback circuit that drives the self-organization of the mitotic chromosome by removing cohesion from all chromatin unless it is between kinetochores. Apart from recruiting the CPC to cohesin, Haspin may also play a positive role in protecting cohesin (Dai et al., 2006).

This insight provides important lessons about the system. First, the feedback loops contain regulators of the various processes (i.e., Sgo1) because they perform their functions as part of this whole centromere network. In other words, Sgo1 performs two functions in the circuit: to recruit more CPC through its interaction with Borealin, and to preserve cohesion (Kitajima et al., 2006; Liu et al., 2015; Tsukahara et al., 2010). The preservation of cohesin would also recruit more CPC through the CSN. Second, the system ensures robustness. When centromeric CPC activity increases the system will recruit more Sgo1/PP2A to ensure that the

cohesin-releasing activity will never overwhelm the preserving activity. Third, the system approaches a steady state that can only be reversed by an external signal. In this case, centromeric cohesion is robustly maintained until the APC/C activates the Separase protease, which cleaves cohesin to drive the segregation of chromosomes. Although this system is robust, it is not a true steady state because cohesin cannot be reattached and chromosomes will eventually lose their cohesion and exit from mitosis, which may contribute to cohesion fatigue (Daum et al., 2011).

CSN regulation of kinetochore-microtubule interaction

Human kinetochores bind approximately 17 microtubules and aneuploidy can develop if a kinetochore is pulled by microtubules attached to opposite poles (merotelly) in anaphase (McEwen et al., 2001; Stukenberg and Foltz, 2010). Thus, mitosis depends upon the sister kinetochores generating bipolar kinetochore microtubule attachments, meaning that one sister kinetochore binds microtubules from one pole, while the other sister kinetochore binds microtubules emanating from the opposite pole. It is likely that cells prevent merotelly by orienting the two sister kinetochores toward the two opposite poles before they make stable attachments (Alexander and Rieder, 1991; Magidson et al., 2015; Stukenberg and Foltz, 2010). It is believed that the motors dynein and Centromere protein E (CENP-E) rotate chromosomes to achieve this orientation (Ditchfield et al., 2003; Magidson et al., 2011; Shrestha et al., 2017). Based on these observations it is suggested that one of the central mechanisms to prevent merotelly is to ensure these motors initially bind microtubules before kinetochores generate “end-on” Ndc80 complex-

mediated attachments that segregate chromosomes in anaphase (Alexander and Rieder, 1991; Magidson et al., 2015).

We suggest that incorporating the CSN into the regulation of kinetochore microtubule attachments enable models with the attributes of a bistable switch (Fig.1-9A). First, the CSN may initially generate a stable system where lateral attachments dominate and end-on attachments are inhibited. Second, after end-on attachments form there is a new stable state where end-on attachments dominate. Third, the first state has mechanisms that ensure the transition to the second state. We will outline each of these states below and note that mathematical modeling is required to test if this is truly a bistable system.

The CSN promotes lateral attachment by recruiting two microtubule motors, CENP-E and Dynein (Johnson et al., 2004; Kasuboski et al., 2011). The CSN plays a crucial role in the formation of motor-dependent attachments by both recruiting and regulating dynein and CENP-E (Johnson et al., 2004; Kasuboski et al., 2011). For example, current models suggest Mps1 and Bub1 recruit, and Aurora B regulates, CENP-E to properly align chromosomes (Abrieu et al., 2001; Cheeseman et al., 2002). Thus, the entire CSN network may be needed to properly control CENP-E (Fig.1-9A).

At the same time CSN promotes lateral attachment it also inhibits “end-on” attachments (Fig.1-9B). Aurora B directly prevents pre-mature “end-on” attachment by phosphorylating the Ndc80 complex and inhibiting its interaction with microtubules (Abrieu et al., 2001; Cheerambathur et al., 2013; Cheeseman et al., 2006; Ghenuiu et al., 2013; Sarangapani et al., 2013). It is unclear how Aurora-B

localized to the inner-centromere phosphorylates Ndc80 at the kinetochore, which is 100s of nanometers away. In Chapter 4 of this thesis I will investigate this question and show data for a new mechanism that suggests the microtubules and centromere bound CPC cooperate to phosphorylate Ndc80 at the kinetochores. Apart from direct phosphorylation of Ndc80 by the Aurora-B the proteins involved in Dynein recruitment to the kinetochore might also inhibit “end-on” attachment (Famulski and Chan, 2007; Gassmann et al., 2008; 2010) and this might also be ultimately controlled by Aurora B (Suijkerbuijk et al., 2012)[97] (Fig.1-9B). Since microtubules displace Mps1 bound to Ndc80 it is reasonable to assume that unattached Ndc80 complex would recruit more Mps1 to the kinetochore (Hiruma et al., 2015; Ji et al., 2015; Nijenhuis et al., 2013). This increase in Mps1 would lead to an increase in the CPC levels at centromeres, due to the CSN, which may further inhibit “end-on” attachment (Hauf et al., 2003; Hiruma et al., 2015; Santaguida et al., 2011; Saurin et al., 2011). This positive feedback loop between Mps1 and the CPC may lead to robust inhibition of “end-on” attachment (Fig.1-9B).

This robust inhibition of end-on attachment through positive feedback by three kinases in the kinetochore sub-network of the CSN has to be controlled to allow the kinetochores to initiate “end-on” attachment (Fig.1-9B). This is accomplished through recruitment of phosphatases by the CSN to decrease and counteract kinase activity. The CSN recruits phosphatase PP2A at two locations: to the inner-centromere, through BUB1 dependent recruitment of Sgo1-PP2A (Boyarchuk et al., 2007; Kawashima et al., 2010; Ricke et al., 2012; Tsukahara et al., 2010; Yamagishi et al., 2010); and to the kinetochore, through BUB1, Plk1 and

Aurora B dependent recruitment of BUBR1-PP2A (Kruse et al., 2013; Nijenhuis et al., 2014; Xu et al., 2013). These two pools of phosphatases allow the formation of initial “end-on” attachments by countering CPC-dependent destabilization of the “end-on” attachment. Sgo1-PP2A reduces the activity of the CPC by dephosphorylating the T-loop of Aurora B thus reducing the overall activity of the CPC (Meppelink et al., 2015). Plk1 mediated BUBR1-PP2A dephosphorylates the kinetochore substrates of the CPC and allows PP1 recruitment to Knl1, which also dephosphorylates the kinetochore substrates and promotes “end-on” attachments (Kruse et al., 2013; Maresca and Salmon, 2009; Nijenhuis et al., 2014; Xu et al., 2013).

Once proper “end-on” attachments begin to form there are at least three events that down-regulate the CSN to stabilize the initial “end-on” attachment (Fig.1-9B). First, the microtubule binding to the Ndc80 complex competes off Mps1 and reduces its levels at kinetochore, which subsequently causes reduction in the CPC levels at the centromere to stabilize “end-on” attachments (Hauf et al., 2001; Hiruma et al., 2015; Ji et al., 2015; Nijenhuis et al., 2013; Santaguida et al., 2011; Saurin et al., 2011; van der Waal et al., 2012). Second, microtubule dependent pulling forces generated by bipolar attachment physically pulls the outer kinetochore away from the inner-centromere localized CPC (Liu et al., 2009; 2010; Uchida et al., 2009). This physical separation of the outer kinetochore from Aurora B would reduce the phosphorylation of the Ndc80 complex (Hiruma et al., 2015; Ji et al., 2015; Liu et al., 2009; 2010; Uchida et al., 2009). Third, recruitment of PP1 to the “end-on” attached kinetochores leads to further stabilization of the attachments (Hagting et al., 2002; Kim et al., 2010). Multiple pools of PP1 are recruited to the

kinetochore that stabilizes “end-on” attachments and localization of most of these pools of PP1 are inhibited by Aurora B activity (Hagting et al., 2002; Kim et al., 2010).

Coordination of Kinetochore-microtubule attachment formation and the Spindle assembly checkpoint (SAC)

The formation of kinetochore microtubule attachments and the spindle assembly checkpoint must be coordinated to ensure faithful genome segregation. The CSN may allow this coordination. Mps1, BUB1 and the CPC, which inhibit end-on attachment and promote lateral attachments, also activate and maintain the spindle assembly checkpoint (Sacristan and Kops, 2015; Stukenberg and Burke, 2015) (Fig.1-9B). This could ensure that the checkpoint is activated at unattached kinetochores. Similarly, the proteins or events involved in promoting end-on attachment (BubR1-PP2A, Knl1-PP1 and Ndc80-microtubule interaction) are also involved in silencing the spindle assembly checkpoint (Maresca and Salmon, 2009; Sacristan and Kops, 2015; Stukenberg and Burke, 2015). In fact, the most important step for spindle assembly checkpoint silencing is Ndc80-mediated end-on attachment itself. Microtubule binding to Ndc80 displaces Mps1 from the kinetochores, which leads to silencing of the spindle assembly checkpoint (Hiruma et al., 2015; Ji et al., 2015). The displacement of MPS1 would also down regulate the CSN to lower Bub1 and Aurora B coupling end-on attachment to dramatic changes to the kinetochore.

Since MPS1 and Bub1 are displaced from metaphase kinetochores, one could imagine that it is difficult to restart the SAC once chromosomes are aligned. Yet, the addition of taxol to metaphase cells quickly reinitiates spindle checkpoint signaling (Jelluma et al., 2008a). It is tempting to speculate that the reversibility of this system is ensured because the cohesion sub-network maintains some CPC at inner-centromeres even when kinetochore sub-network is down regulated, which would enable rapid binding of MPS1 to unattached molecules of Ndc80 (Hiruma et al., 2015; Ji et al., 2015; Nijenhuis et al., 2013).

The generation of the SAC signal involves tens to hundreds of phosphorylation on numerous substrates at each kinetochore by Aurora B, Plk1, Mps1 and Bub1 thus it is an emergent property of the network. The generation of so many phosphorylations can ensure that, once generated, the signal is robustly maintained until there is both active recruitment of phosphatases and down regulation of the kinases that accompanies the transition to mature kinetochore microtubule attachments.

Figure 1-4: Table showing the temporal order of events during mitosis. Spatial and temporal changes to the CPC location on the chromosome, Sister-chromatid cohesion and Kinetochore-microtubule attachment are described as the cell goes through different stages of mitosis. Below, morphology of the cells during each phase of mitosis with the CPC (green) localization on the chromosomes (blue) depicted at each stage of mitosis (mitotic spindle is represented in purple).

	Late G2/ Early prophase	Prophase	Prometaphase	Metaphase	Anaphase
Epigenetic identification of the inner centromere	CPC on the Chromosome arms and at inner centromere	CPC at the inner centromere	CPC at the inner centromere	CPC at the inner centromere	
Cohesion	Cohesin on the Chromosome arms and at the centromere	Cohesin at the inner centromere	Cohesin at the inner centromere	Cohesin at the inner centromere	Cohesin cleaved by seperase
Kinetochore-microtubule attachment	No attachments	No attachments	Dynein/CENP-E-mediated lateral attachment	Stable Ndc80 complex-mediated 'end-on' attachment	Stable Ndc80 complex-mediated 'end-on' attachment

Figure 1-5, The Centromere Signaling Network (CSN) contains sets of proteins that regulate multiple mitotic events. Schematic representation of the CSN is shown with block arrows pointing at the process regulated by the proteins in the CSN.

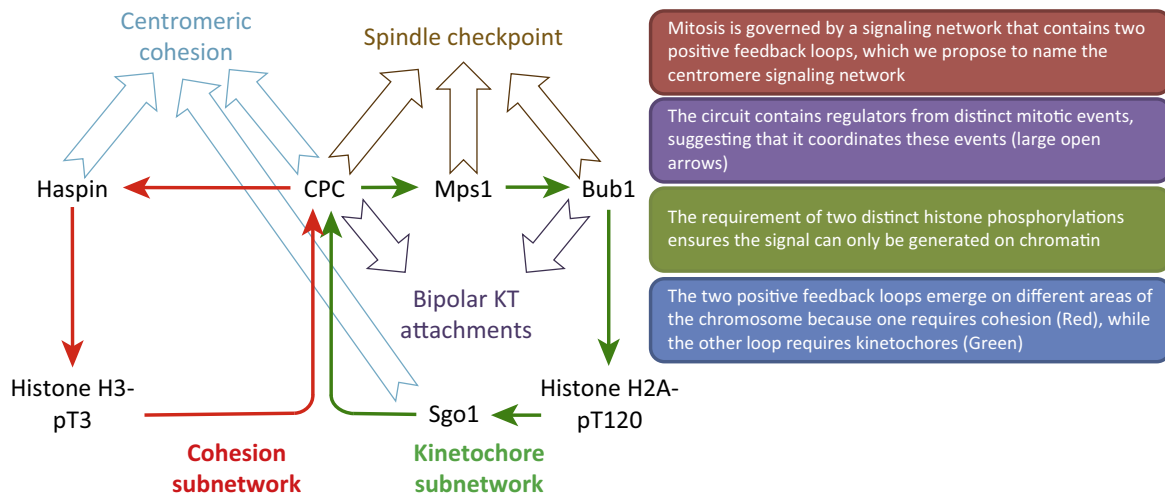


Figure 1-6: CPC localization pathways and epigenetic determination of inner-centromere. (A) Current model of the Chromosome Passenger Complex (CPC) localization to the inner-centromere by binding to two phospho-histone marks (in red). (B) Image showing the CPC (green) localized to the inner-centromere on a mitotic chromosome (original image from [119]). (C) Representation of the centromere signaling network (CSN). (D) Representation of the location of the cohesion and the kinetochore sub-network of the CSN on the mitotic chromosome.

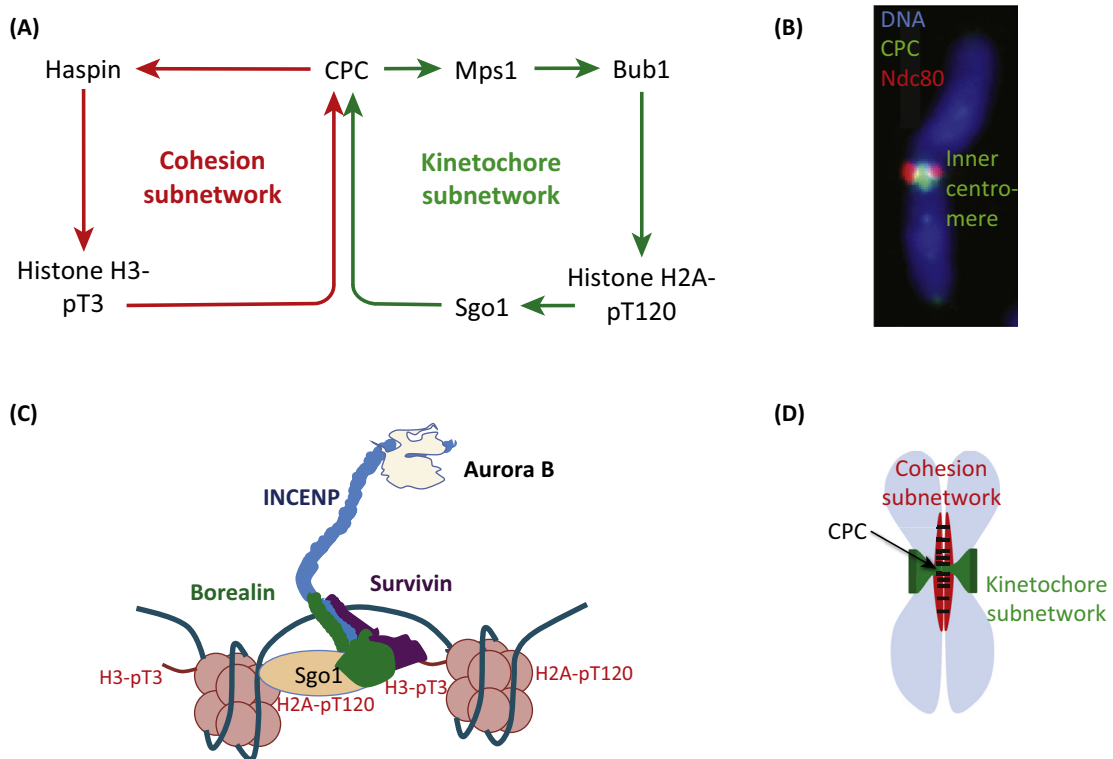


Figure 1-7: Two models of anchoring CPC to the inner-centromere. A) Model 1: The CPC binds H3 pT3 and Cohesin bound Sgo1 at the same time. B) Model 2: The CPC binds H3 pT3 and H2a pT120 at the same time.

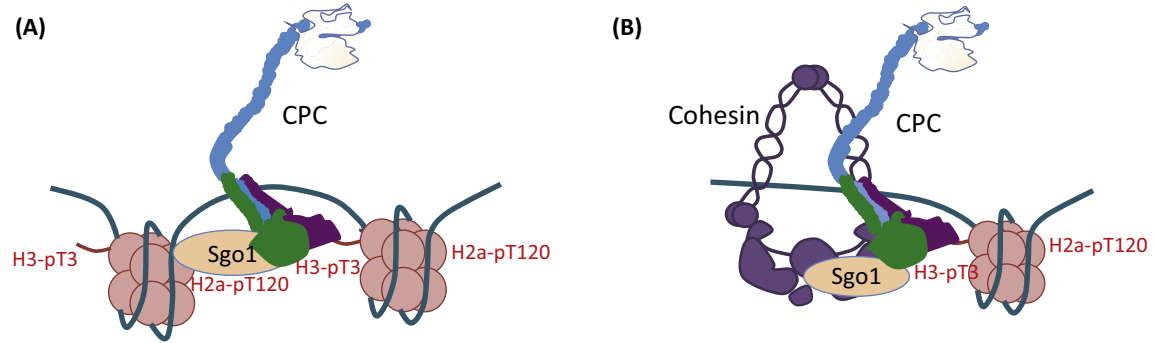


Figure 1-8: Regulation of sister chromatid cohesion by the CSN. (A) Two step cohesin removal from the chromosomes during mitosis. (B) Signaling network regulating sister chromatic cohesion during mitosis. Cohesion removing part of the network is represented by red arrows and green arrows represent cohesion-protecting network. (C) Simplified diagram of the cohesion regulation during the mitosis.

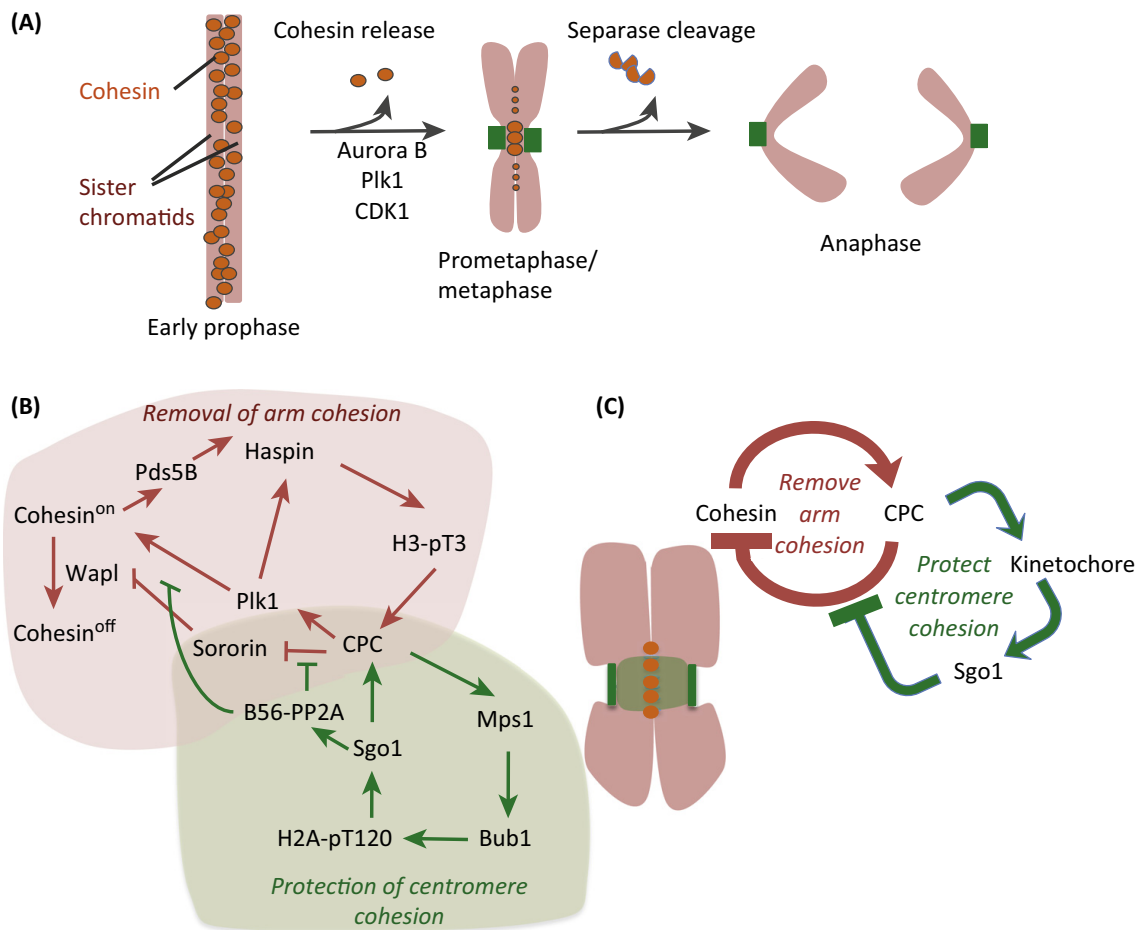
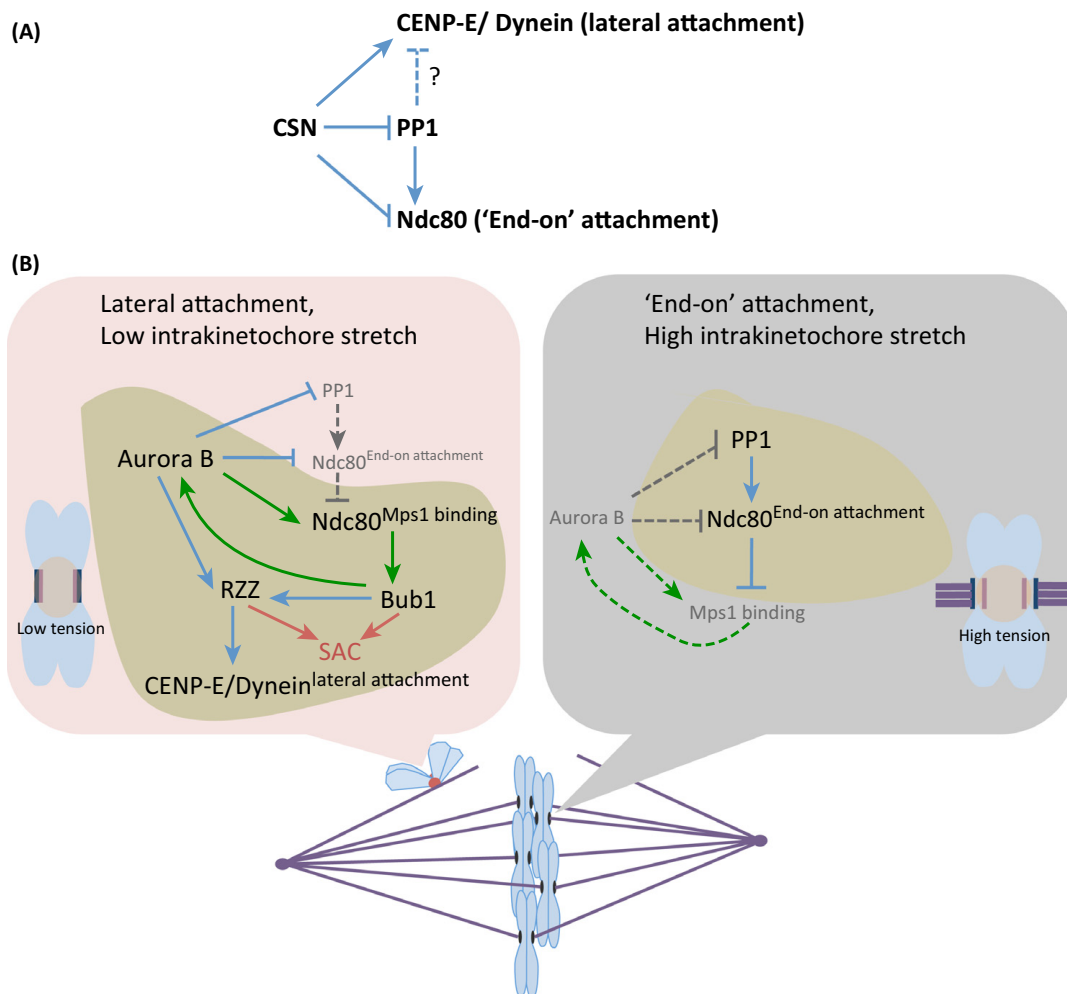


Figure 1-9: Regulation of kinetochore-microtubule interaction by the CSN. (A)

Network coordinating lateral and “end on” kinetochore-microtubule attachment.

(B) Representation of the signaling network that is active on the laterally attached kinetochore (red) or on “end on” attached kinetochore (black). The signaling network represented by green arrows is part of the CSN; the dominant signaling network is represented in the yellow patch. Dotted lines represent inactive or weakened networks. Red lines indicate activation of spindle assembly checkpoint (SAC).



Chapter 2

Phase separation by the chromosome passenger complex
underlies the biophysical organization of the inner centromere

This chapter is from the manuscript titled: “Phase separation by the chromosome passenger complex underlies the biophysical organization of the inner centromere”

Prasad Trivedi and P.Todd Stukenberg. (Submitted to Nature Cell Biology).

Phase separation is emerging as an organizational principle for interphase chromatin but it is unknown if phase separation also underlies the organization and function of mitotic chromosomes. The inner centromere is a specialized chromatin region between the sister kinetochores that displays distinct biochemical composition and behavior from the rest of the mitotic chromosome. Inner centromeres contain high concentrations of the chromosome passenger complex (CPC), which stabilizes sister chromatid cohesion and initiates mitotic signaling (Carmena et al., 2012b; Trivedi and Stukenberg, 2016). Here we demonstrate that subunits of the CPC undergo phase-separation *in vitro* and that inner centromere targeting and mitotic functions of the CPC are dependent on its ability to phase separate. Phase separation occurs at CPC concentrations found at the inner centromeres, but not at cytoplasmic concentrations. CPC coacervates enrich inner centromere components and chromatin and bundles of microtubules induce phase separation. We suggest the CPC is concentrated by phase separation at the inner centromere and the resulting coacervates impart unique biochemical activities to this chromosome territory.

The CPC lies at the heart of a signaling module that allows each mitotic chromosome to measure its local environment and generate outputs such as correcting improper kinetochore-microtubule attachments and generating the spindle checkpoint signal to ensure accurate chromatid segregation (Hindriksen et al., 2017; Trivedi and Stukenberg, 2016). Mitotic signaling is initiated by concentrating the CPC on inner-centromeric chromatin between kinetochores, which stimulates auto-activation of Aurora B kinase (Sessa et al., 2005; Wang et al.,

2011a). The CPC subunits, Survivin and Borealin, facilitate the concentration in the inner centromere by recognizing two-histone phosphorylation marks on histone H2A and H3 (H2ApT120 and H3pT3)(Yamagishi et al., 2010). Survivin directly binds H3 pT3(Kelly et al., 2010; Wang et al., 2010), while Borealin interacts with Sgo1, which binds H2ApT120(Tsukahara et al., 2010).

A number of facts suggest there must be additional mechanisms to localize the CPC to the inner centromere. Aurora B, INCENP, and Borealin subunits are stably attached to inner centromeres as measured by FRAP, while the Survivin anchor turns over approximately five times faster(Bekier et al., 2015; Delacour-Larose et al., 2004; Wheelock et al., 2017). It is also unclear whether the relatively weak (~1-8 uM) affinity between Survivin and a phosphorylated histone tail is sufficient to explain the long-lived chromatin-association of the CPC(Du et al., 2012; Niedzialkowska et al., 2012). In addition, It is unclear how Sgo1 contributes as an anchor for most of the CPC since the concentration of the Sgo1 protein is approximately five times less than that of the CPC components during mitosis, as measured in frog eggs (Wühr et al., 2014).

The property of HP1 to phase separate has been suggested to underlie the organization of interphase heterochromatin(Larson et al., 2017; Strom et al., 2017). The CPC displaces HP1 during mitosis (Fischle et al., 2005; Hirota et al., 2005) and high concentrations of the CPC specifically bind inner centromeric heterochromatin. We therefore tested whether phase separation enables the CPC to localize and organize the inner centromere. First, we asked whether the CPC could phase separate *in vitro*. To do this we expressed the centromeric targeting region of the

CPC containing the proteins Survivin, Borealin, and the 58 N-terminal amino acids of INCENP (ISB) in *E. coli* (Fig.2-1A, Extended Data Fig.2-1A,B). ISB underwent spontaneous phase separation under the condition of high protein concentration, low salt or presence of molecular crowding agent like PEG-3350, which mimic the protein-rich crowded environment of the cell (Fig.2-1B,C,D). We conclude that the centromere-targeting region of the CPC can phase separate *in vitro*.

The ISB coacervates display properties that are characteristic of a liquid-like state similar to what has been seen with other phase separating proteins (Banani et al., 2017; Larson et al., 2017; Strom et al., 2017; Woodruff et al., 2017). They are highly circular in shape, the larger coacervates undergo shear upon placement of a coverslip, and the coacervates also undergo fusion at early time points after phase separation (Fig.2-1E, Extended Data Fig.2-2A, B). We tested the biophysical behavior of these coacervates by Fluorescence Recovery After Photobleaching (FRAP). The recovery kinetics ($t_{1/3}$ -95.44s, 53.7% mobile fraction) is similar to what has been measured for INCENP *in vivo* ($t_{1/2}$ 83.2s \pm 33.5, ~53-60% mobile fraction)(Wheelock et al., 2017) (Fig.2-1G, H; Extended Data Fig.2-2L). Some proteins that phase separate maintain their liquid-like state whereas others undergo gelation over time(Banani et al., 2017). We bleached a sub-region of a GFP-ISB coacervate and saw little internal rearrangement over minutes time scale, suggesting that ISB coacervates undergo gelation over time (Fig.2-1F). The fusion events seen in Fig.2-1E were not observed five minutes or longer after phase separation. We often saw coacervates that appeared to be arrested mid-fusion suggesting gelation occurred before fusion could be completed (Fig.2-2 I, J, K).

The size of ISB coacervates depends on the concentration of salt, ISB protein or on the molecular crowding agent (Extended Data Fig.2-2 C-H). Interestingly, the phase diagram of ISB and salt concentration predicts that the ISB would phase separate near concentrations that are estimated to be present at the inner centromere (10 μM), but exist in a soluble state at cytoplasmic CPC concentrations (0.1 μM) (Mahen et al., 2014; Zaytsev et al., 2016)(Fig.2-1I). In comparison, ISB phase separates at concentrations approximately 30-fold lower than phosphorylated HP1 α (Larson et al., 2017).

A key property of membrane-less organelles is their ability to concentrate macromolecules (Banani et al., 2017). We tested whether inner centromere components interact with the ISB condensates *in vitro*. HP1 α is removed from heterochromatin by Aurora kinase activity (Fischle et al., 2005; Hirota et al., 2005) but then recruited to inner centromeres by direct binding to the CPC during mitosis (Ainsztein et al., 1998; Kang et al., 2011). HP1 α was recruited into ISB coacervates under conditions where HP1 α is unable to phase separate (Fig.2-2A). Aurora-B/INCENP⁷⁹⁰⁻⁸⁴⁷ partitioned into the ISB coacervates (Fig.2-2B). These two parts of the CPC are not been shown to interact and are separated by an elongated α -helix, which suggests that phase separation enables the two regions to interact. We also observed an enrichment of a-satellite RNA and DNA and histone H3.3 mononucleosome in ISB coacervates (Fig.2-2 C,D, Extended Data Fig. 3-3A). In contrast, molecules that either don't interact with CPC or are not inner centromere components such as GFP, GFP-Mad2, or Cy3-azide showed marginal or no enrichment in the ISB phase (Fig.2-2E, Extended Data Fig.2-3B,C.). The CPC is

concentrated at inner centromeres because the Survivin subunit directly binds the N-terminus of histone H3 after it is phosphorylated on threonine-3 by Haspin kinase (Du et al., 2012; Kelly et al., 2010; Niedzialkowska et al., 2012; Wang et al., 2010). ISB coacervates specifically enriched histone H3 peptides phosphorylated at the T3 position more than unphosphorylated peptides. Survivin (H80A), which is deficient in binding H3 pT3 peptides in solution and recruiting the CPC to inner centromeres (Niedzialkowska et al., 2012), did not enrich H3pT3 over H3 peptides in coacervates (Fig.2-2G, H, Extended Data Fig.2-3D). We conclude that ISB coacervates concentrate key inner centromere components and can simultaneously phase separate and recognize histone marks.

Interestingly, α/β -tubulin dimers are also highly enriched in ISB coacervates (Fig.2-2F). Enrichment of the α/β -tubulin in the condensates of centrosome proteins can induce nucleation of microtubules by locally concentrating tubulin dimers above the critical concentration (Woodruff et al., 2017). Similarly, ISB coacervates nucleated microtubules at concentrations of α/β -tubulin dimers that are 20-fold below the critical concentration. No microtubule nucleation was seen in absence of ISB or GTP (Extended Data Fig.2-3E). The physiological importance of this microtubule nucleation activity is unclear. Interestingly, the CPC has been shown to be important for nucleation of microtubules near chromosomes, although this has been attributed to its ability to inhibit the microtubule depolymerase MCAK (Sampath et al., 2004).

ISB spontaneously phase separates in physiological conditions at concentrations approximately 15 μ M, which is higher than that measured at the

inner centromere (10 μ M). We therefore asked whether components found near the inner centromere could induce phase separation of ISB at a concentration below that measured in the inner centromere. Indeed, α -satellite DNA, histone H3.3 polynucleosomes and microtubule bundles induced phase separation under conditions where ISB exists in homogeneous phase (Fig.2-2I-K). These observations suggest that the initial local concentration of the CPC by the phospho-histone marks nucleates phase separation at the inner centromere and other factors such as the presence of chromatin and microtubule can further enhance the phase separation of the CPC at the inner centromere.

We tested whether the CPC exists in a phase-separated state at the inner centromere as suggested by our *in vitro* analysis of the centromere targeting subunits. Since the phase-separation of the ISB is salt sensitive, we tested whether the cell-permeable monovalent cation, ammonium acetate, could disrupt CPC coacervates at inner centromeres, as shown for the phase separation and gelation of repeats containing RNA in cells (Jain and Vale, 2017). 90mM ammonium acetate inhibited phase separation of ISB *in vitro* (Extended Data Fig.2-3A). We found that incubating cells in 90mM ammonium acetate for 2 minutes displaced the CPC from the inner centromere of chromosomes of mitotic cells as measured by quantitative immunofluorescence of Aurora-B (Fig.2-3A-C, Extended Data Fig.2-4A). The approximately two-fold reduction in the amount of inner-centromeric CPC upon treatment with the ammonium acetate was reversible, as we observed a complete recovery of the CPC after washing out the ammonium acetate for an additional two minutes. We found that presence of PEG-3350 allows phase separation to occur in

the presence of high NaCl concentrations *in vitro* (Fig.2-1 B-D, Extended Data Fig.2-4B), which provided an opportunity to determine if the reduction of CPC levels was indeed due to disruption of phase separation and not due to other effects of raising the ionic concentration. We treated mitotic chromosome spreads of HeLa Kyoto cells engineered with a fusion of mCherry on the endogenous INCENP gene with buffer containing either low salt (25mM NaCl) or high salt (200mM NaCl) and measured the amount of inner-centromeric INCENP. High salt significantly reduced the levels of INCENP at inner centromeres. In contrast, the CPC was maintained at high levels in presence of high salt if we also added PEG-3350 (Fig.2-3D-F, Extended Data Fig.2-4B). We propose that the CPC exists in a phase-separated state at inner centromeres.

We identified a mutant of ISB that is defective in phase separation to directly test the hypothesis that phase separation controls CPC localization and function. We deleted two regions, $\Delta 139-160$ and $\Delta 163-180$, in the central unstructured region of Borealin that were predicted to have a high propensity to drive granule formation by catGranule algorithm, which was previously shown to correlate with ability to phase separate (Ambadipudi et al., 2017; Bolognesi et al., 2016) (Fig.2-3G, Extended Data Fig.2-4C-D). We concentrated on basic patches because of the strong regulation of ISB phase separation by ionic concentration *in vivo* and *in vitro*. ISB lacking 139-160 amino acids of Borealin was deficient in both spontaneous and DNA induced phase separation (Fig.2-3H-J). In contrast, the ISB $\Delta 163-180$ behaves similar to ISB^{WT} in these assays. These deletions did not compromise ISB complex formation or caused

any gross structural change as indicated by similar gel-filtration chromatography profiles (Extended Data Fig.2-1A,B).

We depleted the endogenous Borealin by siRNA and complemented with either LAP (GFP and S-peptide) tagged wild-type Borealin (Borealin^{WT}) or lacking the amino acids 139-160 (Borealin^{Δ139-160}) (Extended Data Fig.2-5 A). We then assessed the amount of CPC in the inner centromere and midzone microtubules in anaphase by quantitative immunofluorescence in the first cell cycle following knockdown and replacement. The Borealin^{Δ139-160} had two-fold lower CPC in the inner centromere and midzones compared to the WT (Fig.2-3K-M, Extended Data Fig.2-5B-E). Borealin^{Δ139-160} cells were deficient in both maintaining the spindle assembly checkpoint in response to paclitaxel and correcting improper kinetochore-microtubule attachments (Fig.2-4A-F, Extended Data Fig.2-6A-D). We conclude that phase separation of the CPC is important for its localization to the inner-centromeres and midzone microtubules and its mitotic functions.

Our studies suggest that phase separation underlies the unique properties of the inner centromere. Specifically we demonstrate that apart from recognizing phospho-histone marks the centromere targeting subunits of the CPC also undergo phase separation. The CPC exists in a phase-separated state in the inner centromere. We have also reconstituted a number of biochemical properties of the inner-centromere in the ISB coacervates. We propose that the initial localization of the CPC through phospho-histone marks (nucleation) concentrates the CPC on chromatin until it reaches a critical concentration that induces phase separation on inner centromeric chromatin (Fig.2-4G).

Phase separation of the CPC at the inner centromere has important implications for understanding CPC-dependent mitotic signaling and centromeric cohesion protection that can be explored in further studies. Components of the inner centromere preferentially partition to the ISB condensate, suggesting that the phase separation by the CPC determines the composition of the inner centromere and gives the inner centromere membrane-less organelle like properties that may underlie its key functions in the inner centromere such as cohesion protection (Fig.2-4G). Phase separation by the CPC provides a mechanism for the local enrichment of the Aurora-B kinase at the inner centromere and thus may affect kinase activation kinetics and the gradients of kinase activity emanating from the inner centromere. In addition, the CPC localizes to merotellically-attached kinetochores (Knowlton et al., 2006) where both centromeric chromatin and microtubules are in close proximity. We have shown that both microtubules and chromatin induced phase separation suggesting that phase separation at merotelic attachments drives the prevention or correction of improper kinetochore-microtubule attachments.

Acknowledgements:

The authors thank Dan Foltz and Jan Ellenberg for reagents and Dan Burke for helpful discussions. The work was funded by NIH R24OD023697 and GM118798.

Author Contributions:

PT developed and performed the overall experimental plan with guidance from PTS.

PT analyzed the data under the guidance of PTS. PT and PTS wrote the manuscript.

Figure legends:

Figure 2-1: The centromere-targeting region of the CPC phase separates *in vitro* under physiological conditions. (A) Schematic of the CPC showing various domains in the CPC subunits, where DD is dimerization domain. Red dotted lines indicate interactions between subunits. Orange dotted box indicates the INCENP¹⁻⁵⁸-Survivin-Borealin (ISB) region used for biochemical analysis in this study. (B) DIC micrographs of the ISB coacervates under indicated conditions. (C) Turbidity generated by the phase separation of the ISB complex under indicated conditions. (D) The phase-separated droplets of the GFP-ISB complex contain fluorescence. (E) Time-lapse images demonstration the fusion of ISB coacervates. (F, G, H) FRAP analysis of GFP-ISB coacervates. GFP- INCENP¹⁻⁵⁸ was photo bleached in the ISB coacervates and recovery of florescence was monitored (white dotted box indicates the bleached area). (Top) Pseudo-colored kymograph of the florescent intensity at the orange dotted line (shown in the bottom) of the FRAP experiment. Color corresponds to the florescent intensity as shown on the top right. (Bottom) Time-lapse images from the FRAP experiment (H) Graph of florescence recovery after photo bleaching over time (upon complete coacervate bleaching as shown in G) showing mean and SEM at each time point (n=14). Green line indicates curve fitted with one phase association kinetics equation. Mobile fraction is 50.86% with 95% confidence interval ranging from 48.89% to 52.82%. T1/2 is 99.71 sec with 95% confidence interval ranging from 90.13 to 111.6 sec. (I) Phase diagram of ISB phase separation as a function of NaCl and ISB concentration. Red dotted line indicates

conditions with physiological ionic strength. Blue (homogenous phase) and Red (droplet phase) filled circles show the actual conditions sampled in the experiment. Brown shaded region indicates the cytoplasmic CPC concentration and green shaded region indicates centromeric CPC concentration. Scale bar is 5 μ m.

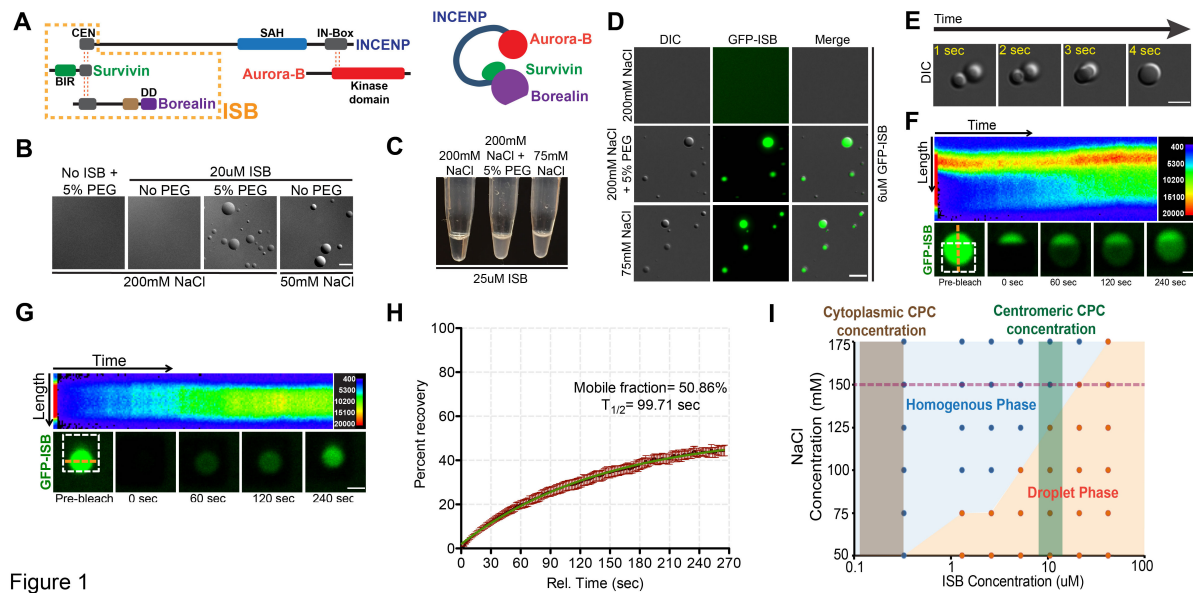


Figure 1

Figure 2-2: Inner centromere components are both specifically concentrated in ISB coacervates and can induce ISB phase separation. A-H ISB coacervates were mixed with the indicated fluorescent inner centromere constituents and images for enrichment. Representative micrograph and graph for respective partition coefficients showing enrichment of (A) alexa553-HP1 α (n=171), (B) alexa553-xAurora-B/INCENP⁷⁹⁰⁻⁸⁵⁶ (n=200), (C) 2X α -satellite DNA-Cy3 (n=193), (D) 2X α -satellite RNA-Cy3 and (E) GFP (n=133) and (F) rhodamine- α/β -tubulin dimer (n=111) in ISB phase. (G) Representative micrographs showing enrichment of FITC-histone H3 peptide or FITC-histone H3pT3 peptide in ISB-WT or ISB-H80A mutant coacervates. Control micrographs for FITC peptide alone and ISB-WT or ISB-H80A mutant coacervates alone are shown in Extended Data figure 3D. (H) Graph showing partition coefficient of the H3 and H3pT3 peptide in ISB-WT or ISB-H80A mutant coacervates from F (at least 63 coacervates were analyzed per condition). For statistical analysis two tailed Mann-Whitney test was applied, *** indicates $P < 0.0001$ and * indicates $P = 0.0386$. I-K, Inner centromere proximal components drive ISB phase separation (I) Micrographs showing phase separation of 12 μ M ISB-WT induced by 60ng/ul 2X α -satellite DNA in presence of buffer containing 165mM NaCl. (J) Micrographs showing phase separation of 8 μ M ISB-WT induced by 60ng/ul H3.3 poly-nucleosomes in presence of buffer containing 150mM NaCl. (K) Micrographs showing phase separation of GFP-ISB induced on bundles of rhodamine labeled microtubules. Scale bar is 5 μ m except for K where it is 3 μ m.

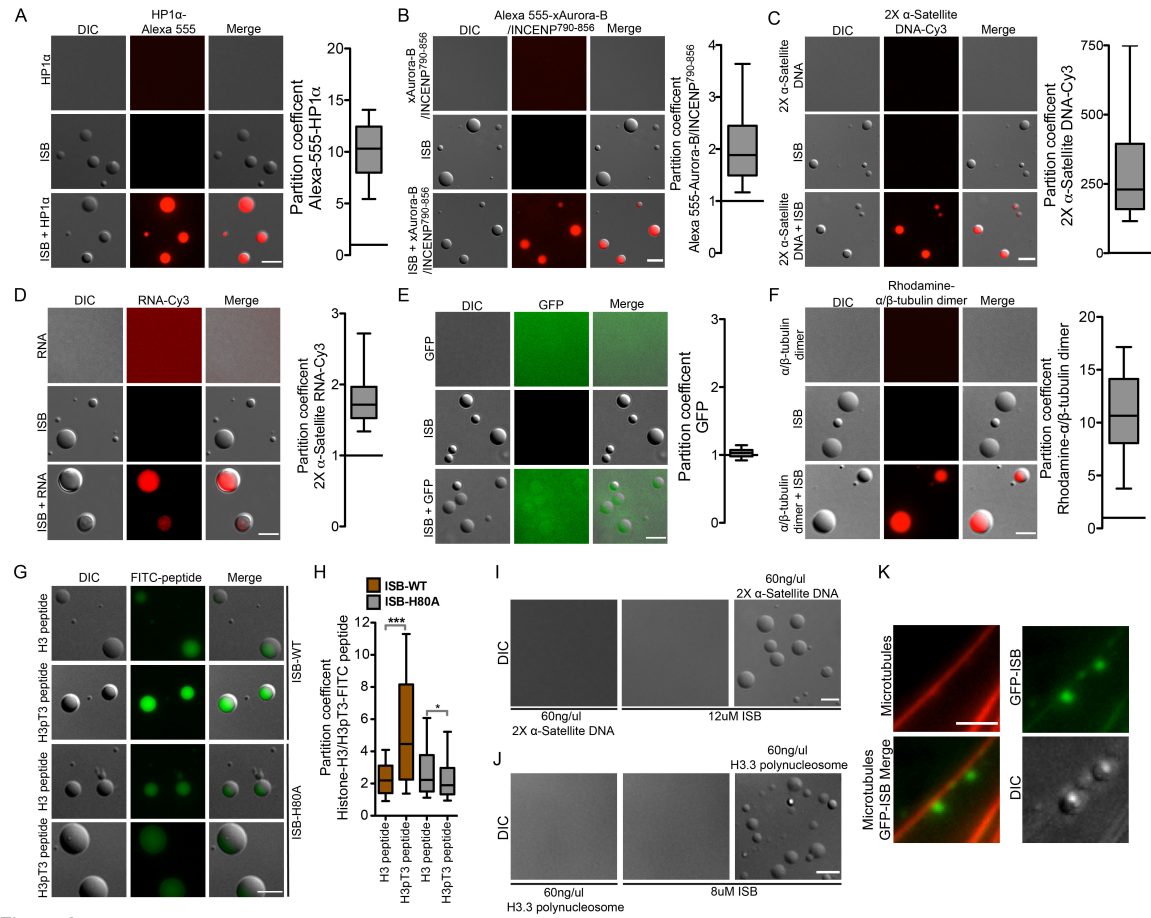


Figure 2

Figure 2-3: The CPC exists in a phase-separated state in inner centromeres. (A) Schematic of the experimental setup for B and C. (B) Images showing localization of CENP-T (red) and Aurora-B (grey) in HeLa-TReX cells in control treatment (no treatment), upon treatment with 90mM NH₄OAc or 2min after NH₄OAc washout. (C) Graph showing normalized fluorescent intensity of Aurora-B/CENP-T under indicated conditions from B. All the inner centromeres from at least 10 cells were analyzed per condition. For statistical analysis One-Way ANOVA followed by Dunn's multiple comparison test was applied. (D) Schematic of the experimental setup for E and F. (E) Images of chromosome spread showing DAPI (blue) and INCENP-mCherry (red) in indicated conditions, white boxes in the images point to the regions that are shown in the magnified insets on the right of the image. (F) Graph showing normalized fluorescent intensity of INCENP-mCherry at the inner centromeres under indicated conditions from E. At least 318 chromosomes were analyzed per condition. For statistical analysis Mann-Whitney test was applied (ns indicated P=0.2873). (G) Cartoon showing distinct regions of the WT and mutant Borealin used in H-L. (H) Graph showing existence of ISB^{WT} or ISB^{Δ139-160} in either droplet phase or homogenous phase under conditions of increasing ISB concentration in buffer containing 150mM NaCl. (I) Graph showing existence of 30uM ISB^{WT}, ISB^{Δ163-180} or ISB^{Δ139-160}, in either droplet phase or homogenous phase under conditions of increasing NaCl concentration. (J) Micrographs showing existence of coacervates at indicated condition in presence or absence of 2X α-satellite DNA. (K) Schematic of the experimental setup for L and M used to analyze first mitosis after knockdown of endogenous Borealin with 3'UTR siRNA and rescue

with either LAP-Borealin^{WT} or LAP-Borealin^{Δ139-160}. (L) Micrographs showing staining of Aurora-B and CENP-T cells rescued with either LAP-Borealin^{WT} or LAP-Borealin^{Δ139-160}. (M) Graph showing normalized intensity of Aurora-B/CENP-T or CENP-T from experiment shown in L. All inner centromeres from at least 11 cells per condition were analyzed. For statistical analysis two-tailed Mann-Whitney test was applied. For the whole figure *** indicates P<0.0001 and ns indicates P>0.05. Scale bar is 5um.

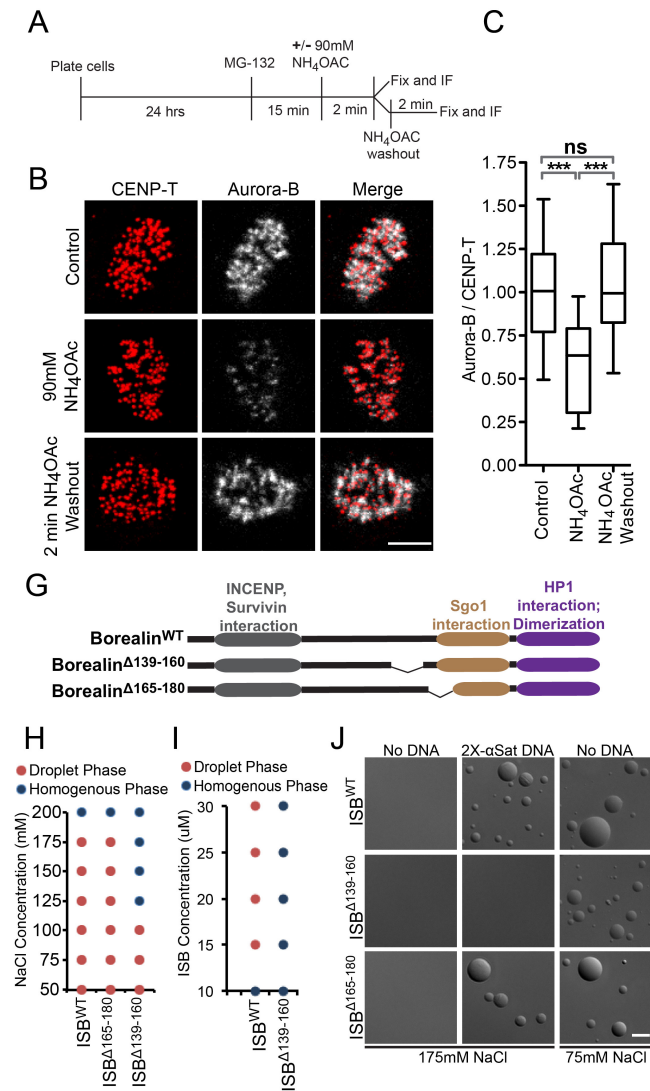


Figure 3

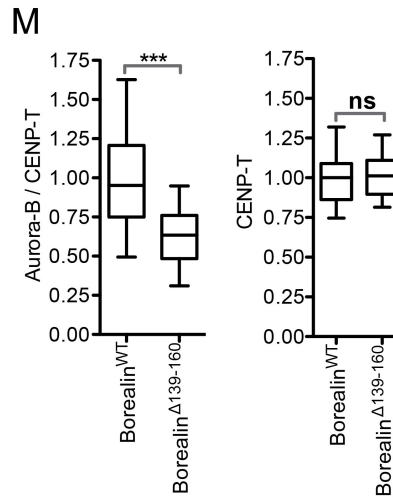
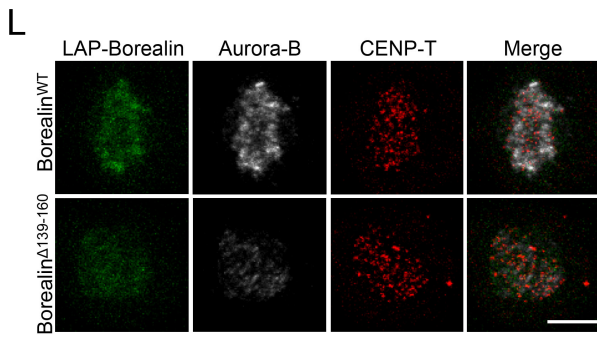
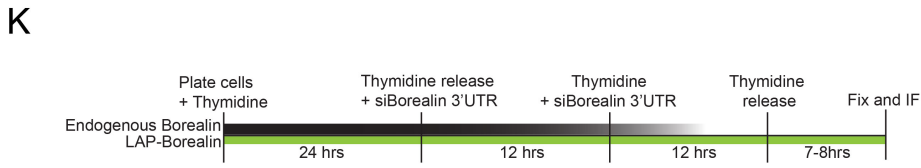
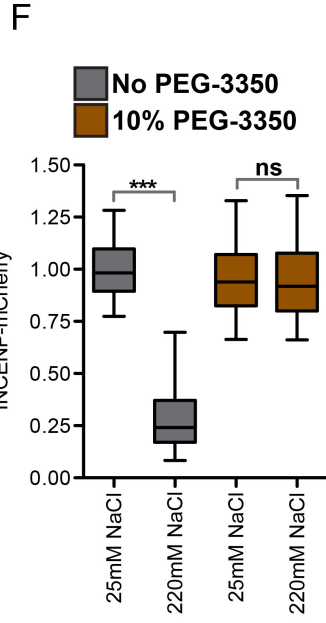
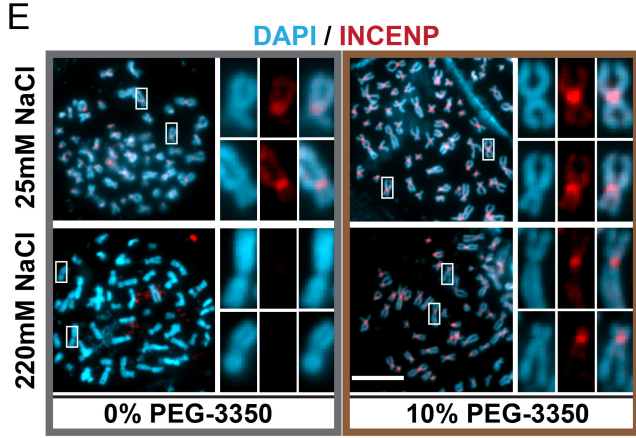
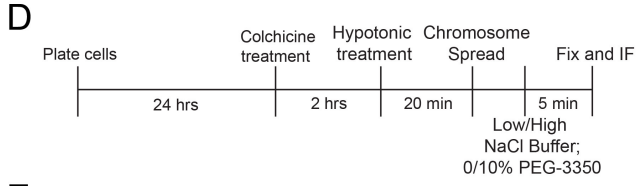


Figure 2-4: The phase separation property of the CPC is important for its mitotic functions. (A) Schematic of the experimental setup for B used to analyze duration of taxol induced mitotic arrest in first mitosis replacement of endogenous Borealin with either LAP-Borealin^{WT} or LAP-Borealin^{Δ139-160}. (B) Representative frames from the time-lapse images of cells undergoing mitosis in presence of 100nM paclitaxel. “NEBD” refers to the time of nuclear envelope break down and “exit” refers to the time of mitotic exit. Duration from NEBD to exit/death is defined as duration of mitotic arrest. (C) Graph showing duration of mitotic arrest in cells rescued with LAP-Borealin^{WT} or LAP-Borealin^{Δ139-160} (at least 220 cells were analyzed from 3 independent experiment per condition). For statistical analysis two tailed students T-test with Welch’s correction was applied. *** Indicates P<0.0001. (D) Schematic of the experimental setup for E used to analyze mitotic progression in first mitosis after knockdown of endogenous Borealin and rescue with either LAP-Borealin^{WT} or LAP-Borealin^{Δ139-160}. (E) Representative frames from the time-lapse images of cells rescued with either LAP-Borealin^{WT} or LAP-Borealin^{Δ139-160} undergoing mitosis. Yellow arrow points to the lagging chromosomes in anaphase. (F) Graph showing percent of anaphases with lagging chromosomes in cells rescued with LAP-Borealin^{WT} or LAP-Borealin^{Δ139-160} (at least 86 cells were analyzed precondition and 3 independent experiment were conducted). For statistical analysis two-tailed unpaired T-test was applied. *** Indicates P=0.0002. For B and D SiR-DNA was used to visualize DNA. Scale bar is 5um. Cumulative frequency graph of duration of taxol arrest and duration of various phases of mitosis is shown in Extended Data figure 3-5. (G) Model for the localization of the CPC to the inner

centromere driven by initial nucleation by phospho-histone marks followed by phase separation of the CPC. Furthermore, some components are enriched in the CPC phase (blue stars), while other are excluded (Purple 8-pointed star).

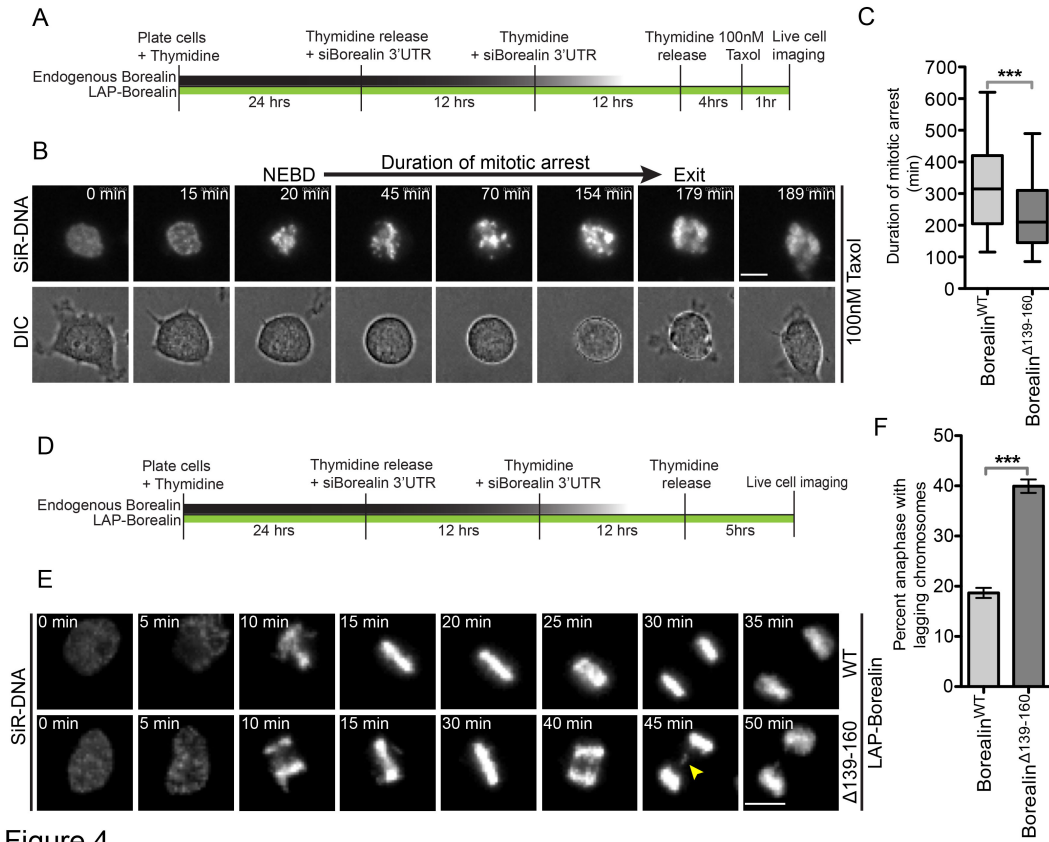
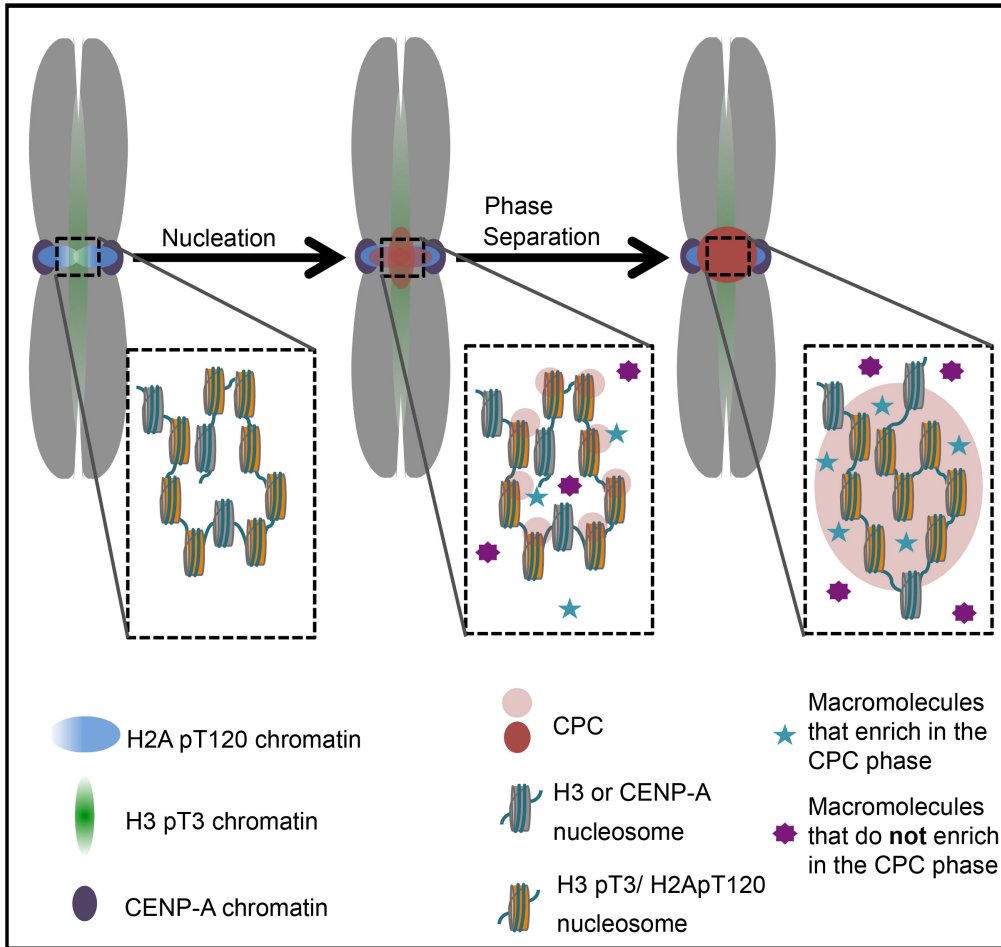
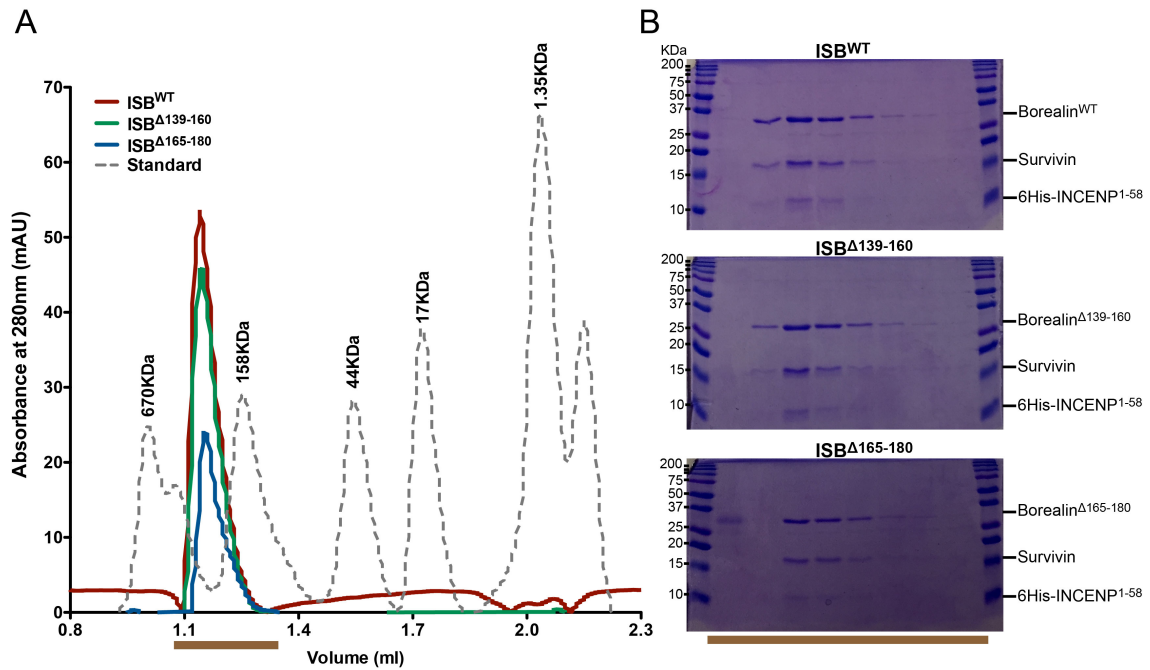


Figure 4

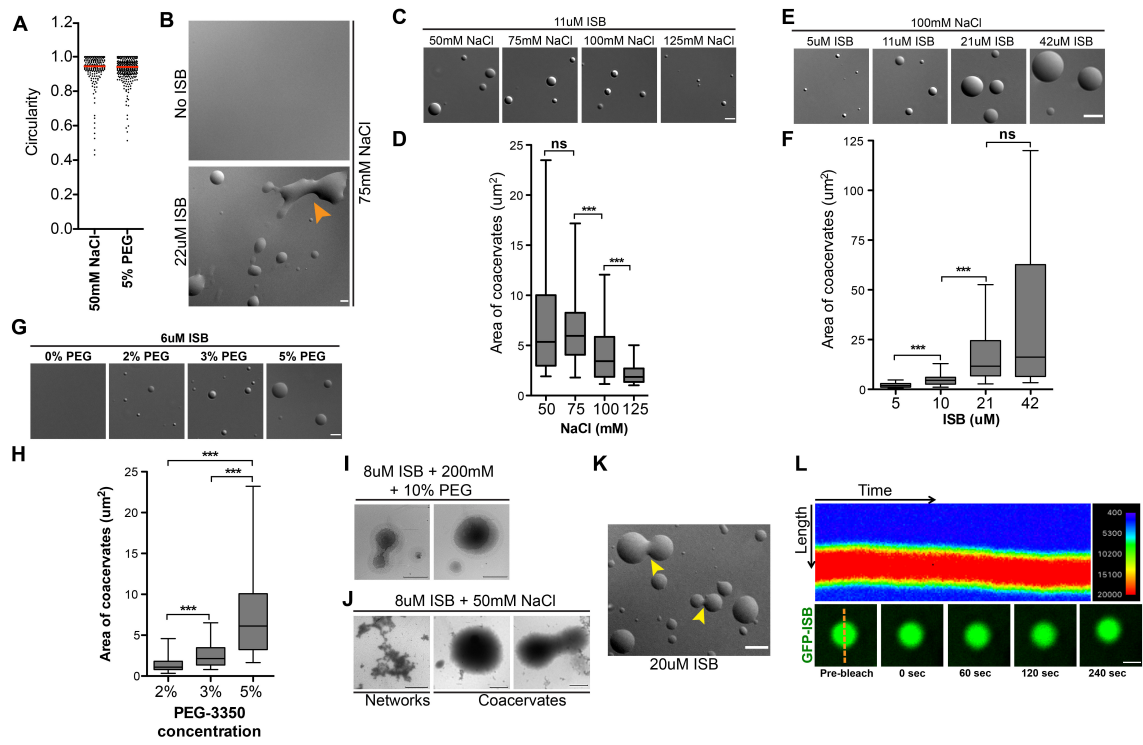
G



Extended Data figure 2-1: ISB-WT and mutant protein complexes. (A) Superdex-200 gel filtration profile of ISB^{WT} (red), ISB^{Δ139-160} (green), and ISB^{Δ163-180} (blue) broken grey line shows the profile of the FPLC standard. Brown bar indicated the fractions from gel filtration run on SDS-PAGE and coomassie stained (B).

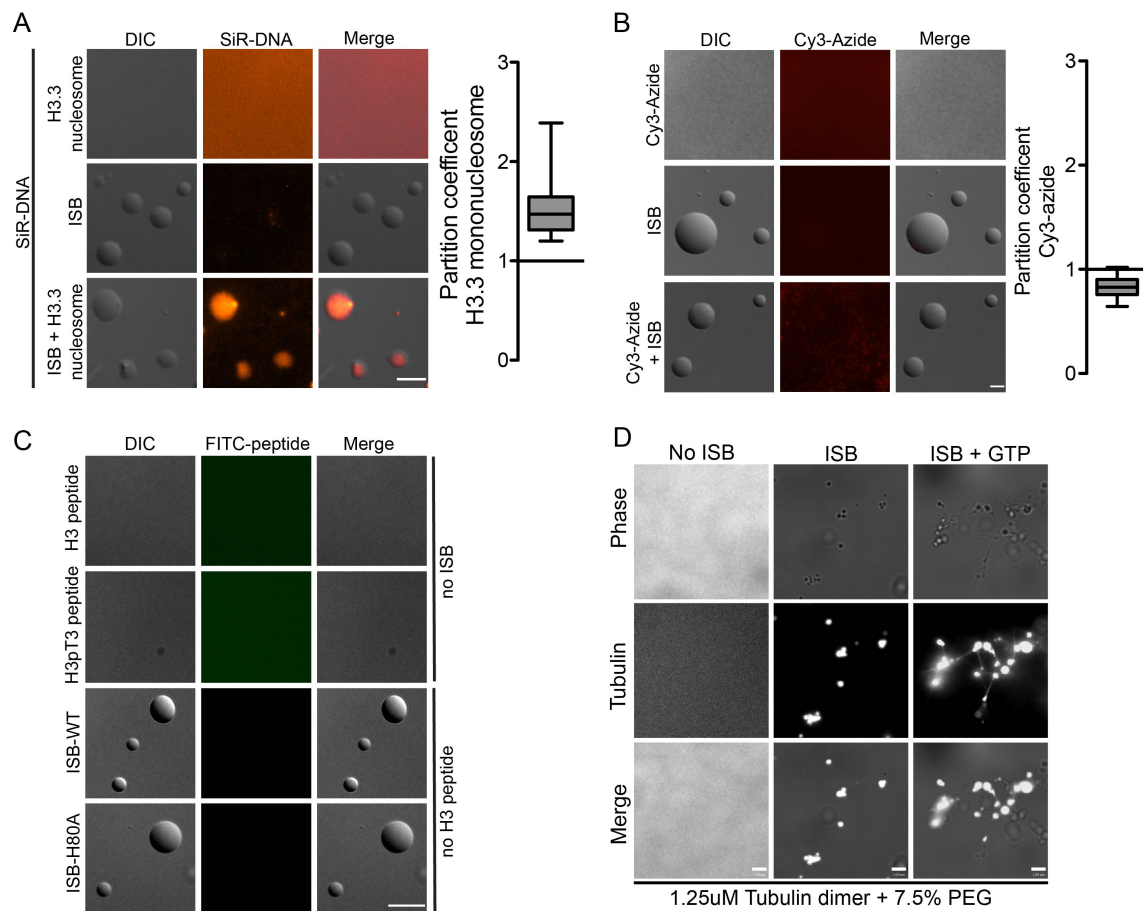


Extended Data figure 2-2: Phase separation properties of the CPC centromere-targeting region. (A) Circularity of the GFP-ISB coacervates from experiment shown in figure 2-1D. (B) Surface wetting and shearing of the ISB coacervates (orange arrow) under the indicated conditions. (C) Micrographs showing ISB coacervates under increasing NaCl concentration. (D) Graph showing area of the coacervates from C under increasing NaCl concentration. (E) Micrographs showing ISB coacervates under increasing ISB concentration. (F) Graph showing area of the coacervates from E under increasing concentration of the ISB. (G) Micrographs of ISB coacervates formed in presence of increasing concentration of PEG-3350. (H) Graph showing area of coacervates under increasing concentration of PEG-3350. For statistical analysis in D, F, and H One-Way ANOVA was applied followed by Dunn's multiple comparison test. (I and J) Electron micrographs of ISB coacervates formed under indicated conditions showing highly circular coacervates and coacervates arrest mid-fusion due to gelation. A few apparently aggregated networks could also be observed under condition of low salt and are shown as contrast to spherical coacervates. (K) DIC micrographs of 20uM ISB showing coacervates arrest mid-fusion (yellow arrow). (L) Control from GFP-ISB FRAP analysis (Fig.2-1F-H) showing no significant bleaching of GFP-ISB coacervates over the duration of imaging. Scale bar 5um except for I and J were it is 1um and for the middle panel in J it is 2um.



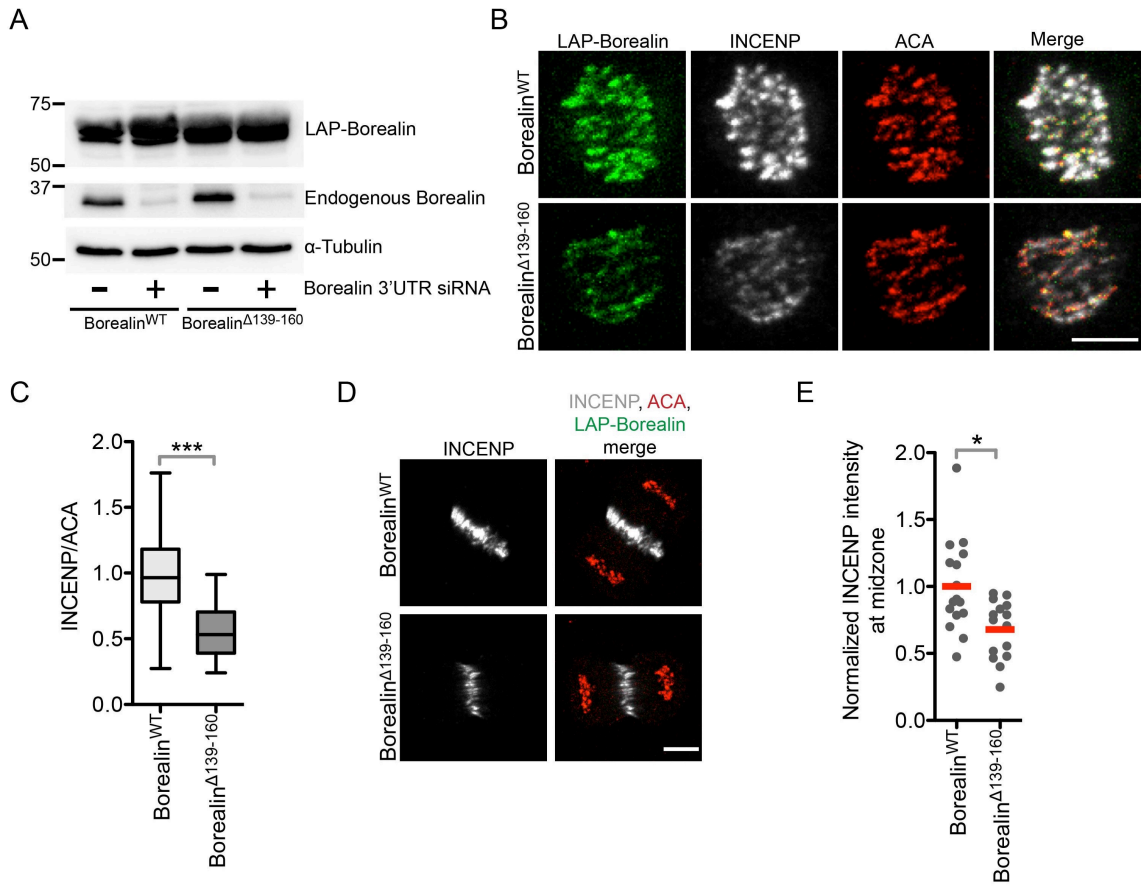
Supplement Figure. 2

Extended Data figure 2-3: Enrichment of macromolecules in ISB phase and nucleation of microtubules from the ISB coacervates. Representative images and graph showing partition coefficient of (A) Histone H3.3 mono-nucleosome, (B) Cy3-azide and (C) GFP-xMad2 in ISB phase. (D) Control images for experiment show in Figure 2-2 G, H. (E) Images showing nucleation of microtubules upon enrichment of Cy3- α/β -tubulin dimers in ISB coacervates. Nucleation was observed from ISB coacervates at 1.25 μ M α/β -tubulin dimers concentration in presence of GTP and not seen in the absence of GTP. Scale bar 5 μ m.

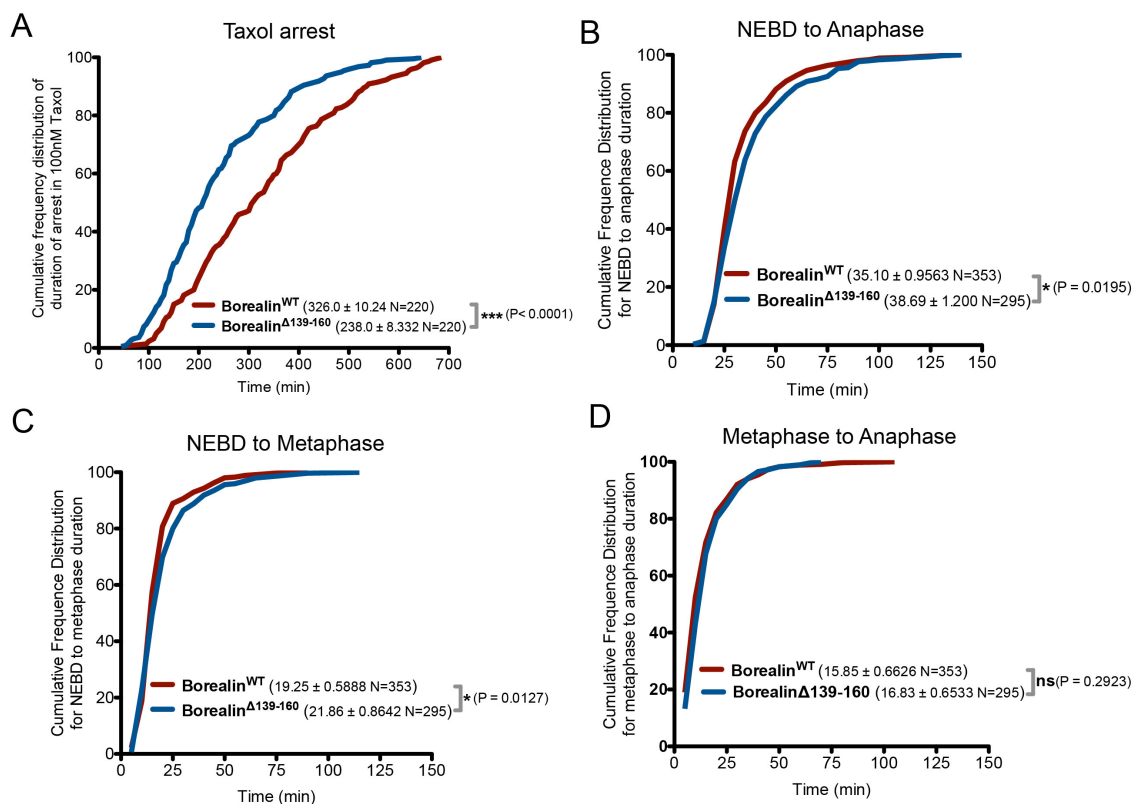


Supplement figure. 3

Extended Data figure 2-5: Phase-separation property of the CPC is important for its inner centromeres localization. (A) Western blots showing endogenous Borealin, LAP-Borealin and Tubulin levels. Cells were treated as indicated in Fig.2-3K and lysates for western blotting were collected 8 hours after second thymidine release. (B) Micrographs showing staining of INCENP and ACA in cells rescued with either LAP-Borealin^{WT} or LAP-Borealin^{Δ139-160}. Cells were treated as shown in Fig.2-3K. (C) Graph showing normalized intensity of INCENP/ACA from experiment shown in B. All inner centromeres from at least 10 cells per condition were analyzed. (D) Micrographs showing staining of INCENP and ACA in anaphase cells rescued with either LAP-Borealin^{WT} or LAP-Borealin^{Δ139-160}. Cells were treated as shown in Fig.2-3K. (E) Graph showing normalized intensity of INCENP at the midzones from experiment shown in D. Midzones from at least 15 cells per condition were analyzed. In C and E, for statistical analysis two-tailed Mann-Whitney test was applied. *** Indicates P<0.0001, * P=0.0108. Scale bar is 5μm.



Extended Data figure 2-6: Phase separation by the CPC is important for maintenance of taxol induced mitotic arrest but only marginally affects the time to align chromosomes. (A) Cumulative frequency plot of the duration of mitotic arrest in presence of 100nM paclitaxel from figure 2-4 A-C. For statistical analysis two-tailed unpaired t-test was applied. Cumulative frequency plot of the duration of Nuclear envelop break down (NEBD) to anaphase (B), NEBD to metaphase (C), and metaphase to anaphase (D); data from experiment shown in figure 2-4 D-F. For statistical analysis two-tailed t-test with Welch's correction was applied. Mean \pm SEM is shown in parenthesis with "n" indicating the sample size.



Materials and methods:

Protein purification:

BL21-pLysS (DE3) cells were transformed with a tri-cistronic pET28a vector containing 6XHis-INCENP¹⁻⁵⁸, Survivin, Borealin (WT, Δ 139-169, or Δ 163-180) sequence; for GFP-ISB, GFP was cloned between 6His and INCENP¹⁻⁵⁸ to yield 6His-GFP-ISB construct. Cells were then grown in presence of 30mg/ml Kanamycin to OD 0.8 and protein expression was induced with 0.45 M IPTG for 16-18hrs at 18°C. The media was also supplemented with 60mg/L ZnCl₂ and 0.2% glucose. Cells were then pelleted and lysed in buffer containing 500mM NaCl; 50mM Tris pH7.5, 0.5mM TCEP, 5% glycerol, 5mM Imidazole and protease inhibitor cocktail (Roche) using EmulsiFlex-C3 Homogenizer. The lysate was then cleared with centrifugation and incubated with Ni-NTA beads (Qiagen) for 4 hours at 4°C. After washing Ni-NTA beads (Qiagen) with 200ml buffer containing 500mM NaCl, 50mM Tris pH7.5, 0.5mM TCEP, 25mM Imidazole, and 5% glycerol. The protein was eluted with buffer containing 500mM NaCl, 50mM Tris pH7.5, 0.5mM TCEP, 250mM Imidazole, and 5% glycerol. The eluted protein was then gel filtered on Superdex-200 column 10/300 GL size-exclusion column (GE Life Sciences) in buffer containing 500mM NaCl, 50mM Tris pH7.5, 0.5mM TCEP and 5% glycerol. The desired fractions were collected and concentrated with Amicon Ultra-4 Centrifugal Filter Unit with 3KDa cutoff. 6His-HP1 α (Larson et al., 2017) and xAurora-B/INCENP⁷⁹⁰⁻⁸⁵⁶(Rosasco-Nitcher et al., 2008) was expressed and purified by following the previously published purification scheme. GFP was expressed from a pET28a-GFP vector in

BL21-pLysS (DE3) cells. Cells were lysed in PBS containing 0.5mM TCEP and 5mM Imidazole and purified using Ni-NTA beads (Qiagen). After washing with PBS supplemented with 0.5mM TCEP and 25mM Imidazole, GFP was eluted in PBS supplemented with 0.5mM TCEP and 250mM Imidazole. GFP was then dialyzed in PBS supplemented with 0.5mM TCEP. GFP-xMad2 was generated by cloning the gene encoding 6His-eGFP onto the N-terminus of Xenopus Mad2 in a Pet28 vector and the protein purified from E. coli on Ni²⁺-Agarose.

Phase separation assay:

Phase separation was induced by diluting the indicated amount of ISB in the low salt buffer (50mM Tris pH7.5, 1mM DTT) to achieve the indicated final concentration of protein and NaCl. To induce phase separation in presence of a molecular crowding agent the ISB at the indicated concentration was incubated in the buffer containing 5% PEG-3350, 50mM Tris pH7.5, 1mM DTT and indicated amount of NaCl. Indicated concentration of 2X- α -satellite DNA, histone H3.3 poly-nucleosome (containing 12 nucleosomes) (Active motif), 2X- α -satellite RNA, or paclitaxel stabilized microtubules was incubated with 8 μ M ISB in buffer containing 150mM NaCl, 50mM Tris pH7.5 and 1mM DTT. Phase separation was observed by adding a drop of the reaction on the coverslip and imaged on 63X objective in Zeiss Observer Z1 wide-field microscope by fluorescence and DIC imaging or on JEOL 1230 for transmission electron microscopy. For time lapse imaging of ISB droplet fusion, ISB droplets were formed in indicated condition and immediately images under DIC every second.

Partitioning of constituents into ISB coacervates:

ISB coacervates were made by incubating 3-6 μ M ISB in buffer containing 150mM NaCl, 50mM Tris pH7.5, 1mM DTT and 5% PEG-3350. 400 μ M (unless otherwise stated) of the indicated agent molecules were incubated with ISB coacervates for 2mins at room temperature and imaged immediately. For calculating partition coefficients with histone peptides the ISB coacervates were generated by incubating 20 μ M of ISB in buffer containing 150mM NaCl, 50mM Tris pH7.5, 1mM DTT. Florescence signal was calculated by using Volocity (V6.3, PerkinElmer). Partition coefficient was calculated by dividing florescence signal per unit area inside the coacervates by the florescence signal per unit area outside the coacervates after subtraction of background florescence. Background florescence was calculated by imaging the coacervates in absence of fluorescent agent molecules.

Unmodified histone H3 or H3 pT3 synthetic peptides (ARTKQTARKSTGGKAPRKQLY-fluorescein (note the additional tyrosine, to allow concentration measurement at 280 nm, and C-terminal fluorescein) (GenScript) were previously described. 400nM rhodamine labeled α/β -Tubulin dimers (Cytoskeleton Inc.), 400nM HP1 α -Alexa555, 100nM xAurora-B/xINCENP⁷⁹⁰⁻⁸⁵⁶-Alexa555, 400nM Cy3-2X- α -satellite DNA, 400nM 2X- α -satellite RNA, 400nM Cy3-azide, 400nM GFP, 400nM GFP-xMad2 were incubated with phase separated ISB coacervates. 2X- α -satellite RNA was made by *in vitro* transcription of 2X- α -satellite-DNA PCR product, which was amplified from vector containing 2X- α -satellite-DNA sequence (a kind gift from Dan Foltz) using primer containing the T7 transcription initiation sequence (Fw:

TAATACGACTCACTATAGGGAGAAAGTGGATATACAGACCCC; Rv:
TCCACTTGCAGACTTTACAAACAG) . The *in vitro* transcription was carried out by using Megascript T7 Transcription Kit (Thermo Fisher) spiked with Cy3-UTP, RNA was then treated with DNAase and isolated by using RNA Clean and Concentrator Kit (Zymo Research). Cy3-2X- α -satellite-DNA was made by PCR, spiked with Cy3-dCTP; using primers listed above and purified using gel extraction. HP1 α -Alexa555 and xAurora-B/xINCENP⁷⁹⁰⁻⁸⁵⁶-Alexa555 was made by purifying HP1 α and xAurora-B/xINCENP⁷⁹⁰⁻⁸⁵⁶ as previously described (REF) and labeling with Mix-n-Stain™ CF-555 labeling kit (Sigma-Aldrich) followed by dialysis to remove unreacted dye molecules.

Microtubule preparation and microtubule dependent phase separation:

Paclitaxel-stabilized microtubules were prepared by polymerizing bovine brain tubulin dimers spiked with rhodamine labeled α/β -Tubulin dimers in BRB80 (80mM PIPES, 1mM MgCl₂, 1mM EGTA, pH 6.8 with NaOH), 1mM DTT and 1mM GTP with increasing concentration of paclitaxel, paclitaxel stabilized MTs were then separated from the un-polymerized tubulin dimers by centrifuging through a 40% glycerol cushion at 137, 000 x g. 6 μ M GFP-ISB was incubated with 1 μ M paclitaxel stabilized rhodamine-MTs in buffer containing 50mM Tris pH7.5, 150mM NaCl, 1mM DTT and 20 μ M paclitaxel for 15min at room temperature. A drop of the reaction was squished between coverslips and images at 63X on Zeiss Observer Z1 wide-field microscope.

Cell culture and stable cell line generation:

HeLa T-REx cell (ThermoFisher Scientific) and HeLa Kyoto cells with endogenously tagged INCENP-mCherry and Aurora-B-GFP (a gift from Jan Ellenberg)(Neumann et al., 2010) were grown in Dulbecco's modified Eagle's medium (DMEM, Invitrogen) supplemented with 10% fetal bovine serum (Gibco) in presence of 5% CO₂ in a humidified incubator at 37°C.

In order to generate HeLa T-REx cells stably expressing LAP-Borealin^{WT} and LAP-Borealin^{Δ139-160}, the Borealin^{WT} transgene fragments were sub-cloned in to pCDNA5/FRT vector (Invitrogen) containing N-terminal LAP (GFP and S-peptide) tag sequence. LAP- Borealin^{Δ139-160} was generated by deleting region coding for Borealin 139-160aa by site directed mutagenesis. The resulting LAP-Borealin^{WT} and LAP-Borealin^{Δ139-160} plasmids were co-transfected with the pOG44 plasmid (Invitrogen) using Lipofectamine 2000 (Invitrogen). Cells were subjected to selection for 15 days in presence of 200ug/ml Hygromycin B (Invitrogen). To get cells with homogenous expression of the transgenes, selected colonies were pooled and FACS sorted for GFP (for LAP-Borealin transgenes) expression.

Plasmid and siRNA transfection:

Plasmid transfection was done using Lipofectamine 2000 (Invitrogen) according to manufacture's protocol.

For knockdown and replacement experiments Borealin 3'UTR siRNA (AGGUAGAGCUGUCUGUUCAdTdT)(Klein et al., 2006) was transfected by using RNAiMAX (Invitrogen) according to manufacturers protocol. To analyze mitotic

phenotypes in the first mitosis after complementation Borealin stable cell lines were plated in presence of 2mM thymidine, 24hrs after plating cells were release in fresh media and siRNA was transfected. Another round of siRNA transfection was done after 12hrs of the 1st siRNA treatment and 2mM Thymidine was added. After 11-44 hours of 2nd siRNA treatment cells were released from thymidine in fresh media. For, immunofluorescence analysis cells were fixed after 8-10 hours and for live cell imaging cell were treated as indicated.

Live cell imaging:

For live cell imaging, cells were plated in the 4 well imaging chamber (Labtek) in presence 2mM thymidine followed by siRNA treatment. 3-4 hours after 2nd thymidine release 200nM SiR-DNA (Cytoskeleton Inc.) dye was added to the cells. 1.5 hours post SiR-DNA treatment time-lapse images were taken 16hrs at 5min interval on a Zeiss Observer-Z1 in an humidified environmental chamber maintained at 37°C in presence of 5%CO₂. Movies were analyzed using Volocity software (V6.3, PerkinElmer).

Fluorescence recovery after photo bleaching (FRAP):

GFP-ISB coacervates were generated by incubating 6uM GFP-ISB in buffer containing 150mM NaCl, 50mM Tris pH7.5, 1mM DTT and 5% PEG-3350 supplemented with oxygen scavenging solution containing 40 mM Glucose, 130 mg/ml Glucose oxidase, and 24 mg/ml Catalase. GFP-ISB coacervates were then placed in a flow chamber constructed by placing two strips of double-sided tape on

a coverslip and placing a second coverslip on top of it to form a groove. FRAP experiment was performed on a Zeiss 880 confocal microscope by acquiring 2 time points before bleaching and then bleaching with 20 cycles of 488 laser at 100% power and imaging every 1.5 sec for 265 sec. Fluorescence intensities were measured using Volocity (V6.3, PerkinElmer). Recovered intensity corrected for photo bleaching that occurred due to imaging was termed as Percent-corrected recovered intensity (Nt) and was calculated by using following equation at each time point.

$$Nt = \left\{ \frac{[(Ft - F0_{postbleach})/Ft_{unbleached}]}{[F0_{prebleach}/F0_{unbleached}]} \right\} * 100$$

Where,

Nt = Percent-corrected recovered intensity.

Ft = Fluorescence intensity at time (t).

$F0_{postbleach}$ = Fluorescence intensity just after bleaching.

$Ft_{unbleached}$ = Fluorescence intensity at time (t) of unbleached coacervate.

$F0_{prebleach}$ = Fluorescence intensity before bleaching.

$F0_{unbleached}$ = Fluorescence intensity of unbleached coacervate at the same time as

$F0_{prebleach}$.

Graph of Nt vs time was fitted with one-phase association equation by least square fitting method using Prism software (GraphPad) (shown in Green in Fig. 1H).

Mobile fraction and $T_{1/2}$ with 95% confidence interval was extracted from this curve using Prism software (GraphPad).

Mitotic chromosome spreads:

100ng/ml KaryoMAX Colcemid (Gibco) was added to HeLa Kyoto cells expressing endogenously tagged INCENP-mCherry and Aurora-B-eGFP for 1 hour. Mitotic cells were collected by mitotic shake off spun down and resuspended in a hypotonic buffer (25mM KCl, 0.27% Na-Citrate in distilled water) for 15min at 37°C. Swollen cells were then broken open and chromosomes were spread on coverslips using a Cytospin 4 (ThermoShandon). The coverslip was then transferred to the indicated buffer (20mM HEPES, 5mM MgCl₂, 25mM NaCl or 220mM NaCl, 0 or 10% PEG-3350, 1mM DTT, 20mM β-glycerophosphate, 1X protease inhibitor cocktail (Roche)) for 5 min and washed once more with the same buffer. The chromosomes were then fixed with 2% PFA in PBS for 15 min. The chromosomes were then stained with DAPI and mounted on a slide for imaging. Chromosomes were imaged at 63X on a Zeiss Observer-Z1. The intensity of INCENP-mCherry and DAPI were quantitated at the inner centromere by using Volocity (V6.3, PerkinElmer). These values were plotted using Prism software (GraphPad) and indicated statistical tests where applied.

Immunofluorescence microscopy:

Cells were seeded on poly-L-Lysine (Sigma) coated coverslips and treated as indicated. Cells were then fixed with 4% paraformaldehyde in PHEM buffer (25mM

HEPES, 60mM Pipes, 10mM EGTA, and 4mM MgCl₂, pH 6.9) containing 0.5% Triton-X 100 for 20 minutes at room temperature. After 3X Tris buffered saline (TBS) wash, cells were blocked for 1hour with 3% BSA in TBS-T at room temperature. Cells were then incubated with primary antibodies in 3% BSA in TBS-T (TBS + 0.1% Tween20) for 1 hour at room temperature. Cells were then washed 3X with TBS-T (10 min each), and incubated with fluorescent secondary antibodies (1:2000) (Jackson Immuno-Research). Cells were then washed 4 times with TBS-T and stained with 0.5µg/ml DAPI for 5 minutes before mounting on the slides using ProlongGold antifade (Invitrogen) and sealed with nail polish. Image acquisition was performed as described previously(Banerjee et al., 2014). Image processing and analysis was done using Volocity (V6.3, PerkinElmer). To quantify fluorescence levels at centromeres, we used an intensity thresholding algorithm to mark all centromeres on the basis of CENP-T or ACA intensity. To eliminate changes in florescence intensity due to differences in centromere size, the total fluorescence intensity was divided by the total volume of the selected area. Background intensity was subtracted and the intensity/volume of the desired channel were normalized against the corresponding CENP-T or ACA intensity/volume. The final normalized intensity values were graphed and analyzed using Prism software (GraphPad) and indicated statistical tests were applied.

Chapter 3

The binding of Borealin to microtubules underlies a tension independent kinetochore-microtubule error correction pathway.

This chapter is from the paper titled: “The binding of Borealin to microtubules underlies a tension independent kinetochore-microtubule error correction pathway”

Prasad Trivedi, Maxim Godzi, Anatoly V. Zaytsev, Fazly I. Ataulakhanov, Ekaterina L. Grishchuk, P. Todd Stukenberg. (Under revision in Nature Communications)

Abstract:

Proper chromosome segregation depends upon regulated kinetochore phosphorylation by the Chromosome Passenger Complex (CPC). Current models suggest the activity of the CPC decreases in response to the inter-kinetochore stretch that accompanies the formation of bi-oriented microtubule attachments. Recent electron microscopy data argue that microtubule bundles initially lie in close proximity to inner centromeres and become depleted by metaphase. Here we find these microtubules control kinetochore phosphorylation by the CPC in a tension independent manner via a novel microtubule-binding site on the Borealin subunit. Disruption of Borealin-microtubule interactions generates reduced phosphorylation of prometaphase kinetochores, improper kinetochore-microtubule attachments and weakened spindle checkpoint signals. Experimental and modeling evidence suggests that kinetochore phosphorylation is greatly stimulated when the CPC binds microtubules that lie near the inner centromere, even if the kinetochores have obtained high inter-kinetochore stretch. We propose the CPC senses its local environment through microtubule structures to control phosphorylation of kinetochores.

Introduction

Human kinetochores bind ~20 microtubules and faithful chromosome segregation requires that the majority of the microtubules attached to one sister kinetochore orient towards one spindle pole, while those of its sister orient towards

the opposite pole(McEwen et al., 2001). The inability to obtain this biorientation is the major source of Chromosomal Instability in human tumors(Cimini et al., 2001; Thompson and Compton, 2011). The Chromosome Passenger Complex (CPC) controls biorientation as well as other mitotic events by regulating kinetochore-microtubule interactions(Cimini et al., 2006; Knowlton et al., 2006; Tanaka et al., 2002) recently reviewed in (Etemad et al., 2015; Lampson and Grishchuk, 2017; Trivedi and Stukenberg, 2016) . The CPC is a four-protein complex consisting of chromatin targeting subunits Survivin and Borealin, the scaffold INCENP and a kinase Aurora-B(Carmena et al., 2012b). Bioriented microtubules bound to kinetochores generate a poleward pulling force that increases the distance of kinetochores from the inner centromere (inter-kinetochore stretch)(Maresca and Salmon, 2009). These forces are countered by centromeric chromatin, which is extended (Lawrimore et al., 2015) after kinetochores are aligned at the metaphase plate and also likely in chromosomes that obtain biorientation before alignment(Itoh et al., 2018; Magidson et al., 2011). Many models have suggested that either the inter-kinetochore stretch or the changes to tension in centromeric chromatin underlie the ability of the CPC to control biorientation(Krenn and Musacchio, 2015; Lampson and Grishchuk, 2017), however the tension independent mechanisms are also likely to be involved because some prometaphase kinetochores may also become stretched due to kinetochore localized motor activity on microtubule bundles that lie in close proximity to inner centromeres(Itoh et al., 2018; Magidson et al., 2011).

The fact that Aurora kinases autoactivate when they are concentrated at subcellular loci underlies their ability to initiate signaling events. The majority of the CPC (~75%) is localized to the inner-centromere, which is the chromatin between kinetochores on mitotic chromosomes, during prometaphase and metaphase (Earnshaw and Cooke, 1991; Mahen et al., 2014). The CPC locates the inner-centromere by binding two distinct histone phosphorylation marks that intersect the mitotic chromosome along two orthogonal axes (Trivedi and Stukenberg, 2016; van der Horst and Lens, 2014; Yamagishi et al., 2010). First, the Haspin kinase phosphorylates histone H3 at threonine 3 (H3pT3) and Survivin directly binds the phosphorylated H3pT3 (Du et al., 2012; Kelly et al., 2010; Niedzialkowska et al., 2012; Wang et al., 2010; 2011b; Yamagishi et al., 2010). Since Haspin is recruited by cohesin (Carretero et al., 2013; Zhou et al., 2017), this mark is initially found along a central “long” axis between sister chromatids. A second axis is generated across chromosomes between kinetochores by the Bub1 kinase (Boyarchuk et al., 2007; London et al., 2012; Shepperd et al., 2012; van der Waal et al., 2012; Yamagishi et al., 2012). Specifically, kinetochore localized Bub1 phosphorylates histone H2A on threonine 120 (H2A pT120) (Boyarchuk et al., 2007; Kawashima et al., 2010; Ricke et al., 2012). This indirectly recruits the CPC because the middle domain of Borealin (170-220aa) binds Sgo1 (Fig.3-1A), which directly binds H2A pT120 (Baron et al., 2016; Tsukahara et al., 2010; Williams et al., 2017; Yamagishi et al., 2010).

Despite this prominent inner centromere localization, the CPC phosphorylates kinetochore proteins that are >500nm away, to correct erroneous kinetochore-microtubule interactions and coordinate the spindle assembly

checkpoint (SAC)(Cheeseman et al., 2002; Cimini et al., 2006; DeLuca et al., 2011; Etemad et al., 2015; Kallio et al., 2002; Knowlton et al., 2006; Lan et al., 2004; Sarangapani et al., 2013; Welburn et al., 2010; Zaytsev et al., 2015; 2014). Aurora-B phosphorylation of kinetochore substrates such as the Ndc80 complex is higher on unaligned kinetochores than metaphase-aligned kinetochores(DeLuca et al., 2011; Welburn et al., 2010). This is caused in part by recruitment of phosphatases to kinetochores after they obtain proper kinetochores attachments(Kim et al., 2010; Liu et al., 2010; Sivakumar et al., 2016; Suijkerbuijk et al., 2012), but most models suggest that the CPC's ability to phosphorylate kinetochores is also decreased in metaphase(Krenn and Musacchio, 2015; Samejima et al., 2015; Zaytsev et al., 2016).

How the CPC phosphorylates kinetochores and why kinetochore substrate phosphorylation is higher in unaligned chromosomes than aligned chromosomes is a matter of intense debate. It has been proposed that centromere anchored CPC uses an extended helix on the INCENP subunit to “reach” the Aurora kinase to kinetochore substrates(Krenn and Musacchio, 2015; Samejima et al., 2015). This model is appealing for its simplicity and the fact that the stretch generated by pulling forces could physically displace substrates from the kinase. It has also been suggested that the highly concentrated centromeric pools initiate a signal by activating soluble CPC that propagates to kinetochores via a reaction-diffusion mechanism(Wang et al., 2011a; Zaytsev et al., 2016). The spreading of the soluble CPC requires dynamic interactions with the chromatin-bound CPC. Modeling suggests that the increased distance between chromatin binding sites that accompanies inter-kinetochore stretching would switch the bistable kinase activity

into the “off” state, providing a plausible explanation for the tension-dependent changes in Aurora-B activity at the kinetochore(Zaytsev et al., 2016). The model has been tested in spreading of CPC activity along chromosome arms but lacks experimental evidence that reaction-diffusion mechanism controls kinetochore phosphorylation(Wang et al., 2011a; Zaytsev et al., 2016). Finally it has even been debated whether centromeric CPC plays a central role in phosphorylating kinetochores and error correction (Haase et al., 2017; Hindriksen et al., 2017; Lampson and Grishchuk, 2017; Wheelock et al., 2017; Yue et al., 2008a). Budding yeast and chicken DT40 cells do not require centromere localization for biorientation(Campbell and Desai, 2013; Fink et al., 2017) (Yue et al., 2008b), but yeast require the ability to bind microtubules(Campbell and Desai, 2013; Fink et al., 2017). It has also been proposed that the CPC can bind directly to kinetochores via the Sgo1 protein in human cells(Caldas et al., 2013; Krenn and Musacchio, 2015). However, direct binding of kinetochores is unlikely to be the only mechanism because depletion of the centromere bound pool or expression of CPC mutants that do not bind H3pT3 compromises Aurora-B ability to phosphorylate its distant substrates(De Antoni et al., 2012; Wang et al., 2011a; Zaytsev et al., 2016).

Importantly, these changes in Aurora-B kinase activity are concomitant with the changes in the mode of kinetochore-microtubule attachments. Kinetochores are initially attached to microtubules laterally, and recent data suggest that high inter-kinetochore stretch can be generated by CENP-E kinesin(Itoh et al., 2018; Magidson et al., 2011). It was recently shown that the initial kinetochore-microtubule attachments in prometaphase place inner centromere regions adjacent to large

bundles of microtubules that also run adjacent to sister kinetochores (Magidson et al., 2011). This suggests that there is a distinct prometaphase state that can specifically have bundles of microtubules that span from inner centromeres to kinetochores. These would be largely reduced by metaphase (Magidson et al., 2011) replaced by the “end-on” attachments when microtubules form kinetochore fibers (K-fibers). In this respect, it is interesting that microtubules themselves, not just tension that they can generate, have been shown to provide added layers of regulation to the CPC. Microtubules stimulate the CPC activity and auto-activation *in vitro* and are required for complete localization of the CPC to the inner-centromere (Banerjee et al., 2014; Rosasco-Nitcher et al., 2008; Tipton et al., 2017; Wheelock et al., 2017). Microtubules are also required for full activation of the CPC in a *Xenopus* extract system where the concentration of CPC by chromatin is replaced by activation by dimerizing antibodies (Tseng et al., 2010). However, the exact mechanism of their action and their relevance to the error-correction function of the CPC is unclear. Previous work identified a microtubule-binding site in the SAH domain of the INCENP subunit (Samejima et al., 2015; van der Horst et al., 2015; Wheatley et al., 2001; Wheelock et al., 2017). Although the SAH domain of INCENP is important for the maintenance of the paclitaxel-dependent SAC arrest, it is unclear if it is required for the error correction function of the CPC (Lens et al., 2006; Wheelock et al., 2017). How microtubules regulate the CPC dependent kinetochore phosphorylation is a major unanswered question.

Here we identify a novel microtubule-binding site in the Borealin subunit of the CPC and show that this interaction is important for proper error-correction and

for maintenance of paclitaxel-induced SAC-dependent arrest. We show that non-centromeric CPC is required to phosphorylate kinetochores and that this requires microtubule binding by Borealin. Using theoretical approaches, we demonstrate that microtubules near the inner centromere up regulate kinase activity at adjacent kinetochores. Interestingly, microtubules extend CPC activity even further than kinetochores at their most stretched state, suggesting that the regulation by microtubules is independent of chromatin changes by tension. Our model also demonstrates that end-on attached K-fiber microtubules do not stimulate phosphorylation of kinetochores to the same extent. Together these findings uncover an unappreciated layer of kinetochore regulation where local changes to microtubules near inner centromeres stimulate kinetochore phosphorylation by the CPC. We suggest that the phosphorylation of kinetochores that underlies faithful mitotic progression requires coordination of the centromere-bound, diffusible and microtubule-bound pools of the CPC.

Results:

The “Centromere targeting region” of the CPC contains a novel microtubule-binding site.

The centromere-targeting region of human CPC was expressed and purified from *E. coli*. Our preparations contained the first 48 amino acids of INCENP tagged on the N-terminus with 6-histidines, and full-length Survivin and Borealin (ISB)). ISB was mixed with paclitaxel-stabilized microtubules and the protein that remained bound to microtubules after sedimentation was quantified by

immunoblot. The ISB sub-complex bound taxol-stabilized microtubules with an apparent K_d of ~164nM (Fig.3-1C, D). Proteins often bind microtubules through the electrostatic interaction between basic amino acids in proteins and the acidic residues on the E-hook of tubulin subunits. There are evolutionarily conserved basic residues at the tip of the triple helix of the ISB structure (Fig.3-1 A, B). Disruption of these basic residues by expression of Borealin^{R17E, R19E, K20E} was previously shown to inhibit cytokinesis, but no effects on early mitotic events were reported (Jeyaprakash et al., 2007). We engineered these mutations into our *E. coli* expression construct to generate ISB^{MTBD}. These charge reversal mutations in the basic patch dramatically reduced the microtubule binding affinity of the ISB complex (apparent K_d of 4,200 nM) (Fig.3-1C, D). Deleting the N-terminal 20 amino acids of Borealin (ISB^{Δ20}) also reduced the affinity for microtubule binding (apparent K_d of 750 nM, Fig.3-1C, D). These mutations did not hinder ISB complex formation or caused any gross structural changes as measured by gel-filtration chromatography (Fig.3-S1A, B, C). We immunoprecipitated tagged Borealin^{MTBM} or Borealin^{WT} that was expressed in HeLa cells and pulled down similar amounts of endogenous untagged Borealin demonstrating that the mutant does not affect dimerization (Fig.3-S1C).

ISB^{WT} complex also bundled paclitaxel-stabilized microtubules in a concentration-dependent manner (Fig.3-1E). Interestingly ISB specifically bound the bundled microtubules; both ISB^{MTBD} and ISB^{Δ20} were deficient in the bundling of paclitaxel-stabilized microtubules (Fig.3-1E). We conclude that the CPC has an additional microtubule-binding site on the N-terminus of the Borealin subunit.

The Borealin-microtubule interaction is important for faithful mitosis.

We generated stable HeLa TReX cells expressing N-terminal LAP (GFP + S-peptide)-tagged Borealin^{WT}, Borealin^{MTBM} or Borealin^{Δ20}. We reduced the endogenous Borealin using a siRNA targeting the 3'UTR (Fig.3-2A, C; 3-S1D) and imaged cells traversing mitosis by time-lapse microscopy with a cell permeable SiRNA dye. It took significantly longer for cells complemented with both Borealin^{MTBM} and Borealin^{Δ20} to traverse mitosis than LAP-Borealin^{WT} cells (Fig.3-2B, D), demonstrating a function for the Borealin-microtubule interaction in early mitosis. We also assessed fidelity of chromosome segregation in absence of Borealin-microtubule interaction. Cell expressing either Borealin^{MTBM} or Borealin^{Δ20} had twice the frequency of anaphases with lagging chromatids than cells complemented with Borealin^{WT} (Fig.3-2E).

To directly test for a role in kinetochore-microtubule error correction we first incubated cells with the Eg-5 kinesin inhibitor STLC to generate improper attachments, then washed the cells out of the drug and followed the fidelity of error correction by quantifying the number of cells in anaphase with lagging chromatids (Lampson et al., 2004). Cells expressing the Borealin^{MTBM} or Borealin^{Δ20} doubled the number of anaphases with lagging chromatids over controls demonstrating a requirement of the Borealin MBD in error correction (Fig.3-S2A). We also replaced the N-terminal 20 amino acids of Borealin with a different microtubule-binding domain from PRC1 (Fig.3-S2B). Cells expressing the chimeric protein resolved kinetochore-microtubule errors significantly better than the

Borealin^{Δ20} demonstrating that the key function of this domain is attachment to microtubules (Fig.3-S2A). We conclude that Borealin microtubule-binding activity plays an important role in preventing and correcting improper kinetochore-microtubule attachments.

To understand the relative contributions of the two CPC microtubule-binding domains, we compared cells lacking the Borealin (Borealin^{MTBM}) or the INCENP (INCENP^{ΔSAH}) MBD or both and determined the percent of cells undergoing anaphase with lagging chromosomes. Cells lacking either the Borealin or the INCENP MBD had two-fold more anaphases with lagging chromosomes (~40%) (Fig.3-2F). Cells lacking both the MBDs had an even worse phenotype, with almost 73-80% cells undergoing anaphase with lagging chromosomes (Fig.3-2F). These cells also showed an increase in duration of mitosis (Fig.3-S2C). We conclude that the Borealin and the INCENP MBDs play different roles in the kinetochore-microtubule error correction process. The interpretation of this experiment is complicated by the fact that the SAH domain is also the region of the INCENP that is hypothesized to stretch in order to phosphorylate the kinetochore in the “dog leash” model (Samejima et al., 2015).

We treated cells depleted of Borealin and complemented with Borealin^{WT}, Borealin^{MTBM} or Borealin^{Δ20} with 100nM paclitaxel and determined the duration of mitosis by live imaging (Fig.3-3A, B). Cells rescued with Borealin^{MTBM} or Borealin^{Δ20} arrested in mitosis for significantly shorter duration than the cells expressing Borealin^{WT}, in presence of taxol (Fig.3-3C). We determined if replacing the MBD of Borealin with the MBD of PRC1 could rescue the defective SAC arrest (Fig.3-S2B).

We observed a partial rescue in the duration of taxol-induced SAC arrest in the cells expressing the PRC1^{MBD}-Borealin^{Δ20} chimeric protein compared to the microtubule-binding mutants of Borealin (Fig.3-3C, D). Increasing the amount of Aurora-B at centromeres by expressing CENPB-INCENP⁷⁴⁷⁻⁹¹⁸ did not rescue the SAC defect (Fig.3-3 E), further arguing that the central defect in the Borealin^{MTBM} is microtubule binding and not the partial reduction in centromeric CPC, which we describe below. We conclude that the reason for deficiency in SAC maintenance in the Borealin mutants is the inability to bind microtubules.

Mathematical modeling suggests that microtubules adjacent to the inner centromere stimulate kinetochore phosphorylation by the CPC

Next, we sought to understand the possible physiological roles for the binding of the CPC to microtubules and how it might affect the phosphoregulation of kinetochores. We extended a previously characterized mathematical model built upon the fact that the Aurora-B kinase can activate itself and forms a complex reaction-diffusion system in combination with soluble phosphatases. Previous work has suggested that this coupled kinase-phosphatase system is capable of controlling the level of kinetochore phosphorylation in response to the increased centromeric stretch(Zaytsev et al., 2016) , such as found on bi-oriented kinetochores. The ability of CPC to bind microtubules could alter this behavior, but because the underlying spatially distributed phosphorylation switch is strongly non-linear, the consequences of this interaction are difficult to predict, warranting theoretical investigation.

In our improved model, Aurora-B engages in binding-unbinding to centromeric chromatin and microtubules, and it also exhibits diffusion along microtubules and in the cytosol, enabling the dynamic exchange of kinase activity between all these pools (Fig.3-4A; see Methods for details). The chromatin-localized CPC binding sites are strongly enriched at the centromere; while their density decreases toward the kinetochores. Aurora-B kinase activity at the tension-free and microtubule-free kinetochores is high in real cells and also in our model (Fig.3-4B)(DeLuca et al., 2011). Adding end-on attached microtubules to these tension-free kinetochores increased the level of phosphorylation even further owing to the contribution of active microtubule-bound CPC (Fig.3-4E, Fig. 3-S3). As shown previously using a similar model lacking CPC-microtubule interactions (Zaytsev et al., 2016), centromeric stretch engages the bi-stable kinase-phosphatase switch, leading to a strong decrease in the fraction of active kinase at the kinetochore, which mirrors low phosphorylation on fully bi-oriented kinetochores in cells. When we incorporated robust CPC binding to microtubules the activity remained high even at fully stretched bi-oriented kinetochores because the microtubule-bound kinase phosphorylated kinetochores even in the presence of tension. We therefore adjusted model parameters and reduced CPC microtubule-binding affinity (see Methods) until low phosphorylation at the bi-oriented kinetochores was restored (Fig.3-4C,E). This seemed reasonable since the localization of the CPC to microtubules is hard to detect by immunofluorescence in pre-anaphase spindles, so its binding affinity is likely to be low.

Having established that our new model is responsive to tension-dependent phosphoregulation, we used this tool to explore consequences of microtubules that lie near the inner centromeres. These “centromere-proximal” bundles appear from three distinct configurations. First, they are seen in prometaphase cells that have microtubules that fill the center of the spindle. It has been suggested that the microtubules are so dense that they exclude chromosomes and their arms must fold back on each other. This orientation places inner centromeres adjacent to the central microtubules (Magidson et al., 2011). Second they can be generated by preformed K-fibers (Banerjee et al., 2014; Maiato et al., 2004). Third, merotelic attachments also bring the merotelic K-fiber microtubules near inner centromeres (Cimini et al., 2001; Knowlton et al., 2006; Thompson and Compton, 2011). In our model, which is a one-dimensional representation, these three states are all equivalent and we represent them simply by the constant level of microtubule-binding sites for CPC. This configuration did not change the overall gradient shape with a peak near the centromere in the model, but it increased the kinase activity at the kinetochores, and expanded the phosphorylation zone along the microtubules (Fig.3-4. D, E). This is remarkable because same model parameters produced negligible kinase activity with a similar concentration of amphitelicly-attached microtubules, which lacked the centromere-proximal segment (Fig.3-4C). To further test whether the expansion of the kinase activity gradient along the centromere-proximal microtubules was indeed induced by their proximity to the centromere, we set the activity of the chromatin-bound Aurora-B kinase to zero. This completely prevented activation of Aurora-B kinase on centromere-proximal

microtubules (Fig.3-4E), demonstrating that centromere-bound kinase pool activates the microtubule-bound kinase. Moreover, preventing CPC binding to the microtubules also abolished the increased kinase activity that extended beyond high-stretched kinetochores in the presence of centromere-proximal microtubules (Fig.3-4E). We then varied the abundance of centromere-proximal microtubules and found that the levels of active microtubule-bound and soluble kinase pools at the kinetochore were responsive to the concentration of these microtubules (Fig.3-3F-H). These findings strongly suggest that the affinity of the CPC to microtubules is capable of controlling kinetochore phosphorylation in response to the presence of centromere-proximal microtubules. Moreover, it suggests that the number of centromere proximal microtubules can act as a rheostat to tightly control kinase activity, and this regulatory mechanism is compatible with the tension-dependent regulation of CPC activity.

Borealin-microtubule interaction enables robust kinetochore phosphorylation in prometaphase by the CPC.

A major prediction of the modeling study is that robust kinetochore phosphorylation on kinetochores with centromere-proximal microtubules depends on both centromeric and the microtubule-bound CPC, which “talk” to each other and the soluble CPC pool. To test whether Borealin-microtubule binding is required for increased phosphorylation of kinetochores, we measured kinetochore phosphorylation by the CPC in prometaphase cells expressing the Borealin^{WT} or Borealin^{MTBM} (Fig.3-5A) using a series of phospho-antibodies by quantitative

immunofluorescence(DeLuca et al., 2011; Welburn et al., 2010). Phosphorylation of a number of CPC substrates at the kinetochore (DSN1 pS109; KNL1 pS60, CenpA pS7 and Hec1 pS44) was reduced when Borealin-microtubule interaction was disrupted (Fig.3-5B-E, 3-S4A-F). In contrast, the chromatin substrate H3 pS10 was not affected (Fig.3-5F, G). The reduction in the CPC phosphorylation was not due to defective kinetochore assembly (Fig.3-S4G-J). Interestingly, we also saw that a recently reported Aurora-A substrate at the kinetochore, Hec1 pS69(DeLuca et al., 2017), was also reduced in the Borealin^{MTBM} compared to the Borealin^{WT} expressing cells (Fig.3-5H, I). Aurora-A centromere localization depends on its interaction with INCENP, which is important for Hec1pS69 phosphorylation(DeLuca et al., 2017), and thus might also depend on Borealin. Phosphorylation by the CPC on DSN1 pS109 was partially rescued by replacing Borealin MBD with PRC1 MBD, which is consistent with our observation that an exogenous MBD can rescue SAC and error-correction functions (Fig.3-S4E, F). These results highlight that our mathematical model lacks Aurora-A-dependent phosphorylation and other such mitotic complexities, but nonetheless they are consistent with the prediction of the importance of CPC-microtubule binding for kinetochore phosphoregulation.

Borealin-microtubule interaction stimulates the localization of the CPC to the inner-centromere.

The interaction of Borealin with microtubules could regulate the amount of the CPC bound to the centromere, the transfer of the signal from the inner centromere to kinetochores or both of these steps. Note that the former is a complexity that was

not included in our model and confounds the interpretation of the above finding. To examine this possibility we measured the levels of the centromeric CPC in cells expressing the Borealin^{MTBM}. The centromeric CPC levels were reduced in the Borealin the microtubule-binding mutants compared to wild type, as assessed by the immuno-staining for Aurora-B, INCENP and Borealin (Fig.3-6A-D). The reduction in the CPC localization is not due the N-terminal LAP-tagging of the Borealin protein as C-terminally tagged Borealin^{MTBM} also shows the same reduction in inner-centromeric CPC localization (Fig.3-S5A, B). Defective centromeric CPC localization is not due to defective dimerization by Borealin, which was shown to regulate CPC localization(Bekier et al., 2015), since disabling MTBD and dimerization domain led to additive reduction in CPC localization, confirming that these are separable functions on the Borealin protein (Fig.3-S5C, D). The reduction in level of activated Aurora-B, measured by T-loop phosphorylation, is comparable to the reduction in total CPC levels in the inner-centromere (Fig.3-S6A,B), indicating that the clustering dependent activation of the inner-centromeric CPC is not affected in cells expressing the Borealin^{MTBM}.

We hypothesized that the Borealin MBD stimulates CPC localization at the centromere indirectly by enabling the CPC to interact with centromere proximal microtubules (Banerjee et al., 2014). In wild type cells, low doses of nocodazole allow short microtubules to remain around centromeres and stimulate the localization of the CPC to the inner centromere(Banerjee et al., 2014). The stimulation of CPC localization was significantly attenuated in cells expressing the Borealin^{MTBM} at low nocodazole concentration (0.33 μ M) (Fig.3-6E, F). In contrast,

the amount of inner-centromeric CPC was similar in mutant and wild type cells in presence of 3.3 μ M nocodazole (high concentration), which completely eliminates centromere proximal microtubules (Fig.3-6E, F). These data suggest that the Borealin MBD interacts with centromere proximal microtubule that stimulates CPC localization to the inner-centromere. Moreover, the fact that the CPC levels are similar in high doses of nocodazole argues that the chromatin binding properties of the CPC are not affected in Borealin^{MTBM}.

To gain insight into molecular mechanism of this stimulation, we examined whether the Borealin MBD controls either of the two-histone phosphorylation feedback loops that localize the centromeric CPC. Both the H2A pT120 phospho-histone mark and the Sgo1 levels at the kinetochores are both reduced about 25% in the microtubule-binding mutants (Fig.3-7B, C; Fig.3-S6C, D). However, the Haspin-dependent Histone H3pT3 phospho-mark is unchanged in the Borealin WT and the MTBM expressing cells (Fig.3-7D, E). We conclude that Borealin MBD stimulates the kinetochore-axis of the CPC localization pathways. This result is consistent with reduced kinetochore phosphorylation in cells expressing the Borealin^{MTBM}, since the CPC controls the H2ApT120 pathway by phosphorylation of kinetochore substrates MPS1 and the Ndc80 complex (Hiruma et al., 2015; Ji et al., 2015; Saurin et al., 2011; van der Waal et al., 2012).

The Borealin MBD on non-centromeric CPC is required to transfer CPC activity from inner centromeres to kinetochores.

We next sought to dissect microtubule-dependency of kinetochore phosphoregulation and test directly whether the Borealin microtubule interaction was controlling the transfer of the CPC activity from the inner centromere to kinetochores, as predicted by the model. We first tested whether the diffusible non-centromeric pool of the CPC contributes to kinetochore phosphorylation in human cells by developing an assay that allowed us to manipulate the non-centromeric CPC without affecting the amount of Aurora-B at centromeres. Specifically, we artificially targeted the Aurora-B kinase to the centromere by fusing Aurora-B binding domain of INCENP, INCENP⁷⁴⁷⁻⁹¹⁸ with the DNA binding domain of the CENP-B, which recognizes alpha satellite DNA. This chimeric protein should be incapable of stretching significant distances and binding microtubules since it cannot bind Borealin and Survivin and lacks the SAH domain of INCENP (Fig.3-8B). We inhibited the targeting of the endogenous CPC to the inner-centromere by adding the Haspin inhibitor (3-ITU) and depleting Bub1 (Fig.3-S7A, B) and measured Aurora-B kinase activity at the outer kinetochore using two different antibodies raised against Hec1-pS44 and Hec1-pS55. In these conditions, we found that Hec1 was still phosphorylated. This is consistent with recent reports(Hengeveld et al., 2017; Wheelock et al., 2017) and argues that the elongated stretch of INCENP or “dog leash” model cannot be the only mode of kinetochore phosphorylation (Fig.3-8A, C, D; 3-S7C, D). These results support the reaction-diffusion model, in which combination of the diffusible and chromatin-bound CPC pools coordinates the phosphorylation of the kinetochore(Lampson and Grishchuk, 2017; Wang et al., 2011a; Zaytsev et al., 2016). We specifically inhibited the soluble pool of the CPC by

depleting the Borealin subunit in cells expressing CENP-B-INCENP⁷⁴⁷⁻⁹¹⁸. Strikingly, depleting Borealin in these cells reduced Hec1 pS44 and Hec1 pS55 compared to control cells, even though the amount of Aurora-B at the centromere was unaffected (Fig.3-8A, C, D; 3-S7C, D). Since the CENP-B DNA binding domain that is used to target the Aurora-B is known to turnover (Wang et al., 2011a), it likely has a soluble pool of its own. Therefore, the requirement of Borealin suggests that the non-centromeric pool of the CPC must use some activity that is lacking in the CENP-B-INCENP⁷⁴⁷⁻⁹¹⁸ to phosphorylate kinetochores.

We hypothesized that the diffusible pool of the CPC is activated by the inner centromere pool and then uses microtubules to “travel” to the kinetochore to phosphorylate kinetochore substrates as predicted by the model. As an initial test of this idea we measured the requirement for Borealin-microtubule interaction in our system that isolated the requirement for soluble CPC to phosphorylate kinetochores (Fig.3-S7E). Specifically, we compared cells rescued with Borealin^{WT} or Borealin^{MTBM} in cells expressing CENP-B-INCENP⁷⁴⁷⁻⁹¹⁸ and depleted of the endogenous CPC localization pathways (Fig.3-S7H). We found that even though active Aurora-B was targeted to the inner centromere, robust phosphorylation of kinetochores still required the Borealin MBD on the diffusible pool of the CPC (Fig.3-8E-I; 3-S7F-G). In conclusion, we have identified two roles for microtubule binding in Borealin activity. First, the Borealin MBD allows the centromere-activated CPC to ignite the microtubule-bound pool of the CPC, leading to elevated combined activity of all pools at the kinetochore and up regulating its phosphorylation. Second, this

kinetochore phosphorylation affects the Bub1-Sgo1-CPC localization pathway increasing the amount of CPC in the inner centromere.

Discussion:

Phosphorylation of the kinetochore proteins by the CPC controls many mitotic events, but it is unclear how Aurora-B phosphorylation is coordinated as each chromosome first laterally binds microtubules and then converts these attachments to end-on (Shrestha et al., 2017). Here we provide evidence that a newly identified microtubule-binding site on the Borealin subunit of the CPC is required for resolving kinetochore microtubule attachment errors and spindle checkpoint activation and suggest a possible mechanism for such regulation.

Borealin is a multifaceted CPC subunit that binds both centromeric chromatin and microtubules.

A MTBD in the N-terminus of Borealin resides just outside the triple helix that acts as the interface between INCENP, Survivin and Borealin. Charged amino acids on Borealin are critical to bind microtubules suggesting that electrostatic interactions in ISB bind the negatively charged microtubule surface. Interestingly, INCENP also has basic residues in this region (R43, R47) so it may also contribute to a composite microtubule-binding surface. However, mutating the positively charged residues on Borealin was sufficient to inhibit microtubules binding and bundling *in vitro*.

The ISB MTBD described here is the third direct microtubule-binding region on the CPC (Fig.3-9A). The extended alpha helix in the INCENP subunit contains a PR/SAH domain that binds microtubules(Fink et al., 2017; Wheatley et al., 2001; Wheelock et al., 2017). In addition, a complex of the C-terminus of INCENP and the Aurora-B kinase subunit binds microtubules *in vitro* and microtubules can stimulate kinase activity of this region of the CPC(Banerjee et al., 2014; Rosasco-Nitcher et al., 2008). CPC also binds a kinesin MKLP-2, which drives the interaction of the CPC with microtubules in anaphase(Hümmer and Mayer, 2009; Krupina et al., 2016). EB1 and GTSE1 also regulate the activity of the CPC during mitosis(Banerjee et al., 2014; Sun et al., 2008; Tipton et al., 2017). While most studies have focused on the ability of microtubules to regulate kinase activity, it is unclear if there are additional reasons why the CPC requires these multiple microtubule interactions. A possible answer is that the CPC help to build microtubule structures during mitosis. The ISB complex drove the formation of microtubule bundles from individualized paclitaxel stabilized microtubule *in vitro*. In addition, the ISB complex bound bundles of microtubules, but was not detected on single microtubules. It is difficult to know if this activity is important for their *in vivo* functions. However, *in vivo* the CPC is intimately tied to microtubule bundle structures, as it both localizes to and coordinates the assembly of midzone microtubules in anaphase and preformed K-fibers in prometaphase cells(Banerjee et al., 2014; Earnshaw and Cooke, 1991; Glotzer, 2009; Sampath et al., 2004; Tulu et al., 2006).

Microtubule binding by the non-centromeric CPC plays a role in robust outer kinetochore phosphorylation.

The MTBD of Borealin is important for full kinetochore phosphorylation and mitotic functions. This finding explains recent results demonstrating that the centromere-targeting domain of the CPC has roles independent of centromere targeting during paclitaxel dependent checkpoint arrest (Wheelock et al., 2017), and it suggests the multiple-microtubule binding domains that are required for viability in yeast (Campbell and Desai, 2013; Fink et al., 2017) represent a conserved function of the CPC. How the CPC in the inner centromere controls phosphorylation of adjacent kinetochores is an important unanswered question. Due to presence of multiple feedback loops that regulate the inner-centromeric localization of the CPC, mechanistic studies that tease out localization of the CPC from phosphorylation of the outer kinetochore phosphorylation have been difficult. We developed a system to remove the feedback loops and restore centromeric Aurora-B activity. In corroboration of the reaction-diffusion model of Aurora-B activity, we found that a pool of non-centromere targeted CPC is critical for robust phosphorylation of outer kinetochores. Moreover, by combining the above-mentioned strategy with the microtubule-binding mutants of Borealin we show that microtubule binding is important for this robust phosphorylation of the outer kinetochore by the non-centromeric CPC.

We suggest that the reduced CPC levels in the inner centromere in cells expressing the Borealin^{MTBD} can at least be partially explained by reduced kinetochore phosphorylation. We measured levels of histone H2ApT120 in these

cells and it was reduced 25%, which suggests that the CPC containing Borealin^{MTBD} is deficient at recruiting MPS1 to kinetochores, which in-turn would reduce the recruitment of the Bub1 kinase that phosphorylates histone H2A.

A combined model for tension-dependent and microtubule-dependent kinetochore phosphorylation by the CPC.

Electron microscopy on prometaphase cells suggests that the initial attachments by kinetochore to microtubules can generate microtubule structures that lie proximal to the inner centromere because chromosomes fold along the centromere axis (Itoh et al., 2018; Magidson et al., 2011) (Fig.3-9A,B). We suggest these structures stimulate CPC phosphorylation of kinetochores. The maturation of these microtubule attachments into “end-on” attached K-fibers is concomitant with the depletion of centromere-proximal microtubules and decrease in the CPC’s ability to phosphorylate kinetochore substrates. As suggested by the reaction-diffusion model, the inner-centromeric pool of the CPC in all these configurations activates Aurora-B because this is the place of the highest Aurora-B concentration. This pool is in a constant exchange with the soluble CPC pool, which helps to sustain high kinase activity and propagates it to the areas where chromatin-bound CPC is less abundant (Fig.3-9B). With increased tension, however, the concentration of chromatin bound CPC near the kinetochore falls below threshold for activation, so phosphorylation at the kinetochores drops despite presence of the soluble pool. Here we tested a hypothesis that this drop can be prevented by centromere-proximal microtubules (Fig.3-4). Our theoretical model confirms that this scenario is

feasible and the centromere-proximal microtubule bundles can help to propagate CPC activity, up regulating phosphorylation even at the fully stretched kinetochores. This effect provides additional regulatory layer to the tension-dependent regulation. Our mathematical model is simplified and it does not include other complexities, such as kinetochore phosphorylation by Aurora-A kinase, kinetochore-localized phosphatase or induction of CPC recruitment to centromere. However, this “proof of principle” model is highly informative because it demonstrates that phosphoregulation at the kinetochore results from highly complex biochemical system, in which chromatin-bound, microtubule-bound and soluble CPC pools exchange dynamically. Indeed, we show that in cells these pools are also required for high phosphorylation of prometaphase kinetochores. Thus, our data provides important *in vivo* support for the reaction-diffusion model of CPC activity. Based on these results we suggest that prometaphase microtubule structures that are in immediate vicinity to the centromere, such as preformed K-fibers, or lateral attachments enable robust phosphorylation of the kinetochores (Kajtez et al., 2016; Khodjakov et al., 2003; Mitchison and Kirschner, 1985) (Fig.3-9B). Similarly, merotelic attachments that bring kinetochore fibers in close proximity to inner centromeres during metaphase could also stimulate Aurora-B kinase (Fig.3-9B). The generation of amphitelic kinetochore-microtubule attachments during bi-orientation should reduce the number of inner centromere proximal microtubules and this would help to reduce outer kinetochore phosphorylation (Fig.3-9B). In addition, the concomitant recruitment of the phosphatase to “end-on attached” kinetochores would further stabilize correct attachments (Fig.3-9B).

It remains to be seen whether the mechanism we propose regulates specifically the Ndc80 complexes that are bound to the merotelic K-fibers or it affects Ndc80 on all microtubules attached to such kinetochore. It is also still unclear whether microtubules can somehow bias the diffusion of the centromere activated soluble CPC towards the kinetochores, for example via a gradient of H2ApT120 emanating from kinetochores. Microtubules might be more efficient than soluble pool at directing the CPC since “lateral” attached microtubules would reduce the dimensionality of diffusion from 3D to 1D and provide a more direct path to kinetochores. In addition, the stimulation of activity by microtubules (Banerjee et al., 2014; Rosasco-Nitcher et al., 2008) could also allow the activity to be maintained or to even activate more soluble CPC that is concentrated on the microtubule (Fig.9A,B). Other mechanisms for outer-kinetochore phosphorylation have been suggested, such as the “dog leash” model in which the inner-centromeric CPC stretches out to the outer kinetochore and phosphorylates its substrates (Samejima et al., 2015; Santaguida and Musacchio, 2009), a kinetochore localized pool of the CPC has also been suggested to play a role in outer kinetochore phosphorylation (Caldas et al., 2013; Krenn and Musacchio, 2015). Perhaps such mechanisms could contribute together to robust phosphorylation the outer-kinetochore. The model proposed in this study can be thought of as a tension independent model for error correction in the sense that the amount of kinetochore phosphorylation depends on the proximity of the microtubules and the inner-centromere, which in turn would be a function of the geometry between

kinetochores and microtubules, and not on the tension across kinetochores or the distance of the kinetochore from inner centromeres per se. We propose that spatial separation mechanisms allow robust phosphorylation in the absence of microtubules in prophase or nocodazole while chromatin/microtubule-dependent spreading of the CPC enables robust kinetochore phosphorylation independent of tension until the obtainment of end-on attachments.

Author contributions

P.T. performed all the biochemical and cell biological experiments under the supervision of P. T. S.. M.G and A.V.Z. carried out all the theoretical analyses under the supervision of F.I.A and E.L.G.. P.T.S, P.T and E.L.G. wrote the paper.

Acknowledgements:

This work was supported by grants from the NIH to P.T.S. (1R01GM118798) and E.L.G. (R01-GM098389). E.L.G. is supported in part by Research Scholar Grant RSG-14-018-01-CCG from the American Cancer Society. Theoretical part of this work (Figure 4) was supported by grant from Russian Science Foundation (16-14-00-224) to FIA. PTS and PT would like to thank Limin Liu and Anindya Dutta for their support, Dan Burke for critical reading of the manuscript and Dan Foltz, Arshad Desai, Susanne Lens, Jennifer Deluca and Iain Cheeseman for reagents.

Materials and Methods

Cell culture:

HeLa T-Rex cell (ThermoFisher Scientific) were grown in Dulbecco's modified Eagle's medium (DMEM, Invitrogen) supplemented with 10% fetal bovine serum (Gibco) in a humidified incubator at 37°C in presence of 5% CO₂.

Stable cell lines generation:

In order to generate HeLa T-Rex cells stably expressing LAP-Borealin^{WT}, LAP-Borealin^{MTBM}, LAP-Borealin^{Δ20}, LAP-PRC1^{MBD}-Borealin^{Δ20}, LAP-Borealin^{T230E} and LAP-Borealin^{MTBM/T230E}, the Borealin^{WT} transgene fragment was sub-cloned in to pCDNA5/FRT vector (Invitrogen) containing N-terminal LAP (GFP and S-peptide) tag sequence. QuickChange II XL site directed mutagenesis kit (Agilent) was used to generate all the point mutations and deletions constructs. For generating HeLa T-Rex cells expressing GFP-CENP-B^{DBD}-INCENP⁷⁴⁷⁻⁹¹⁸ and mCherry-Borealin^{WT} or mCherry-Borealin^{MTBM} transgenes, the GFP-CENP-B^{DBD}-INCENP⁷⁴⁷⁻⁹¹⁸ was sub-cloned downstream of Tet-operator binding site. CMV promoter containing fragment of mCherry-Borealin^{WT} or mCherry-Borealin^{MTBM} was cloned at the 3' end of GFP-CENP-B^{DBD}-INCENP⁷⁴⁷⁻⁹¹⁸. This whole cassette of GFP-CENP-B^{DBD}-INCENP⁷⁴⁷⁻⁹¹⁸ and mCherry-Borealin^{WT} or mCherry-Borealin^{MTBM} was then cloned into pCDNA5/FRT vector (Invitrogen). The resulting plasmids were co-transfected with the pOG44 plasmid (Invitrogen) with Lipofectamine 2000 (Invitrogen). Hygromycin B (Invitrogen) 200ug/ml was added one-day post transfection and the cells were selected for 15 days. After the selection period, the surviving colonies were pooled

and FACS sorted for GFP (for LAP-Borealin transgenes) or mCherry (for GFP-CENP-B^{DBD}-INCENP⁷⁴⁷⁻⁹¹⁸ and mCherry-Borealin^{WT} or mCherry-Borealin^{MTBM} transgenes) expression to get cells expressing equal amount of the transgene.

For generating cells expressing vsv-INCENP^{WT}-GFP or vsv-INCENP^{ΔCC}-GFP with mCherry-Borealin^{WT} or mCherry-Borealin^{MTBM} transgenes. The Tet-inducible HeLa T-REx cells expressing vsv-INCENP^{WT}-GFP or vsv-INCENP^{ΔCC}-GFP (a kind gift from S. Lens) were infected with virus carrying mCherry-Borealin^{WT} or mCherry-Borealin^{MTBM} transgenes in the presence of 8μg/ml polybrene (Sigma). The double stable cells were then selected for 10-12 days in presence of Puromycin (Invitrogen) at 1ug/ml and Hygromycin B at 200ug/ml. The surviving colonies were pooled and FACS sorted for mCherry expression to obtain double stable cell lines.

Virus production:

For making retrovirus, mCherry-Borealin^{WT} or mCherry-Borealin^{MTBM} transgenes were cloned into pBABE-Puro retrovirus vector using cold fusion cloning kit (System Biosciences). HEK 293 GP cells were co-transfected with pBABE-Puro-mCherry-Borealin (WT or MTBM) and VSVG plasmid in order to package pseudotyped MULV viruses. The viruses were collected 3-day post transfection by filtering the media through 0.45um syringe filter.

Plasmid and siRNA transfection and STLC washout assay:

For plasmid transfection cells were grown to 80-90% confluence followed by plasmid transfection using Lipofectamine 2000 (Invitrogen) according to the manufacture's protocol.

In case of siRNA transfection in order to avoid the indirect effect we analyzed the first mitosis after depletion of the target proteins. To achieve this cells were plated in presence of 2mM thymidine, 24hrs after plating, cells were released into fresh media and siRNA was transfected using RNAiMAX (Invitrogen) according to the manufacturer's protocol. Another round of siRNA transfection was done after 10-12hrs of 1st siRNA treatment and at the same time 2mM Thymidine was added. Cells were released into fresh media 12 hours after the second siRNA treatment. For immunofluorescence analysis cells were fixed after 8-10 hours of second thymidine release or after the indicated treatment.

For STLC washout assay 6-7 hours after the second thymidine release 5uM STLC was added and cells were incubated for 2 hours. After 2 hours of incubation STLC was washed out of the cells by washing with PBS followed by 1.5 hours of incubation at 37°C in presence of 5% CO₂. Cells were fixed and stained with DAPI and mounted on coverslips using ProlongGold antifade (Invitrogen).

Live cell imaging:

For live cell imaging, cells were plated in the 4 well Lab-Tek II chambered coverglass (Thermo Fisher Scientific) in presence 2mM thymidine followed by siRNA treatment. After 3-4 hours of the 2nd thymidine release 200nM SiR-DNA (Cytoskeleton Inc.) dye was added to the cells. One and a half hour after SiR-DNA

treatment time-lapse images were taken at 5min interval for 15hrs on a Zeiss Axio-observer-Z1 in a humidified environmental chamber maintained at 37°C in presence of 5%CO₂.

Immunoprecipitation (IP):

For immunoprecipitation, HeLa cells were synchronized to mitosis with 0.33uM nocodazole for 16 hours. Mitotic cells were collected and lysed in CPC lysis buffer (250mM NaCl, 50mM Tris-HCl pH7.5, 5mM EDTA, 0.5% NP-40, 1mM DTT, 20mM Beta-glycerophosphate, 50mM NaF, 1mM Na-orthovanadate, 1x protease inhibitors cocktail (Roche) and sonicated using Bioruptor-300 (Diagenode) for 30 cycles with 30 seconds on and 30 seconds off at 4 °C. The whole cell lysate was cleared by centrifugation at 14000g for 10 minutes and the supernatants was incubated with GFP antibody (a kind gift from Dan Foltz) for 3 hours at 4°C. Equilibrated protein-A beads (GE lifesciences) were then incubated with the antibody lysate mixture for an additional hour. The beads were washed with lysis buffer 3 times. The washed beads were re-suspended in 2X sample buffer and loaded on to SDS-PAGE gel after brief boiling at 95°C, desired proteins were detected in the immune-precipitate by western blotting

Immunofluorescence microscopy:

HeLa T-REx cells were seeded onto coverslips coated with poly-L-Lysine (Sigma) and indicated siRNA transfection and subsequent indicated treatment were done. The cells were then co-fixed with 4% paraformaldehyde in PHEM buffer

(60mM Pipes, 25mM Hepes, 10mM EGTA, and 4mM MgCl₂, pH 6.9) supplemented with 0.5% Triton-X 100 for 20 minutes at room temperature. The cells were then washed 3 times with Tris buffered saline (TBS), followed by 1hour blocking with 3% BSA at room temperature. Fixed cells were then incubated with indicated primary antibodies for 1 hour at room temperature. After washing three times with TBS-T (TBS + 0.1% Tween20), cells were incubated with fluorescent secondary antibodies (1:2000) (Jackson Immuno-Research). After washing 4 times with TBS-T, the cells were stained with 0.5µg/ml DAPI for 5 minutes and the coverslips were mounted onto slides using ProlongGold antifade (Invitrogen) and sealed with nail polish. Image acquisition was performed as described previously (Banerjee et al., 2014). Images were processed and analyzed using Volocity (V5.5, PerkinElmer). To quantify fluorescence levels at centromeres, we used an intensity thresholding algorithm to mark all centromeres on the basis of ACA or GFP (for Fig.8, S7) intensity. To eliminate the size difference of each marked centromere the total fluorescence intensity was divided by the total volume of the selected area. Upon background subtraction the intensity/volume values of the desired channel were normalized against the corresponding ACA intensity/volume. When cells were not stained with a centromere marker or when the staining pattern was not encompassed by ACA background subtracted intensity/volume was reported. These values were plotted (box and whisker plots showing 3-95% percentile (whiskers) and box representing 23-75 percentile and median is the line in the boxes) using Prism software (GraphPad) and indicated two tailed statistical tests where applied.

Protein Purification:

INCENP¹⁻⁵⁸-Survivin-Borealin complex was expressed in BL21-pLysS (DE3) cells from a tri-cistronic pET28a vector containing 6XHis-INCENP¹⁻⁵⁸-Survivin-Borealin sequence in 2XYT media in presence of 30ug/ml Kanamycin. Protein expression was induced at O.D. 0.6 by addition of 0.45 mM IPTG and the media was supplemented with 0.2% glucose 60ug/ml ZnCl₂, protein expression was carried out for 16-18hrs at 18°C. Cells were subsequently pelleted and lysed in buffer containing 50mM Tris, pH 7.5; 500mM NaCl; 0.5mM TCEP; 5mM Imidazole; 5% glycerol and protease inhibitor cocktail (Roche) using EmulsiFlex-C3 Homogenizer. Lysate was cleared by centrifugation. Cleared lysate was then mixed with Ni-NTA beads (Qiagen) for 4 hours at 4°C. Ni-NTA beads (Qiagen) were then washed with 200ml buffer containing 25mM Imidazole, 50mM Tris pH7.5, 500mM NaCl, 0.5mM TCEP and 5% glycerol. The Protein was then eluted with buffer containing 250mM Imidazole, 50mM Tris pH7.5, 500mM NaCl, 0.5mM TCEP and 5% glycerol. Upon elution the proteins were gel filtered on Superdex-200 column 10/300 GL size-exclusion column (GE Life Sciences). Gel filtration was done in buffer containing 50mM Tris pH7.5, 500mM NaCl, 0.5mM TCEP and 5% glycerol. Upon gel filtration the desired fractions were pooled and concentrated with Amicon Ultra-4 Centrifugal Filter Unit with 3KDa cutoff.

Microtubule co-sedimentation assay and microtubule bundling assay:

Taxol-stabilized microtubules were prepared by polymerizing bovine brain tubulin dimers in BRB80 (80mM PIPES, 1mM MgCl₂, 1mM EGTA, pH 6.8 with

NaOH), 1mM DTT and 1mM GTP with increasing concentration of taxol, taxol stabilized microtubules were then separated from the un-polymerized tubulin dimers by centrifuging through a 40% glycerol cushion at 137000g. Various concentrations of taxol-stabilized microtubules were mixed with 100nM of ISB (WT, MTBM or $\Delta 20$) in BRB80, 1mM DTT, 50mM NaCl and 20 μ M paclitaxel. Samples were allowed to equilibrate at room temperature for 15 min. Samples were then layered onto a 50% glycerol cushion and centrifuged at 279,000g for 10 min, and both the supernatant (S) and pellet (P) were collected and resuspended in SDS sample buffer, and equal amounts of supernatant and pellet were run on 15% SDS-PAGE gels followed by western blotting. Quantification of the relative amounts of ISB in supernatants and pellets was performed using ImageJ (National Institutes of Health, Bethesda, MD). The dissociation constants measured by fitting the data from three separate experiments to the one-site specific binding equation using Prism software (GraphPad).

For bundling assay indicated concentrations of ISB complex were incubated with the 1 μ M microtubules in BRB80, 1mM DTT, 50mM NaCl and 20 μ M paclitaxel for 15 min at room temperature. The reaction was then fixed with 1% glutaraldehyde in BRB80 for 5 min. The fixed reaction was then pipetted on the coverslips and was allowed to adhere for 10 min at room temperature. The coverslips were then blocked with 3% BSA in TBS for 30 min. The coverslips were then probed with DM1a and 6-His antibody in blocking solution for 1 hour at room temperature. After washing 3 times with TBS fluorescent secondary antibodies were added for 1 hour in blocking solution at room temperature. The coverslips were

then washed 4 times with TBS and mounted in Prolong gold followed by imaging at 63X objective using a Zeiss Observer Z1 wide-field microscope.

Description of mathematical model.

General model framework. Quantitative analysis of the spatial distribution of Aurora-B kinase activity was carried out based on our previously published mathematical model (Zaytsev et al., 2016). Briefly, the model incorporates biochemical reactions of Aurora-B phosphorylation-dependent autoactivation (in cis and in trans) and its phosphatase-dependent inactivation, the reactions of kinase binding/unbinding to the centromere-localized binding sites and diffusion of the soluble kinase and phosphatase pools. Additionally, we have now incorporated into this model the interactions between kinase and microtubules. Soluble Aurora-B molecules can bind to microtubules, and the bound kinase can diffuse along the microtubules. We assume a rapid equilibrium in the binding-unbinding of Aurora-B to chromatin and microtubule binding sites, so the model considers only the steady-state distributions of all kinase pools.

Assumptions about kinase activity of different pools. Soluble Aurora-B kinase can phosphorylate other soluble kinase molecules, as well as the chromatin-bound and microtubule-bound molecules, thereby activating them (trans-activation). The bound forms of kinase can phosphorylate soluble kinase molecules with similar enzymatic rate constants, but the catalytic rate constant for microtubule-bound kinase is assumed to be 3-fold more active (Table 1), reflecting findings in (Banerjee

et al., 2014; Rosasco-Nitcher et al., 2008). The bound forms of the kinase can also phosphorylate each other; such activity is assumed to be 100-fold lower relative to the soluble form to account for possible steric limitations in the bound state. For simplicity, only the soluble form of phosphatase is considered; the phosphatase dephosphorylates all forms of Aurora-B kinase with the same activity, thereby partially inactivating. Phosphatase characteristics, as well as the diffusion rate of kinase on microtubules are not known, so these parameters were adjusted to optimize model behavior.

Spatial distribution profiles of bound kinase pools. For simplicity, simulations were carried out in one dimension along the centromere-kinetochore axis. Steady-state distribution of the chromatin-bound kinase along this axis, $Profile(x)$, is based on the experimentally measured metaphase Aurora-B localization (Liu et al., 2009), similar to approach employed by (Zaytsev et al., 2016):

$$Profile(x) = B_0 \cdot k / [(1 + \exp(-s(x \cdot k + cent))) \cdot (1 + \exp(-s(x \cdot k - cent)))],$$

where $B_0 = 10 \mu\text{M}$ is the maximum concentration of chromatin-bound kinase at centroid (midpoint between sister kinetochores at $x = 0$). Parameter $s = 6 \mu\text{M}^{-1}$ defines steepness of this profile. Parameters $cent$ and k are used to scale the profile in response to tension: with no tension $k=1.1$ and $cent = 0.55$ (corresponding to Ndc80-Ndc80 distance $1.02 \mu\text{m}$), while for the fully stretched centromere $k=2.3$ and $cent = 0.8$ (corresponding to Ndc80-Ndc80 distance $1.64 \mu\text{m}$).

The concentration profile of the microtubule-bound kinase for bi-oriented configuration (end-on attachments) is given by:

$$MT \text{ Profile}(x) = [MT] / (1 + \exp(q(x_0 - x))),$$

where $[MT]$ is concentration of microtubule-bound Aurora-B kinase, $q = 100 \mu\text{m}^{-1}$ and x_0 is parameter that defines position of the microtubule ends at the kinetochore. For configuration with no tension $x_0 = 0.45 \mu\text{m}$, for the fully stretched centromere $x_0 = 0.8 \mu\text{m}$.

The concentration profile of the microtubule-bound kinase for centromere-proximal kinetochore bundle (merotelic configuration) is given by:

$$MT \text{ Profile}(x) = [MT].$$

Concentration of microtubule-bound Aurora-B kinase, $[MT]$, is not known, but judged from fluorescent images of Aurora-B localization in metaphase cells (Liu et al., 2009), it is significantly smaller than the peak concentration of Aurora-B kinase at the centromere. We used $[MT] = 2 \mu\text{M}$, then titrated this concentration to show that this parameter regulates concentration of active kinase at the Ndc80 site of the kinetochore.

Full set of model equations. The following system of differential reaction-diffusion

equations was used:

$$\left\{ \begin{aligned}
 \partial A^* / \partial t &= A \cdot k_{cis} + [AA^*] \cdot (2k_{cat}^a + k_r^a) - A^* \cdot A \cdot k_f^a - (A^* \cdot B + A^* \cdot T) \cdot k_f^a + ([AB^*] + [AT^*]) \cdot k_{cat}^a + \\
 &\quad + ([BA^*] + [TA^*]) \cdot (k_{cat}^a + k_r^a) + [A^* PPase] \cdot k_r^p - A^* \cdot PPase \cdot k_f^p + D \cdot \partial^2 A^* / \partial x^2 \\
 \partial B^* / \partial t &= B \cdot k_{cis} + [BB^*] \cdot (2k_{cat}^a + k_r^b) - B^* \cdot A \cdot k_f^a - B^* \cdot B \cdot k_f^b + [BA^*] \cdot k_{cat}^a + [AB^*] \cdot (k_{cat}^a + k_r^a) + \\
 &\quad + [B^* PPase] \cdot k_r^p - B^* \cdot PPase \cdot k_f^p \\
 \partial T^* / \partial t &= T \cdot k_{cis} + [TT^*] \cdot (2k_{cat}^a + k_r^T) - T^* \cdot A \cdot k_f^a - T^* \cdot T \cdot k_f^T + [TA^*] \cdot k_{cat}^a + [AT^*] \cdot (k_{cat}^a + k_r^a) + \\
 &\quad + [T^* PPase] \cdot k_r^p - T^* \cdot PPase \cdot k_f^p + D_{MT} \cdot \partial^2 [T^*] / \partial x^2 \\
 \partial A / \partial t &= -A \cdot k_{cis} + ([AA^*] + [AB^*] + [AT^*]) \cdot k_r^a - A \cdot (A^* + B^* + T^*) \cdot k_f^a + [A^* PPase] \cdot k_{cat}^p + \\
 &\quad + B \cdot k_{Boff} + D \cdot \partial^2 A / \partial x^2 \\
 \partial B / \partial t &= -B \cdot k_{cis} + [BA^*] \cdot k_r^a + [BB^*] \cdot k_r^b - B \cdot A^* \cdot k_f^a + B \cdot B^* \cdot k_f^b + [B^* PPase] \cdot k_{cat}^p \\
 \partial T / \partial t &= -T \cdot k_{cis} + [TA^*] \cdot k_r^a + [TT^*] \cdot k_r^T - T \cdot A^* \cdot k_f^a + T \cdot T^* \cdot k_f^T + [T^* PPase] \cdot k_{cat}^p \\
 &\quad + D_{MT} \cdot \partial^2 [T] / \partial x^2 \\
 \partial [AA^*] / \partial t &= A \cdot A^* \cdot k_f^a - [AA^*] \cdot (k_{cat}^a + k_r^a) + D \cdot \partial^2 [AA^*] / \partial x^2 \\
 \partial [BA^*] / \partial t &= B \cdot A^* \cdot k_f^a - [BA^*] \cdot (k_{cat}^a + k_r^a) \\
 \partial [AB^*] / \partial t &= A \cdot B^* \cdot k_f^a - [AB^*] \cdot (k_{cat}^a + k_r^a) \\
 \partial [BB^*] / \partial t &= B \cdot B^* \cdot k_f^b - [BB^*] \cdot (k_{cat}^a + k_r^b) \\
 \partial [TA^*] / \partial t &= T \cdot A^* \cdot k_f^a - [TA^*] \cdot (k_{cat}^a + k_r^a) + D_{MT} \cdot \partial^2 [TA^*] / \partial x^2 \\
 \partial [AT^*] / \partial t &= A \cdot T^* \cdot k_f^a - [AT^*] \cdot (k_{cat}^a + k_r^a) + D_{MT} \cdot \partial^2 [AT^*] / \partial x^2 \\
 \partial [TT^*] / \partial t &= T \cdot T^* \cdot k_f^T - [TT^*] \cdot (k_{cat}^a + k_r^b) + D_{MT} \cdot \partial^2 [TT^*] / \partial x^2 \\
 \partial [A^* PPase] / \partial t &= PPase \cdot A^* \cdot k_f^p - [A^* PPase] \cdot (k_r^p + k_{cat}^p) + D \cdot \partial^2 [A^* PPase] / \partial x^2 \\
 \partial [B^* PPase] / \partial t &= PPase \cdot B^* \cdot k_f^p - [B^* PPase] \cdot (k_r^p + k_{cat}^p) \\
 \partial [T^* PPase] / \partial t &= PPase \cdot T^* \cdot k_f^p - [T^* PPase] \cdot (k_r^p + k_{cat}^p) + D_{MT} \cdot \partial^2 [T^* PPase] / \partial x^2
 \end{aligned} \right.$$

where A – concentration of the partially active soluble kinase; A^* – concentration of active soluble kinase; B – concentration of partially active chromatin-bound kinase; B^* – concentration of active chromatin-bound kinase; T – concentration of partially active microtubule-bound kinase; T^* – concentration of active microtubule-bound kinase, $PPase$ – concentration of soluble phosphatase. Two-letter symbols in square brackets denote concentrations of enzymatic complexes of the corresponding forms. All model parameters and their values are listed in (Table 1).

Boundary conditions were chosen to avoid the flow of soluble components:

$$\left. \frac{dA}{dx} \right|_{x=0,R} = 0$$

$$\left. \frac{dA^*}{dx} \right|_{x=0,R} = 0$$

$$\left. \frac{d[AA^*]}{dx} \right|_{x=0,R} = 0$$

$$\left. \frac{d[A^*PPase]}{dx} \right|_{x=0,R} = 0$$

$$\left. \frac{dT}{dx} \right|_{x=0,R} = 0$$

$$\left. \frac{dT^*}{dx} \right|_{x=0,R} = 0$$

$$\left. \frac{d[TA^*]}{dx} \right|_{x=0,R} = 0$$

$$\left. \frac{d[AT^*]}{dx} \right|_{x=0,R} = 0$$

$$\left. \frac{d[T^*PPase]}{dx} \right|_{x=0,R} = 0$$

where $x = 0$ for the left boundary and $x = R$ for the right boundary of the simulated spatial segment. Calculations here were carried out for $R = 3 \mu\text{m}$.

Following *initial conditions* were used:

$$\begin{cases} B^* \Big|_{t=0} = Profile(x) \\ T^* \Big|_{t=0} = MT Profile(x) \\ \{A^*, A, B, [AA^*], [BA^*], [BB^*], [AB^*], [TA^*], [TT^*], [AT^*], [A^*PPase], [B^*PPase], [T^*PPase]\} \Big|_{t=0} = 0 \end{cases}$$

Additionally, the sums of all bound and soluble kinase forms and soluble phosphatase forms were constrained:

$$Profile(x) = B + B^* + 2 [BB^*] + [AB^*] + [B^*PPase] + [TB^*] + [BT^*] + [BA^*]$$

$$MT Profile(x) = T + T^* + 2 [TT^*] + [AT^*] + [T^*PPase] + [TB^*] + [BT^*] + [TA^*]$$

$$A_o = A + A^* + 2 [AA^*] + [AB^*] + [BA^*] + [A^*PPase] + [AT^*] + [TA^*]$$

$$PPase_o = PPase + [A^*PPase] + [B^*PPase] + [T^*PPase]$$

Equations were solved numerically using Mathematica software (Wolfram Research) with total simulation time 50,000 s using automatic time and space step size option to ensure convergence.

Table 1. Enzymatic and other model constants.

symbol	description	value	units
k_f^a	rate constant for the formation of the enzyme-substrate complex of active and partially active kinase molecules in case at least one of the molecules is soluble	0.1	$\mu\text{M}^{-1} \text{s}^{-1}$
k_f^b	rate constant for the formation of the enzyme-substrate complex of active and partially active kinase molecules in case both molecules are chromatin-bound	0.001	$\mu\text{M}^{-1} \text{s}^{-1}$
k_f^T	rate constant for the formation of the enzyme-substrate complex of active and partially active kinase molecules in case both molecules are microtubule-bound	0.001	$\mu\text{M}^{-1} \text{s}^{-1}$
k_r^a	rate constant for the dissociation of the enzyme-substrate complex of active and partially active soluble kinase molecules	5.1	s^{-1}
k_r^b	rate constant for the dissociation of the enzyme-substrate complex of active and partially active chromatin-bound kinase molecules	0.21	s^{-1}
k_r^T	rate constant for the dissociation of the enzyme-substrate complex of active and partially active kinase molecules in case both molecules are microtubule-	0.21	s^{-1}

	bound		
k_{cat}^a	catalytic rate constant for active soluble or chromatin-bound kinase toward all forms of the partially active kinase	2.3×10^{-2}	s^{-1}
k_{cat}^{MT}	catalytic rate constant for active microtubule-bound kinase toward all forms of the partially active kinase	4.6×10^{-2}	s^{-1}
k_{cis}	rate constant for kinase cis-activation, all forms	7.28×10^{-6}	s^{-1}
k_f^P	rate constant for the formation of the enzyme-substrate complex of phosphatase and active kinase, all forms	0.6	$\mu M^{-1} s^{-1}$
k_r^P	rate constant for the dissociation of the enzyme-substrate complex of phosphatase and active kinase, all forms	0.09	s^{-1}
k_{cat}^P	catalytic rate constant for phosphatase toward active kinase, all forms	2.0×10^{-3}	s^{-1}
D	diffusion coefficient of soluble kinase	1	$\mu m^2 s^{-1}$
D_{MT}	diffusion coefficient of microtubule-bound kinase	0.005	$\mu m^2 s^{-1}$
$PPase_0$	total concentration of phosphatase	0.047	μM
A_0	total concentration of soluble kinase	0.01	μM

Antibody	Concentration	Application	Source animal	Company/source	Item number
pH3S10	1 in 800	IF	Rb	EMD Millipore	06-570
pH3T3	1 in 1500	IF	Rb	EMD Millipore	07-424
pH2a T120	1 in 1000	IF	Rb	Active motif	61195
Sgo1	1 in 100	IF	Ms	Abcam	ab58023
Aur-B pT232	1 in 200	IF	Rb	Rockland	600-401-677S
Aurora-B	1 in 250	IF	Ms	BD Biosciences	611083
Borealin	1 in 1000	IF/WB	Rb	Stukenberg lab(Banerjee et al., 2014) (986)	
INCENP	1 in 1000	IF	Ms	Abcam	ab23956
ACA	1 in 200	IF	Hu	Antibodies Inc.	13-234-0001
CENPA pS7	1 in 100	IF	Rb	EMD Millipore	07-232
Dsn1 pS109	1 in 1000	IF	Rb	Ian Cheeseman lab(Welburn et al., 2010)	
Kn1 pS60	1 in 2000	IF	Rb	Ian Cheeseman lab(Welburn et al., 2010)	

Hec1 pS44	1 in 1500	IF	Rb	Deluca lab(DeLuca et al., 2011)	
Hec1 pS55	1 in 250	IF	Rb	Stukenberg lab (974)	
Hec1 pS69	1 in 1000	IF	Rb	Stukenberg lab (974)	
Hec1 (9G3.23)	1 in 2000	IF	Rb	Genetex	GTX70268
Kn1	1 in 1000	IF	Rb	Arshad Desai lab(Cheeseman et al., 2008)	
Bub1	1 in 1000	WB	Rb	Genetex	GTX30097
mCherry	1 in 1000	WB	Rb	Genetex	GTX128508
INCENP	1 in 1000	WB	Rb	Sigma	I5283
Survivin	1 in 1000	WB	Rb	cell signaling	2808
Tubulin (Dm1a)	1 in 500	IF/WB	Ms	Sigma	T6199

Antibodies used in this study:

Sequences of siRNA used in this study:

siRNA	Sequence	Publication
siBorealin 3'UTR	AGGUAGAGCUGUCUGUUCAdTdT	(Klein et al., 2006)
siLuciferase (siLuc)	CGUACGCGGAAUACUUCGAdTdT	(van der Horst et al., 2015)

siINCENP 3'UTR	GGCUUGGCCAGGUGUAUAUdTdT	(van der Horst et al., 2015)
siBub1	CCCAUUUGCCAGCUCAAGCdTdT	(Jia et al., 2016)

Small molecules used in this study:

Small molecules	Concentration / duration
STLC	5uM for 2hr
3-Iodothio	2uM for 30-45'
MG132	10uM
Nocodazole	0.33uM or 3.3uM for 20-30min

Figure 3-1: Borealin binds microtubules through its N-terminal region. (A) Schematic showing multiple protein interaction regions on Borealin (microtubule-binding region is characterized in this paper). Multiple sequence alignment of Borealin, basic residues are shown in green, residues important for microtubule binding are indicated with blue asterisk. (B) Crystal structure of INCENP-survivin-Borealin (PDB: 2QFA); microtubule binding residues R17, R19 and K20 are highlighted in dark blue. (C) Western blots of input, supernatant (S) and pellet (P) fraction of microtubule co-sedimentation assay with 100nM ISB^{WT}, ISB^{MTBM} and ISB^{Δ20} and indicated concentration of microtubules; probed with anti-Borealin antibody. (D) Graph from 3 independent microtubule co-sedimentation assays (mean ± SD), small graph is log₁₀ scale and large graph is linear scale. ISB^{WT} is in red, ISB^{MTBM} is in green and ISB^{Δ20} is in blue. (E) Images from microtubule bundling assay ISB^{WT}, ISB^{MTBM} and ISB^{Δ20} were incubated with 1uM taxol stabilized microtubules and probed with anti-tubulin and anti-6His antibody. 6His-ISB is shown in green and microtubules are shown in red.

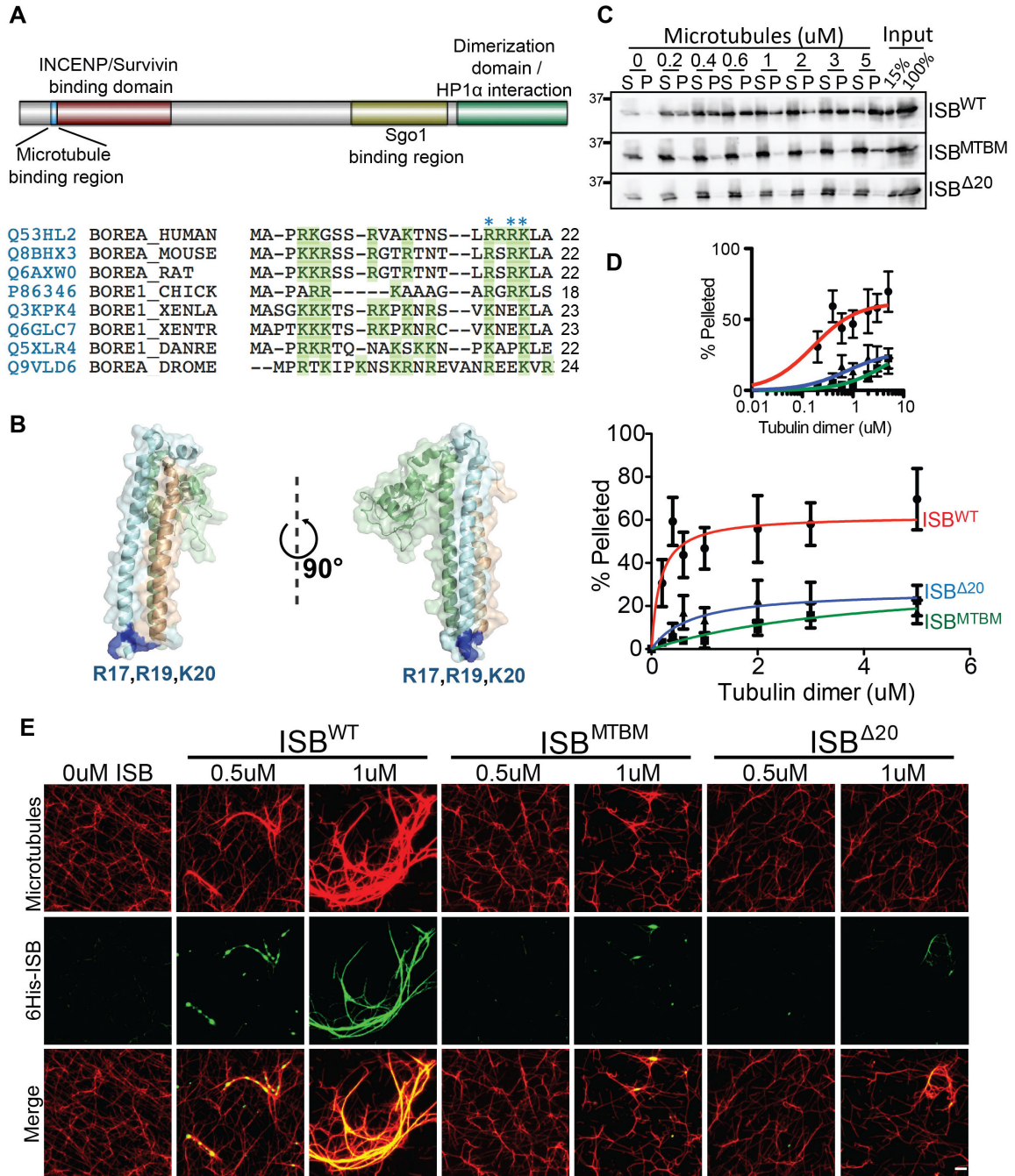


Figure.1

Figure 3-2: Interaction of both Borealin and INCENP with microtubules is important for error free mitosis. (A) Schematic of siBorealin mediated knockdown rescue experiment. (B) Representative frames from time-lapse imaging of SiR-DNA labeled cells treated with Borealin siRNA and rescued with expression of indicated Borealin transgene. (C) Western blots of cells expressing indicated transgene and treated as in A with Borealin or control siRNA, showing endogenous Borealin and LAP-Borealin expression. Tubulin staining is used as loading control. (D) Box and whisker graph of NEBD to anaphase duration from time-lapse movies. Statistical analysis was performed using one-way ANOVA (Kruskal-Wallis test) and Dunn's Multiple Comparison Test (combined data from 3 independent experiments and at least 182 cells in total were analysed). (E) Bar graph showing percent of cells undergoing anaphase with lagging chromosomes, cells were treated as described earlier in A and rescued with indicated Borealin transgene (data from 3 independent experiments, at least 50 cells were analyzed per experiment). (F) Bar graph showing percent of cells undergoing anaphase with lagging chromosomes, treatment was done as in A, except during siRNA transfection step both Borealin and INCENP siRNA were added and the experiment was carried out in presence of 1ug/ml Doxycycline to ensure INCENP transgene expression (data from 2 independent experiments, 50-110 cells were analyzed per experiment). Statistical analysis was performed using one-way ANOVA and Bonferroni's Multiple Comparison Test for both D and E. Bonferroni's Multiple Comparison Test was used for F. *** P<0.001; ** P<0.01, * P<0.05. Scale bar is 5um. Error bars in E and F are \pm SD.

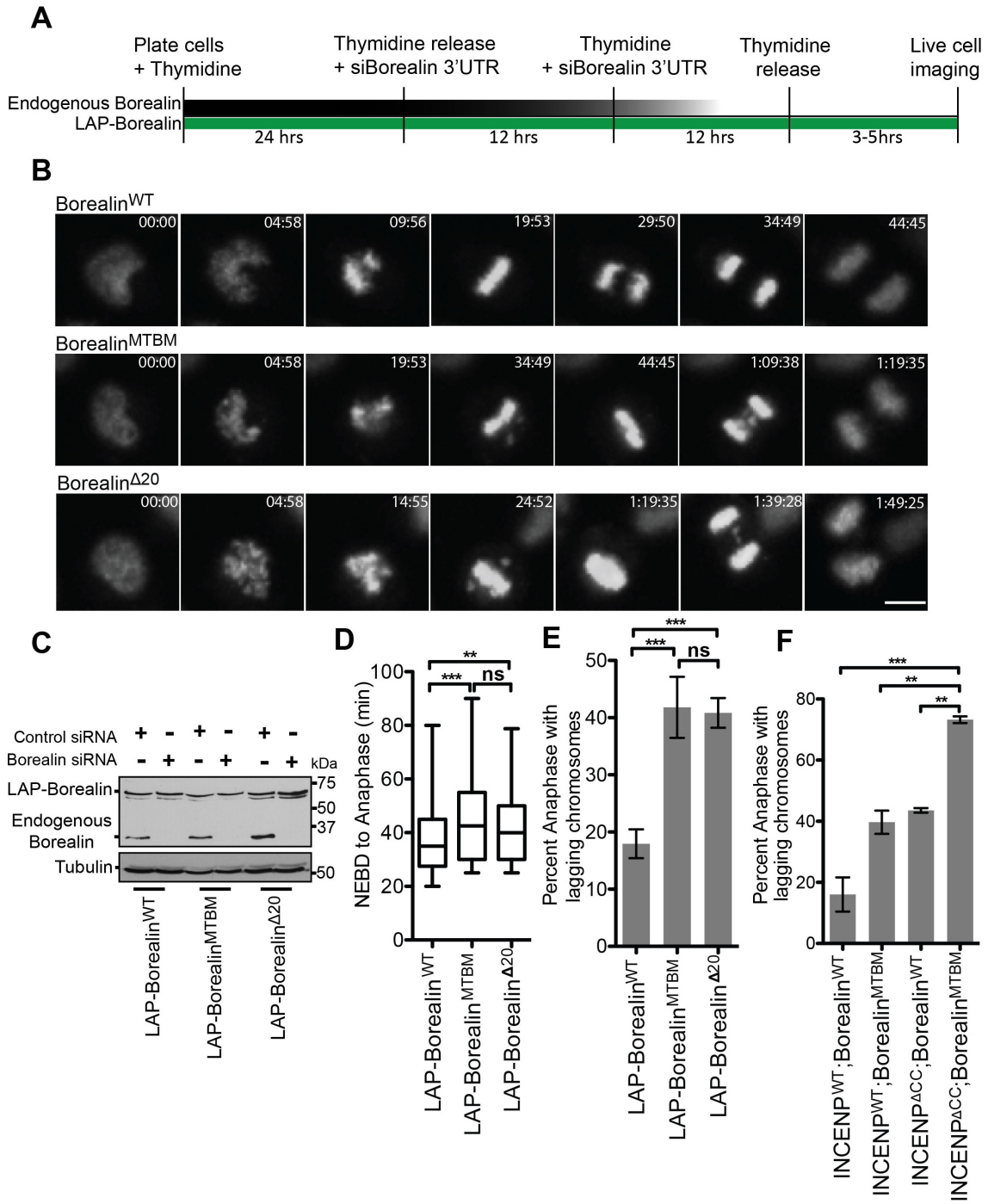


Figure.2

Figure 3-3: CPC-microtubule interaction is important for maintenance of taxol dependent spindle assembly checkpoint arrest. (A) Schematic of experimental procedure for B-D. (B) Representative time-lapse phase-contrast images of a cell treated as in A. Arrow head points to the cell that enters mitosis and is arrested in presence of 100nM taxol and exits mitosis, time of mitotic entry and exit are depicted. Duration of mitotic arrest is the duration between mitotic entry and exit. (C) Box and whisker graph of duration of mitosis in cells expressing the indicated Borealin transgene (between 106-260 cells were analyzed per condition). (D) Graph of data from C showing cumulative frequency distribution of duration of mitosis for the cells expressing indicated Borealin transgene. (E) Box and whisker graph of duration of mitosis in presence of 100nM taxol. Cells were treated as in A with the exception that 1ug/ml of doxycycline was added, at the time of second thymidine addition, for induction of CenpB^{DBD}-INCENP⁷⁴⁷⁻⁹¹⁸ expression (at least 105 cells per condition were analyzed). Statistics performed using Dunn's Multiple Comparison Test, *** P<0.001; ** P<0.01, * P<0.05 and ns P>0.05. Scale bar is 5um.

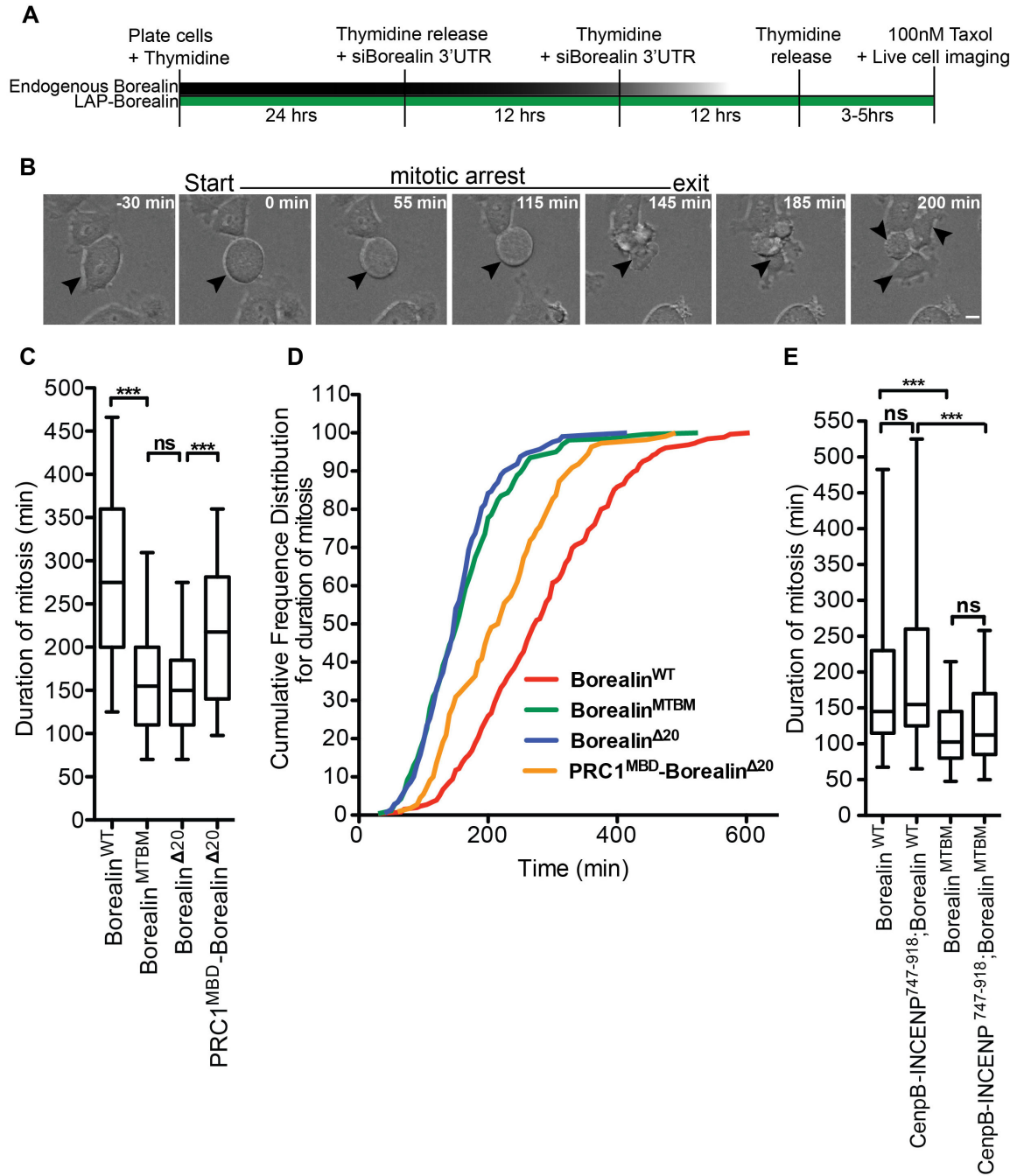


Figure.3

Figure 3-4: Mathematical model of tension-dependent and microtubule configuration-dependent phosphoregulation at kinetochores. (A) Schematic for dynamically exchanging CPC pools. Kinase within each pool becomes activated by autophosphorylation and inactivated by soluble phosphatase, see Methods for details. Calculations for all panels were done using same model parameters (listed in Table 1) but for different centromeric tension and/or microtubule configurations. (B) Concentration of chromatin-bound kinase (blue) decreases from centromere centroid to outer-kinetochore containing Ndc80 substrate (position shown with broken line). Red line (right axis) shows overall decrease in the fraction of active kinase, which nonetheless remains relatively high at this kinetochore. (C, D) Profiles as in B but additionally showing spatial distributions for microtubule-bound kinase (green). The presence of amphitelic microtubules (Bioriented) (C) vs. centromere-proximal (CP-MT) (D) was modeled with constant level of microtubule-bound kinase. Additional concentration profiles are shown in Supplementary Figure 3-3. (E) Calculated concentration of active kinase (sum of all pools) at kinetochore for indicated configurations. The last two columns correspond to model predictions where centromere-proximal microtubules are included but kinase binding to either chromatin or microtubules was removed. (F) Spatial distribution for active microtubule-bound kinase for reduced size of microtubule bundles relative to the level in panel D, which was taken as 1. (G, H) Fraction of active kinase in the microtubule-bound pool (G) and soluble pool (H) responding to the size of centromere proximal microtubule bundle. (Data for this figure was provided by the Grishcuk lab).

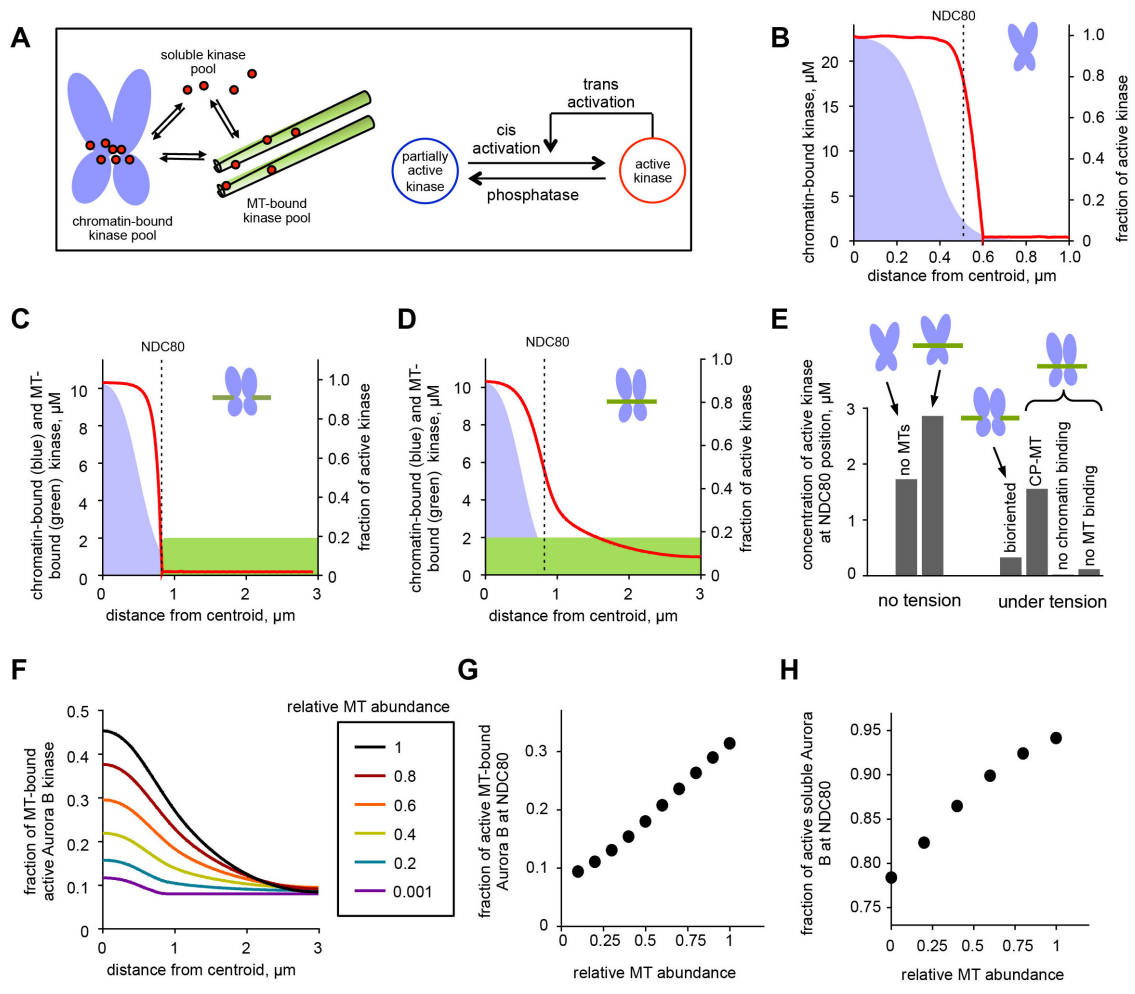


Figure.4

Figure 3-5: Borealin-microtubule interaction contributes to robust phosphorylation of the kinetochore substrates by the CPC. (A) Schematic of Borealin siRNA mediated knockdown rescue experiment. HeLa-TReX cells stably expressing LAP-Borealin^{WT} or ^{MTBM} were treated with Borealin 3'UTR siRNA and cells were immunostained in first mitosis after knockdown of endogenous Borealin. Kinetochore phosphorylation was assessed by immunostaining with (B) DSN1 pS109, (D) Knl1 pS60, (H) Hec1 pS69, antibodies. (F) Chromatin phosphorylation was assessed by immunostaining with histone H3 pS10. Box and whisker (3-95%) graphs of normalized intensity from (C) DSN1 pS109 (8), (E) Knl1 pS60 (8), (G) H3 pS10 (11) and (I) Hec1 pS69 (6), staining (number in the parenthesis indicates the minimum number of cells analyzed per condition). Statistical analysis was performed using Mann Whitney Test, *** P < 0.0001 and ns P > 0.05. Scale bar is 5µm.

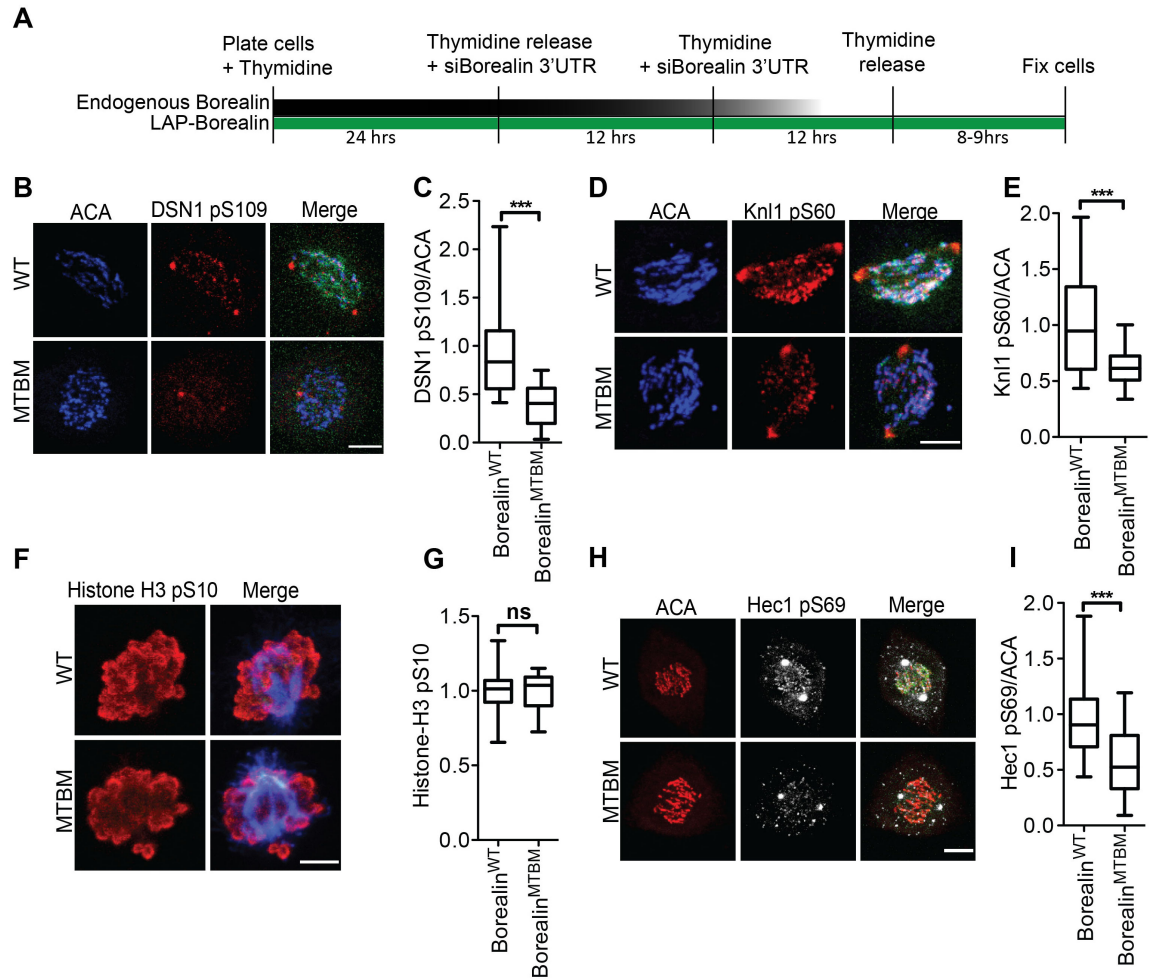


Figure.5

Figure 3-6. Borealin-microtubule interaction drives microtubule dependent enhancement of the CPC localization to the inner-centromere. HeLa-TReX cells expressing LAP-Borealin^{WT} or ^{MTBM} were treated with siRNA as described in A, and immunostained with ACA and Aurora-B (A) or Borealin (C) or INCENP (C) antibodies. (B) Quantification of Aurora-B intensity normalized to ACA (P<0.0001) and absolute ACA intensity (P=0.1396), Unpaired T-test with Welch's correction was applied (data from at least 10 cells per condition). (D) Quantification of INCENP (P<0.0001) and Borealin (P<0.0001) intensity normalized to ACA (data from at least 8 cells per condition). Statistical analysis was performed using Mann Whitney Test. (E) HeLa-TReX cells expressing LAP-Borealin^{WT} or ^{MTBM} were treated as described in A, and incubated with either 0.33uM or 3.3uM nocodazole for 45min followed by immunostaining with ACA and Aurora-B. (F) Quantification of Aurora-B intensity normalized to ACA (data from at least 8 cells per condition). Statistics performed using Dunn's Multiple Comparison Test, *** P<0.001; ** P<0.01, * P<0.05 and ns P>0.05. Scale bar is 5um.

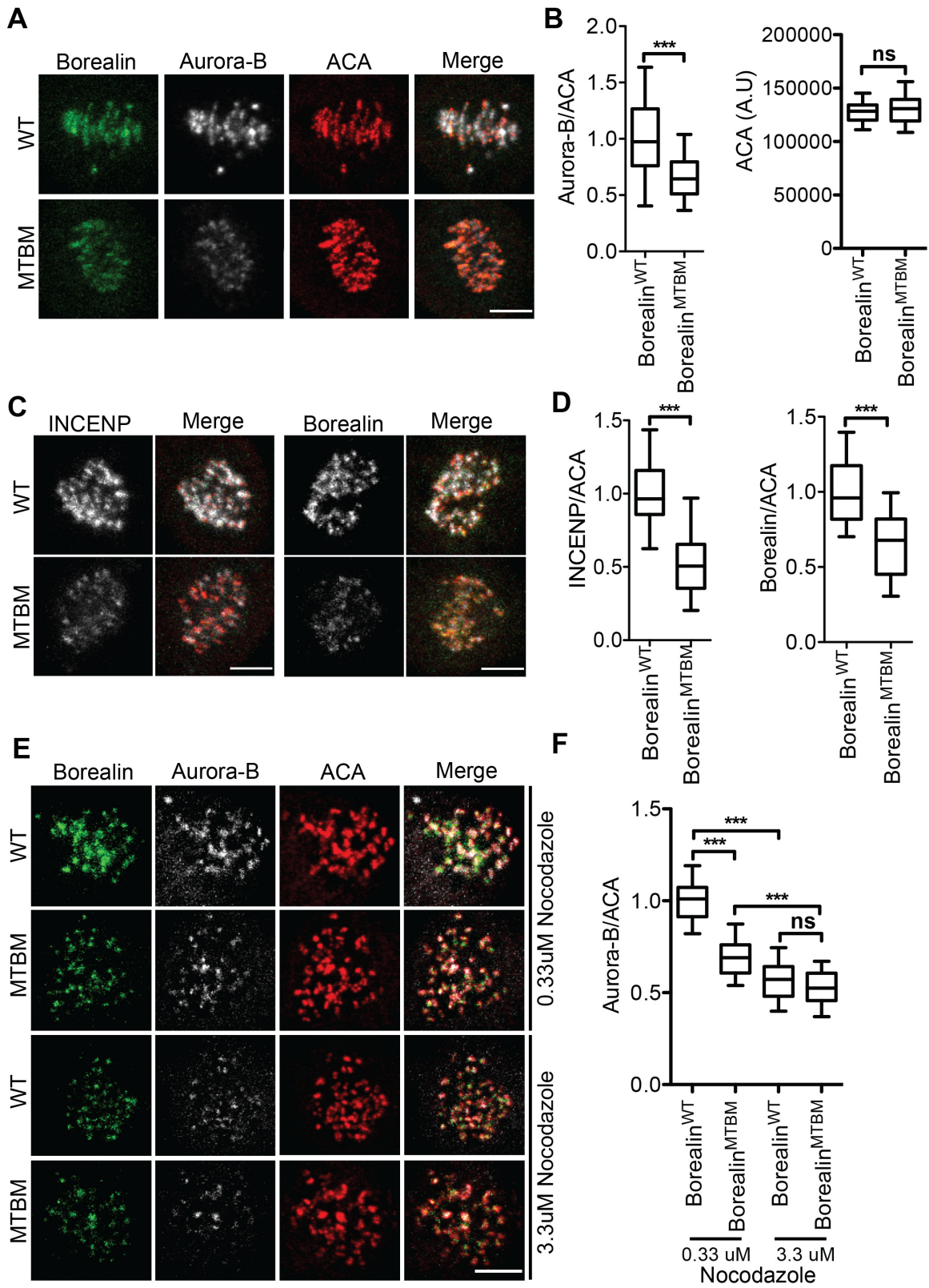


Figure.6

Figure 3-7: Borealin-microtubule interaction enhances kinetochore sub-network of the CPC inner-centromere localization pathway. (A) Schematic of Borealin siRNA mediated knockdown rescue experiment. (B, D) HeLa-TReX cells stably expressing LAP-Borealin^{WT} or ^{MTBM} or ^{Δ20} were treated as in A and immunostained with histone H2a pT120 and H3 pT3 antibodies. (C) Box and whisker graph of histone H2a pT120 intensity normalized by ACA intensity (data from at least 11 cells per condition). (D) Box and whisker graph of histone H3 pT3 intensity (data from at least 10 cells per condition). Statistical analysis was performed using one way ANOVA (Kruskal-Wallis test) with Dunn's Multiple Comparison Test, *** P<0.001; ** P<0.01, * P<0.05 and ns P>0.05. Scale bar is 5μm.

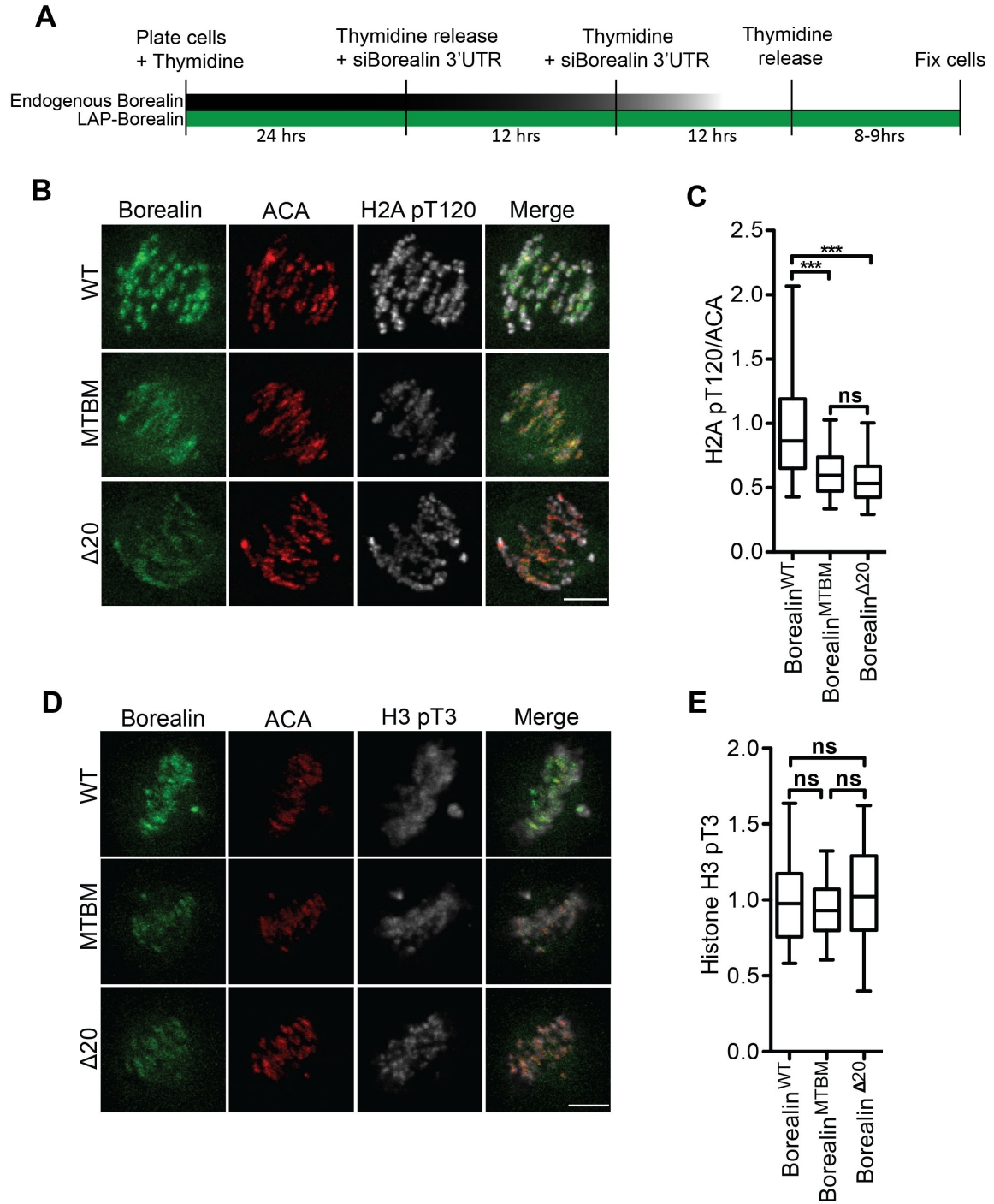


Figure.7

Figure 3-8: Borealin mediated non-centromeric CPC-microtubule interaction is required for robust phosphorylation of the kinetochore substrates by the CPC. (A) Schematic of experimental procedure, for C and D, Borealin and Bub1 siRNA mediated knockdown of endogenous Borealin and Bub1 in cells expressing chimeric CenpB^{DBD}-INCENP⁷⁴⁷⁻⁹¹⁸ transgene. (B) Cartoon showing domain structure of INCENP^{WT} and chimeric LAP-CenpB-INCENP⁷⁴⁷⁻⁹¹⁸ protein. (C) Cells expressing LAP-CenpB- INCENP⁷⁴⁷⁻⁹¹⁸, for targeting Aurora-B to the centromeres, were treated with control siRNA (siLuc) or siBorealin to deplete endogenous Borealin as shown in A. Bub1 siRNA and Haspin inhibitor, 2uM 3-ITU, were added before fixation in order to remove the inner-centromeric CPC localization signal. Cells were immunostained with antibodies against Hec1 pS44 and Aurora-B and representative images are shown. (D) Box and whisker graph of normalized Hec1 pS44 intensity and normalized Aurora-B intensity (data from at least 12 cells per condition) (E) Schematic of experimental procedure for F-I. (F) Cells were treated as in E, LAP-CenpB- INCENP⁷⁴⁷⁻⁹¹⁸ and LAP-Borealin^{WT} or LAP-Borealin^{MTBM} expressing cells were treated with siBub1 and haspin inhibitor (2uM 3-ITU) to delocalize the endogenous CPC from the inner-centromere. Endogenous Borealin was depleted with siBorealin treatment and cells were immunostained with Hec1 pS44 (F) and Aurora-B (H) antibodies, representative images are shown. (G) Box and whisker graph of normalized Hec1 pS44 and normalized GFP intensity from F (data from at least 10 cells per condition). (I) Box and whisker graph of normalized Aurora-B and GFP intensity from H (data from at least 10 cells per condition). Statistical analysis performed using Mann Whitney Test, *** P< 0.0001 and ns P> 0.05. Scale bar 5um.

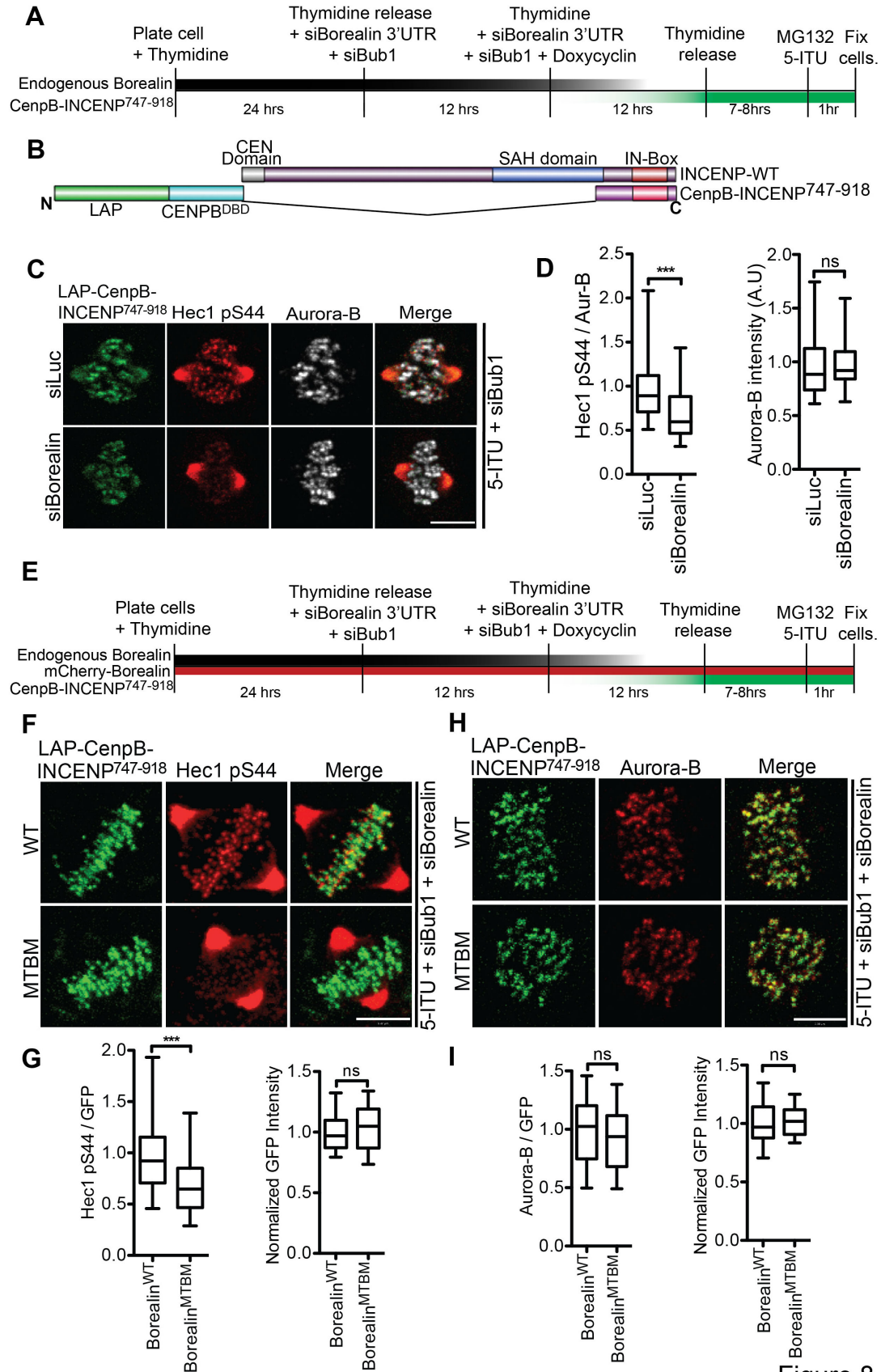


Figure.8

Figure 3-9: Model for kinetochore phosphorylation by the CPC. (A) Model showing phosphorylation of kinetochore by the CPC. Inactive diffusible pool of CPC is auto-activated by centromeric pool. Microtubule binding by the diffusible activated CPC leading to robust kinetochore phosphorylation. The box in the right shows three microtubule-binding domains on the CPC, Borealin MBD (1), INCENP PR/SAH (2) and INCENP^{IN-Box}/Aurora-B (3), different binding modes of the CPC to microtubules are also shown. (B) Cartoon showing effect of the above mechanism on kinetochore phosphorylation by the CPC and its implication to the error correction process. The effective range and amount of centromere activated diffusible CPC is increase by the presence of microtubules in close proximity to the inner-centromere (laterally attached kinetochores or merotelic kinetochores). This increase in amount of the centromere activated non-centromeric CPC near laterally attached or on merotelically attached kinetochores leads to robust kinetochore phosphorylation and release of attachment. During metaphase a relatively larger separation between microtubules and inner-centromere, would lead to reduction in the amount of centromere activated non-centromeric CPC and the concomitant recruitment of phosphatases to the kinetochore in metaphase would lead to stabilization of end-on attachment.

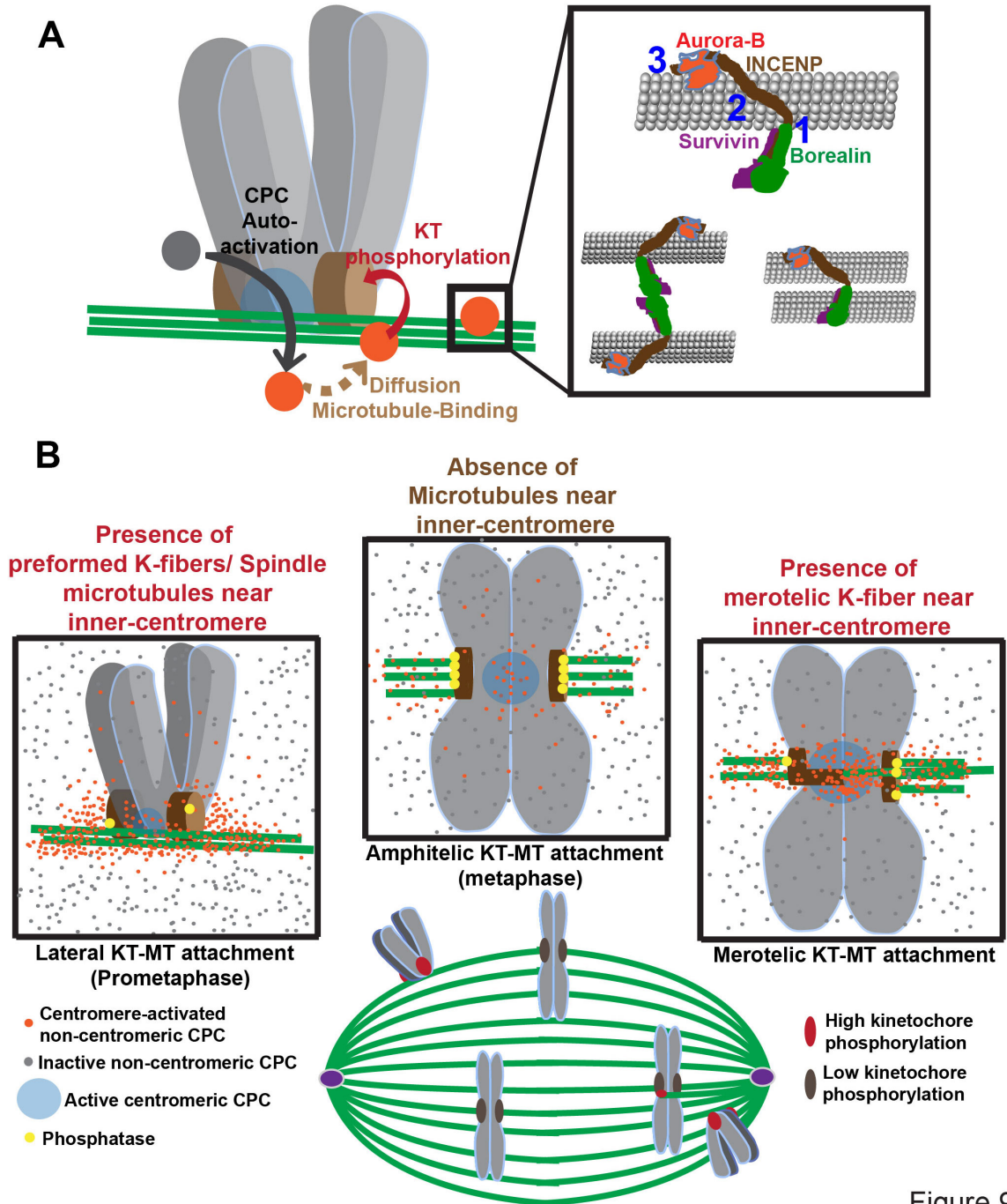
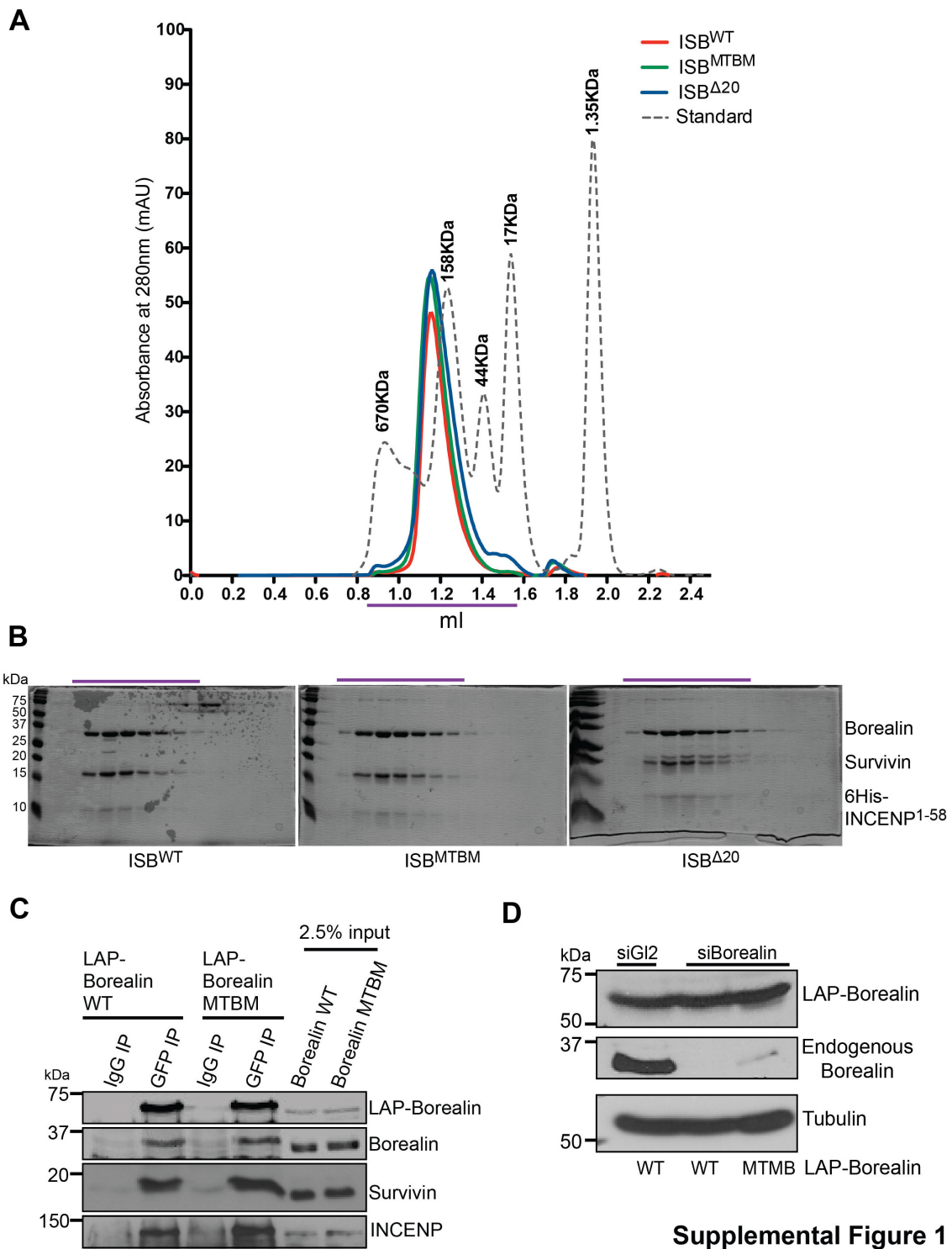
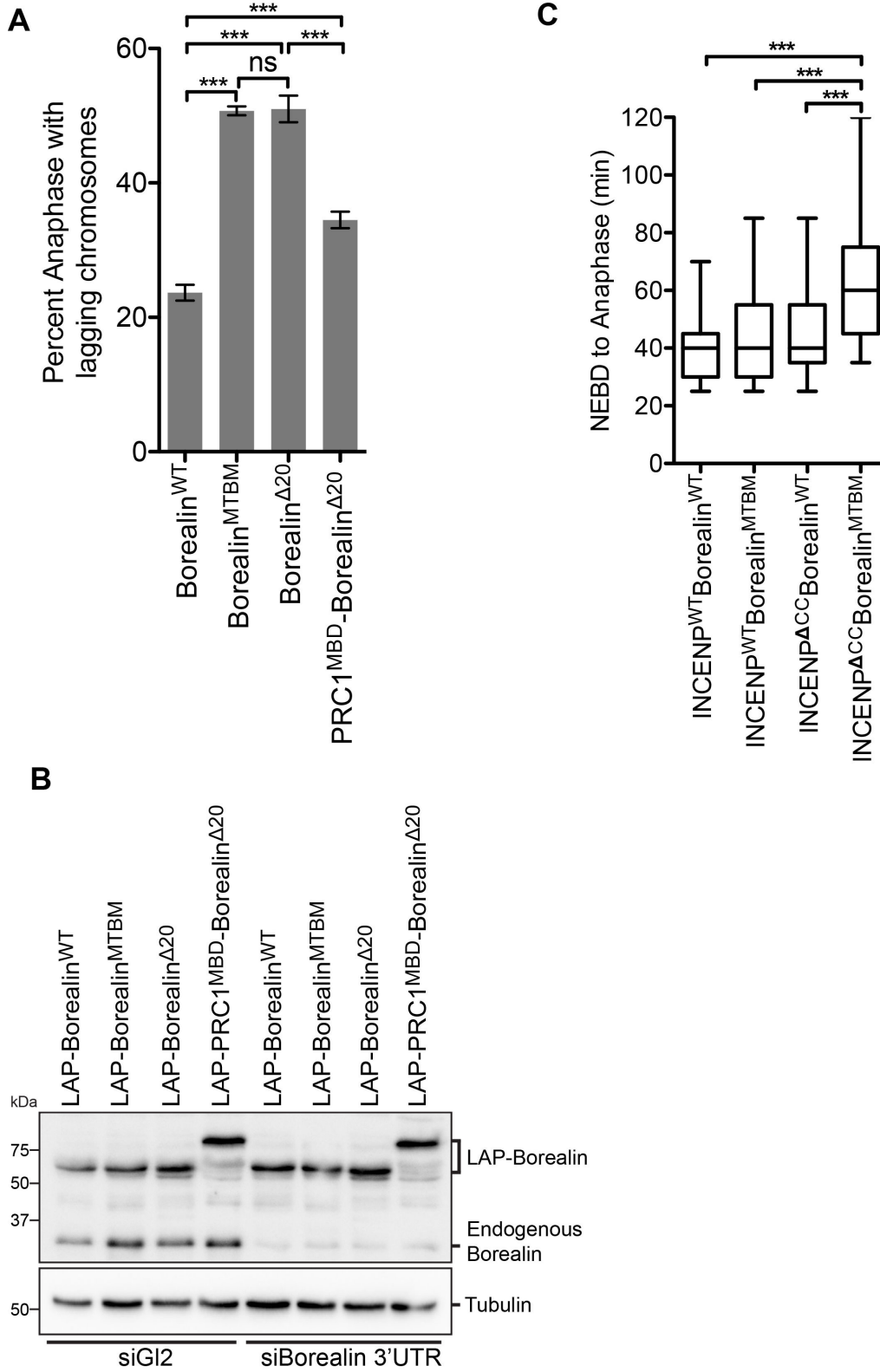


Figure.9

Supplementary figure 3-1: The microtubule binding mutations of Borealin have no effect on the ISB or the CPC complex formation. (A) Graph of the FPLC gel-filtration run on a superdex S-200 column. ISB^{WT} (red), ISB^{MTBM} (green), ISB^{Δ20} (Blue) and FPLC standard (dashed line). (B) Coomassie stained gel of the fractions from the gel filtration run shown in A, purple line on the graph in A and on the coomassie stained gel images indicates the fractions from the FPLC gel-filtration that were loaded on the gel. (C) Western blots from the IP experiment are shown. LAP-Borealin^{WT} and LAP-Borealin^{MTBM} were immuno-precipitated from the nocodazole arrested cell lysate using an anti-GFP antibody. The western blot was probed with antibodies raised against GFP, Borealin, survivin and INCENP. (D) Western blot of the whole cell lysate from the Borealin knockdown rescue experiments as described in 3-2A. Blots were stained with anti-Borealin antibody and GFP antibody; tubulin staining was used as a loading control.

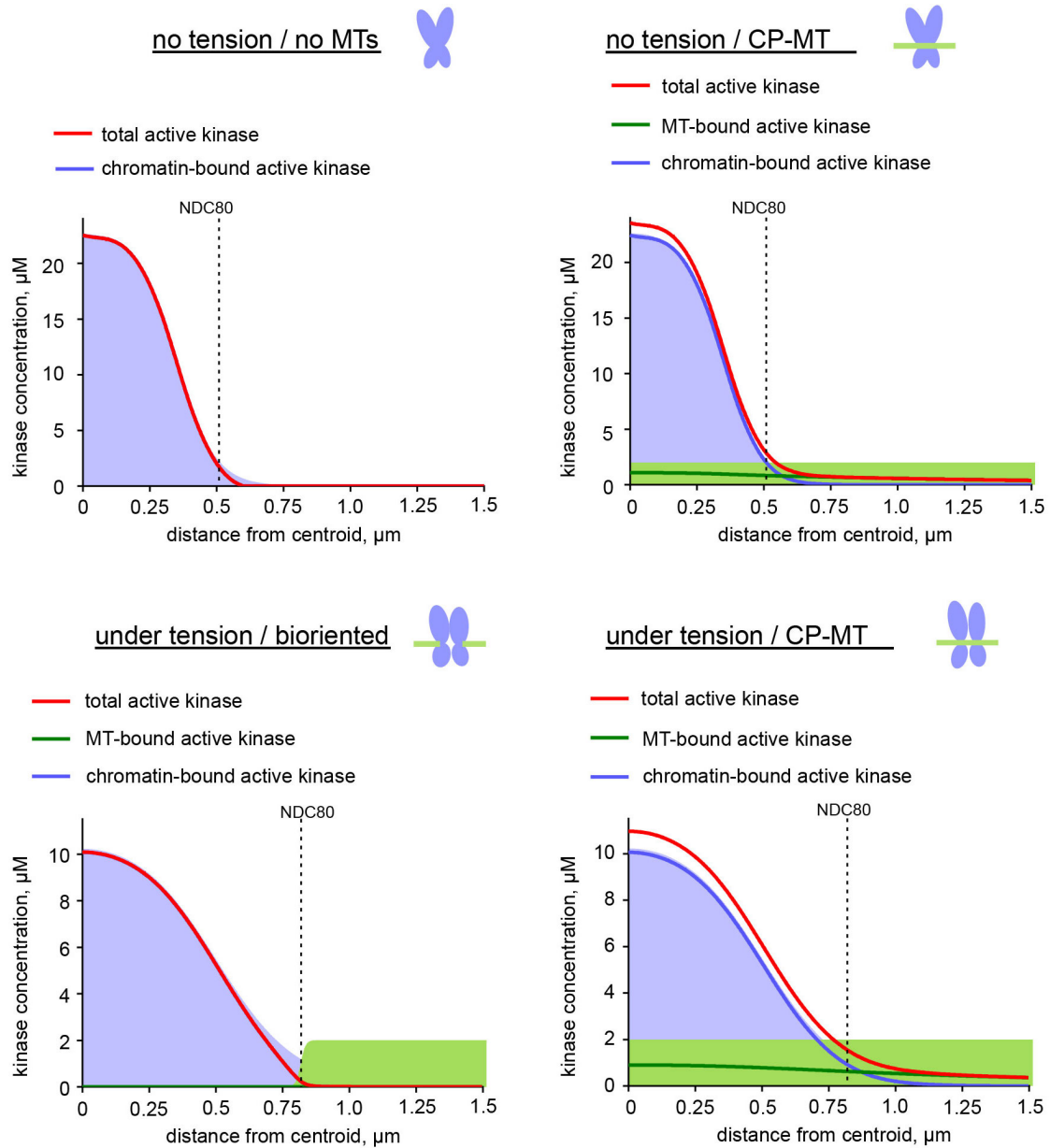


Supplementary figure 3-2: Both Borealin and INCENP microtubule binding domain is important for error free mitosis. (A) Bar graph showing percent of cells undergoing anaphase with lagging chromosomes after STLC release assay, cells were treated as described earlier in 3-2A and rescued with indicated Borealin transgenes. STLC was added 6 hours post 2nd thymidine release for 2 hours. STLC was then washed out and 2 hours post washout cells were fixed (data from 3 independent experiments, at least 84 cells were analyzed per experiment). Error bars represent \pm SD. Statistical analysis was done using one-way ANOVA and Bonferroni's multiple comparison test for both D and E. *** P<0.001; ** P<0.01, * P<0.05. (B) Western blots of the cells expressing the indicated transgenes and treated with siRNA as in 3-2A. (C) Box and whisker graph of nuclear envelope breakdown (NEBD) to anaphase duration for experiment shown in 3-2E. Statistical analysis was performed using Dunn's Multiple Comparison Test *** P<0.001.



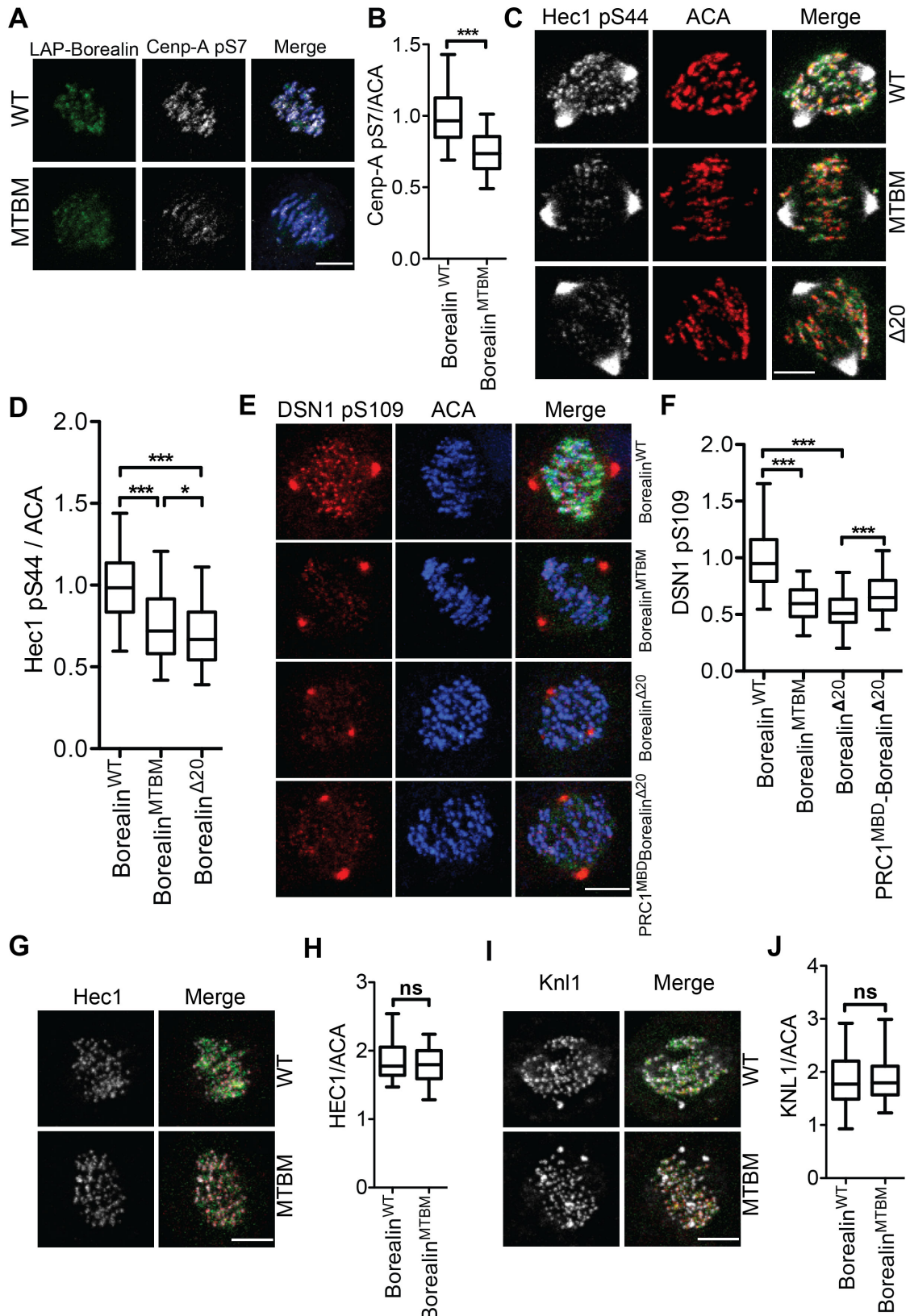
Supplemental Figure 2

Supplementary figure 3-3: Modeling results for spatial distribution of different kinase forms. Concentration profiles along centromere-kinetochore axis as in Fig. 4 B-D but additionally showing active chromatin-bound, active microtubule bound and total active kinase. (Data for this figure was provided by the Grishcuk lab).



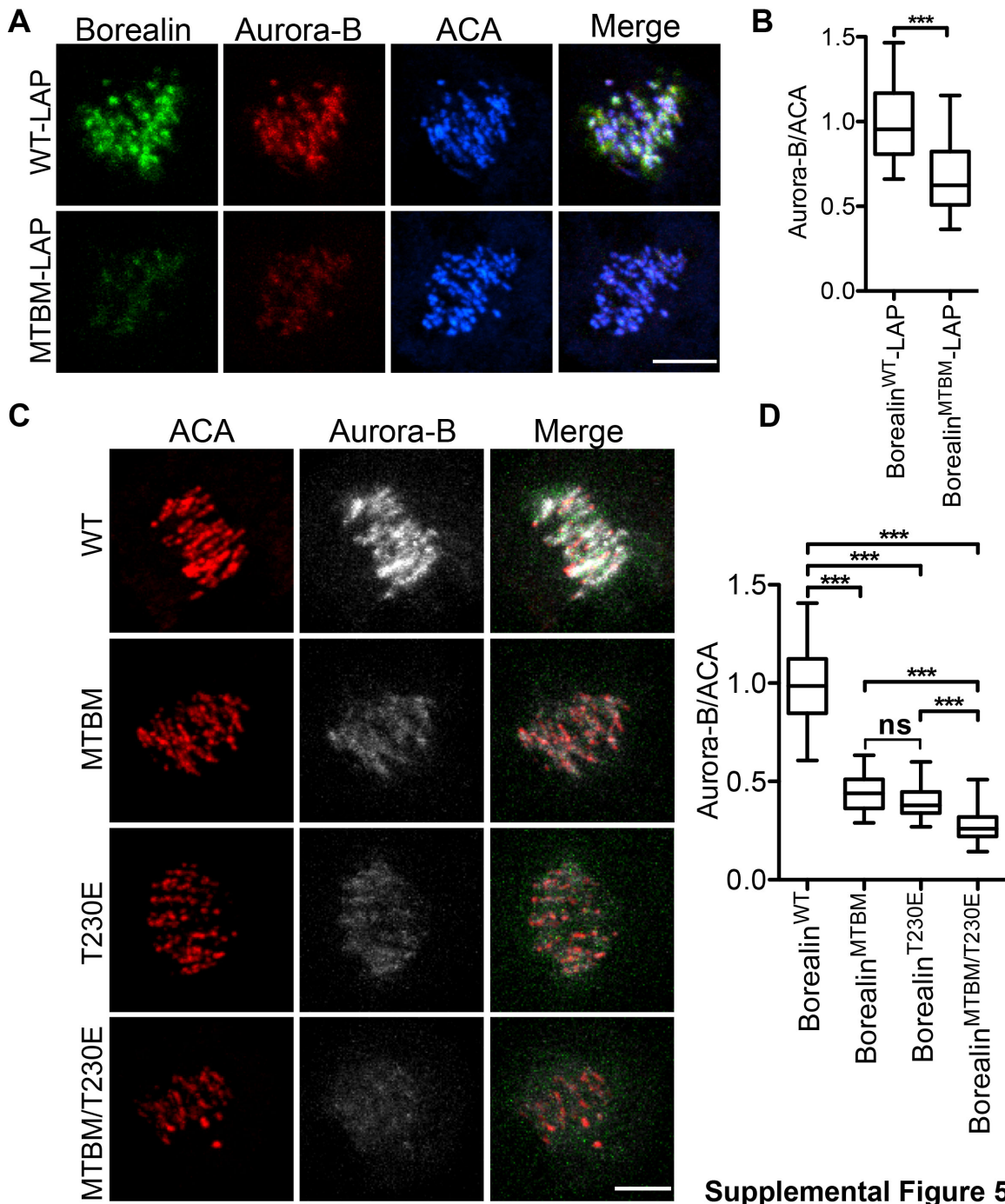
Supplemental Figure 3

Supplementary figure 3-4: Borealin-microtubule interaction is important for robust kinetochore phosphorylation by the CPC. (A) Cells expressing LAP-Borealin^{WT} and LAP-Borealin^{MTBM} were treated as shown in 3-5A and immunostained for CenpA pS7; representative images are shown. (B) Box and whisker graph of normalized CenpA pS7 intensity (data from at least 8 cells per condition). Statistical analysis was performed using Mann Whitney Test, *** P<0.0001. (C) Cells expressing LAP-Borealin^{WT}, LAP-Borealin^{MTBM} and LAP-Borealin^{Δ20} were treated as described in 3-5A and immunostained with Hec1 pS44. Representative images are shown. (D) Box and whisker graph of the normalized Hec1 pS44 intensity from C (data from at least 10 cells per condition). (E) Cells expressing LAP-Borealin^{WT}, LAP-Borealin^{MTBM}, LAP-Borealin^{Δ20} and LAP-PRC1^{MBD}-Borealin^{Δ20} were treated with Borealin siRNA as described in 3-5A. Cells were then immunostained with DSN1 pS109 and ACA. Representative images of the experiment are shown. (F) Box and whisker graph of the normalized DSN1 pS109 intensity from E (data from at least 8 cells). For D and F statistical analysis was done using one way ANOVA (Kruskal-Wallis test) with Dunn's Multiple Comparison Test, *** P<0.001; ** P<0.01, * P<0.05 and ns P>0.05. Cells were treated as described in 3-5A and immunostained with Hec1 (G) or Knl1 (I); representative images are shown. Box and whisker graph of normalized Hec1 (H) or Knl1 (J) intensity (data from at least 6 cells per condition). Statistical analysis was performed using Mann Whitney test for H (P=0.3131) and J (P=0.4431). Scale bar 5μm.

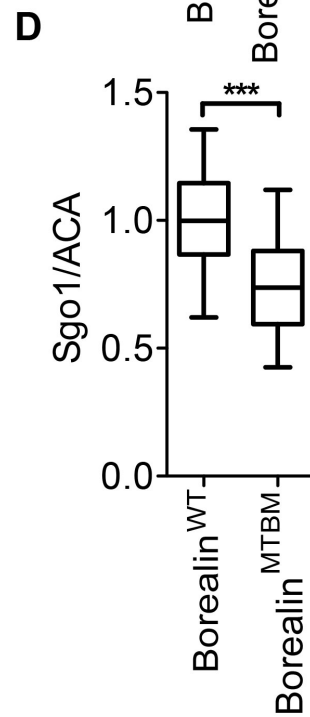
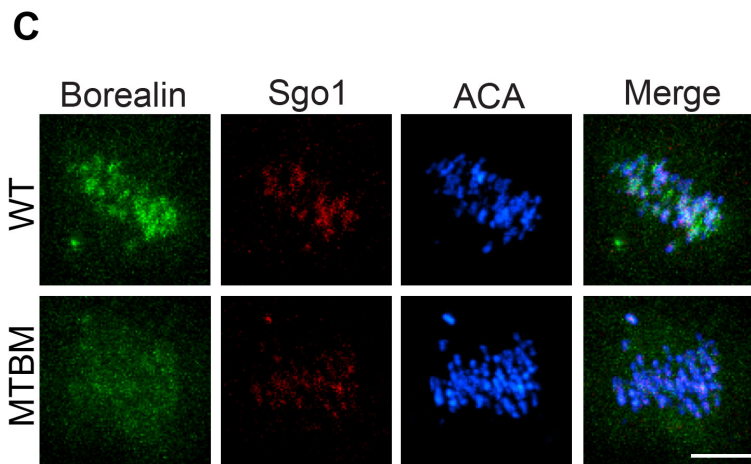
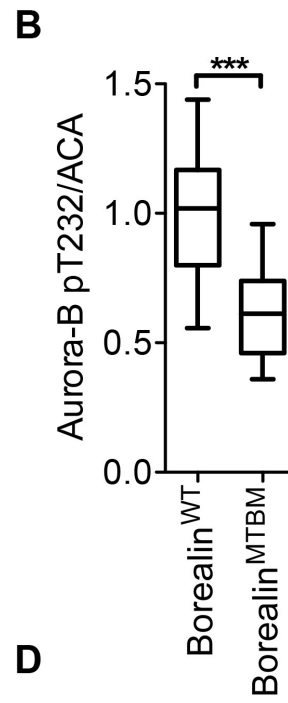
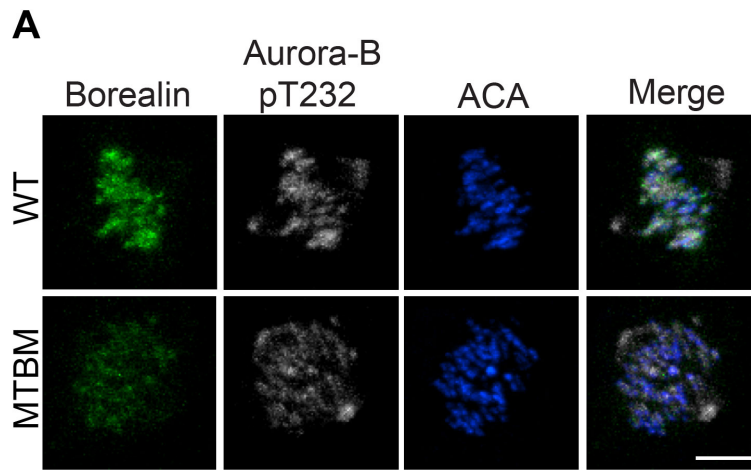


Supplemental Figure 4

Supplementary figure 3-5: Borealin microtubule-binding domain and dimerization domain independently enhance inner-centromere localization of the CPC. (A) Cells expressing C-terminal LAP tagged Borealin^{WT} or Borealin^{MTBM} were treated as in 3-5A and immunostained with antibodies against Aurora-B and ACA. Representative images from the experiments are shown. (B) Box and whisker graph of the normalized Aurora-B intensity from A (data from at least 5 cells per condition). Statistical analysis was performed using Mann Whitney Test, *** P<0.0001. (C) Representative images are shown from the experiment were cells expressing LAP-Borealin^{WT}, LAP-Borealin^{MTBM}, LAP-Borealin^{T230E} (Borealin dimerization mutant) and LAP-Borealin^{MTBM/T230E} were treated as in 3-5A and immunostained with antibodies against Aurora-B and ACA. (D) Box and whisker graph of the normalized Aurora-B intensity from C (data from at least 7 cells per condition). Statistical analysis was done using one way ANOVA (Kruskal-Wallis test) with Dunn's Multiple Comparison Test, *** P<0.001; ** P<0.01, * P<0.05 and ns P>0.05. Scale bar is 5um.

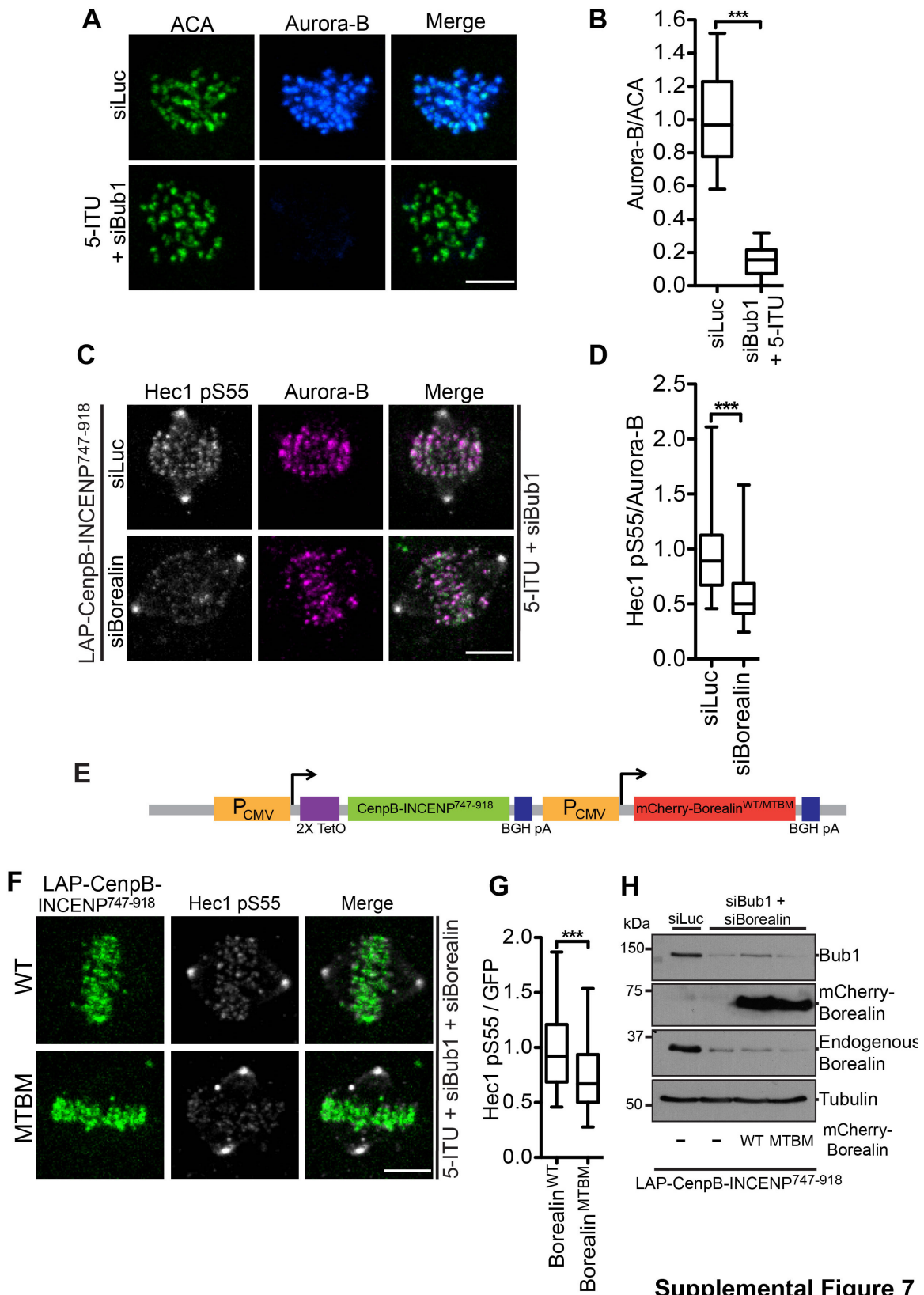


Supplementary figure 3-6: Borealin-microtubule interaction is important for proper centromeric Sgo1 localization. Representative images are shown from the experiment where cells expressing LAP-Borealin^{WT} and LAP-Borealin^{MTBM} were treated as in 3-5A and immunostained with Aurora-B pT232 (A), Sgo1 (C) and ACA. Representative images are shown in A and C. Box and whisker graph of normalized Aurora-B pT232 intensity (B) (data from at least 10 cells) and normalized Sgo1 intensity (D) (data from at least 8 cells per condition) in cells expressing LAP-Borealin^{WT} and LAP-Borealin^{MTBM}. Statistical analysis was performed using Mann Whitney Test, *** P< 0.0001. Scale bar is 5um.



Supplemental Figure 6

Supplementary figure 3-7: Borealin mediated non-centromeric CPC-microtubule interaction is required for robust phosphorylation of the kinetochore substrates by the CPC. (A) HeLa-Trex cells were either treated as in 3-8A (siBub1 and 2uM 3-ITU), with the exception of doxycycline treatment, or untreated (control). Cells were stained for Aurora-B and ACA after treatment with 3.3uM Nocodazole. (B) Box and whisker graph of normalized Aurora-B intensity from experiment shown in A (data from at least 8 cells per condition). Statistical analysis was done using Mann Whitney Test, *** $P < 0.0001$. Scale bar 5um. (C) Cells were treated as described in figure 3-8A followed by immunostaining with Hec1 pS55 and Aurora-B antibody. Representative images are shown. (D) Box and whisker graph of normalized Hec1 pS55 from experiment shown in C (data from at least 9 cells per condition). (E) Schematic of the construct used for making cell lines stably expressing LAP-CenpB^{DBD}-INCENP⁷⁴⁷⁻⁹¹⁸ under doxycycline induction and constitutively expressing mcherry-Borealin^{WT} or ^{MTBM}. (F) Cells were treated as described in figure 8E followed by immunostaining with Hec1 pS55. Representative images are shown. (G) Box and whisker graph of normalized Hec1 pS55 from experiment shown in F (data from at least 8 cells per condition). Statistical analysis was done using Mann Whitney Test, *** $P < 0.0001$. Scale bar 5um. (H) Western blot showing Borealin and Bub1 knockdown and expression of mCherry-Borealin^{WT} or ^{MTBM} transgene in cells expressing LAP-CenpB-INCENP⁷⁴⁷⁻⁹¹⁸. Tubulin blot is used as loading control.



Supplemental Figure 7

Chapter 4

Outer kinetochore maintenance requires Plk1 and Aurora-B activity before but not after end-on attachment.

This chapter is from the paper under preparation titled: “Outer kinetochore maintenance requires Plk1 and Aurora-B activity before but not after end-on attachment.”

Prasad Trivedi and P. Todd Stukenberg.

Kinetochores are multi-proteins assemblies that mediate the interaction of mitotic chromosomes with the spindle microtubules and act as the scaffold for initiation of the spindle assembly checkpoint (SAC) arrest. Understanding the kinetochore assembly and dynamics is important in order to understand the mechanisms that ensure genomic stability. Although it is clear from the light microscopy studies that the core kinetochore undergoes a major structural change before and after end-on attachment. The molecular basis for this change has remained mysterious. Here, we find that the kinase Plk1 plays a critical role in maintenance of the core KMN complex at the kinetochores before, but not after, end-on kinetochore-microtubule attachments. The HIKM complex recruits Plk1, which regulates an interaction between HIKM and the Ndc80 complex. The KMN that is recruited by Plk1 is proficient at generating spindle checkpoint signals. We also show that Plk1 and Aurora B kinase play a parallel role in maintenance of KMN before end-on attachment and this activity is required to maintain the SAC arrest in absence of microtubules. Our observations suggest that the core kinetochore is maintained differentially before and after end-on attachment and the current model of kinetochore organization, that are largely based on the *in-vitro* reconstitution studies, are more representative of metaphase kinetochore.

Introduction:

Kinetochores undergo dramatic changes after they bind the plus ends of spindle microtubules using the Ndc80 complex (end-on attachment) (Howell et al., 2001; Magidson et al., 2015; Smith et al., 2016; Varma et al., 2013; Wynne and

Funabiki, 2015; 2016). Before this critical event they generate spindle assembly checkpoint signals (SAC) that prevent the onset of anaphase (Stukenberg and Burke, 2015). Moreover, at the stage before end-on attachment the major attachments to microtubules are likely through the microtubule-motors CENP-E and dynein (Tanaka, 2012). In addition, there is growing data that before end-on attachment kinetochores assemble preformed K-fibers (Maiato et al., 2004; Mishra et al., 2010; Sikirzhytski et al., 2018; Tulu et al., 2006), which are bundles of microtubules that extend out from kinetochores to increase the frequency of capture events. In contrast, it is thought that these activities are silenced after kinetochores obtain end-on attachments and new activities that control the movements of chromosomes are activated.

These change in the function of kinetochore correlates with the change in the protein composition of the kinetochore. A number of proteins important for SAC or lateral attachment are increased at the kinetochores before end-on attachment and their recruitment is further enhance upon arresting cells for longer duration in absence of microtubules (Sacristan et al., 2018; Thrower et al., 1996; Wynne and Funabiki, 2015; 2016). These proteins are often removed after end-on attachments by dynein dependent process termed as stripping (Howell et al., 2001). Apart from changes in the amounts of fibrous corona proteins changes in the organization and amount of the core outer-kinetochore proteins have also been observed before and after end-on attachment (Magidson et al., 2015; Wynne and Funabiki, 2015; 2016). The mechanisms underlying these organizational changes in kinetochore before and after end-on attachment are still mysterious and may underlie proper kinetochore

function and spacio-temporal coordination between discrete processes at the kinetochores.

Apart from the structural changes in kinetochore one of the most conspicuous changes that occur after end-on attachment is the reduction of key mitotic kinases like Mps1, Aurora-B and Plk1 at the centromere/kinetochore and a concomitant recruitment of phosphatase PP1 to the kinetochores (Hiruma et al., 2015; Ji et al., 2015; Lénárt et al., 2007; Liu et al., 2010; Nijenhuis et al., 2014; Salimian et al., 2011; Sivakumar et al., 2016; Stukenberg and Burke, 2015; Trivedi and Stukenberg, 2016). Although it is clear that the change in kinase and phosphatases before and after end-on attachment is critical for the function of kinetochore, how these changes control the structural dynamics of the kinetochore is still mysterious.

The key components for outer kinetochore is the KMN network (Knl1, Mis12 complex and Ndc80 complex), which is a 10-protein assembly consisting of the Knl1 complex (consisting of Knl1 and Zwint), Mis12 complex (consisting of Mis12, Dsn1, Nnf1, and Nsl1), and Ndc80 complex (consisting of Ndc80, Nuf2, Spc24, and Spc25). KMN forms the core of the outer kinetochore and mediates the attachment of the spindle microtubules with the chromatin and is responsible for coupling the force generated by the depolymerizing microtubules to the chromosomes in order to move the chromosomes during mitosis (Musacchio and Desai, 2017). In absence of the end-on kinetochore-microtubule attachment KMN also serves as the scaffold on which the spindle assembly checkpoint proteins localize and initiate SAC (Stukenberg and Burke, 2015). KMN is thus central to both SAC and kinetochore-microtubule attachment, it is, therefore, important to understand the dynamics of

the pathways that control KMN recruitment/maintenance before and after end-on kinetochore-microtubule attachment to understand the structural changes that occur at kinetochores. KMN members display some organizational changes at level of light microscopy before and after end-on attachment in human cells, the mechanism regulating these changes are still mysterious (Magidson et al., 2015; Maresca and Salmon, 2009; Smith et al., 2016; Wynne and Funabiki, 2015; 2016).

KMN is assembled in a phosphorylation-dependent manner on the inner kinetochore, which comprises of the CCAN complexes that make direct contact with the CENP-A nucleosomes (Emanuele et al., 2008; Gascoigne and Cheeseman, 2013; Huis in 't Veld et al., 2016; Yang et al., 2008). Two elongated proteins CENP-C and CENP-T in the CCAN complex recruit majority of the KMN complex to the kinetochores. Each CENP-C molecule through its N-terminal region can recruit one KMN complex in an Aurora-B dependent manner (Kim and Yu, 2015; Rago et al., 2015; Screpanti et al., 2011; Yang et al., 2008). On the other hand, each CENP-T molecule can recruit two Ndc80 complex and one KMN complex through CDK1 dependent interaction with its N-terminal region (Huis in 't Veld et al., 2016; Rago et al., 2015). Apart from CENP-T and CENP-C, another CCAN component CENP-I also plays a role in recruiting some Ndc80 molecules either directly or through CENP-T and this is important for maintenance of SAC in absence of Aurora-B activity and microtubules (Basilico et al., 2014; Kim and Yu, 2015; Matson et al., 2012). It is largely though that the same interactions drive the KMN network recruited to the inner kinetochore throughout mitosis. Given a global switch in kinase and phosphatases that occurs at kinetochores before and after end-on attachment it is

unclear how the KMN stability is maintained before and after end-on attachment given a phospho-dependent assembly mechanism.

Here we describe a mechanism for KMN maintenance that is regulated by the attachment status of the kinetochores. We show that KMN maintenance at the kinetochore requires Aurora-B and Plk1 activities before but not after end-on attachment. Aurora-B and Plk1 activity are required for KMN maintenance in absence of microtubules even when the CDK1 is still present. We also show that Aurora-B and Plk1 regulate parallel pathways for Ndc80 recruitment. Plk1 regulates the Ndc80 complex recruitment through the CENP-I dependent Ndc80 recruitment pathway. We further show that CENP-I and Ndc80 interact before the end-on attachment but not after the formation of end-on attachment. Finally, we demonstrate that Aurora-B and Plk1 ensure the maintenance of SAC arrest in absence of microtubules by stabilizing KMN at the kinetochores.

Results:

Treating cells with the Eg5 inhibitor (STLC) generates monopolar spindles and is an ideal system to study the effect of kinetochore microtubule attachments since the two sister kinetochores often have different attachment states. Specifically, the poleward-facing sister has end-on attachments, while the anti-poleward sister generates preformed k-fibers using lateral attachments. We quantified the amount of Ndc80 at poleward and anti-poleward sister kinetochores and the amount of Ndc80 was significantly reduced at anti-poleward kinetochores (Fig.4-1A-C), suggesting that there may be different modes of recruitment of Ndc80 to

kinetochores in different attachment states.

We next arrested cells in a monopolar state, then treated them with Plk1 inhibitor (BI2536) and measured the level of Ndc80 by immunofluorescence. Note we added Plk1 inhibitors to cells already arrested in mitosis by STLC to avoid complications of kinetochore assembly pathways. There was a greater reduction of Ndc80 from the anti-poleward sister after the addition of Plk1 inhibitors compared to cells treated with DMSO, while the reduction in the Ndc80 levels at the poleward sister was subtle upon treatment with Plk1 inhibitor (Fig.4-1A-C). These data suggest that Plk1 activity maintains Ndc80 at kinetochores before, but not after, end-on attachment.

Plk1 is known to play a role in Aurora-B activation during mitosis (Carmena et al., 2014; Ghenoiu et al., 2013; Zhou et al., 2014) and given an established role of Aurora-B in recruiting KMN to the kinetochores (Kim and Yu, 2015; Rago et al., 2015; Yang et al., 2008); it is possible that the reduction of the Ndc80 levels at the kinetochore upon Plk1 inhibition was indirectly due to lowered Aurora-B activity. To test whether Plk1 regulates Ndc80 at unattached kinetochore by activating Aurora-B we treated the cells arrested in mitosis, with high dose of nocodazole, with either Aurora-B inhibitor (ZM), Plk1 inhibitors (BI) or both inhibitors. Consistent with an established role of Aurora-B in recruiting KMN to the kinetochore we found that Ndc80 levels are reduce at centromeres (~25%) upon treatment with the Aurora-B inhibitor, confirming a role for Aurora-B in KMN maintenance before end-on attachment. Interestingly, for cells in nocodazole the Ndc80 levels were drastically reduced (~70%) upon simultaneous inhibition of both Aurora-B and

Plk1 (Fig.4-1D-F) and this reduction in Ndc80 levels at kinetochore was more severe than the reduction seen upon inhibition of either one of the kinases. Note we also included MG-132 to prevent the cells from exiting mitosis (see below) and this also ensured that Cyclin-B-Cdk1 activity remained high, which is important for the recruitment of Ndc80 to CENP-T. Other KMN members (Mis12, Zwint and Knl1) and outer kinetochore proteins, ZW10 and CENP-F, were also severely reduced or absent from the kinetochores upon inhibition of Aurora-B and Plk1 (Fig.4-1J). In contrast, the CCAN components CENP-C and CENP-I did not change upon Aurora-B and Plk1 inhibition (Fig.4-1J). This observation suggests that the Plk1 and Aurora-B play an independent role in maintenance of KMN and other outer kinetochore components at the kinetochore in absence of microtubules. Moreover, the difference in reduction of Ndc80 levels upon Plk1 inhibition alone in STLC and nocodazole suggests that Ndc80 is actively removed from the anti-poleward kinetochores in a microtubule dependent manner, which is likely dynein stripping.

Plk1 and Aurora-B levels are reduced upon end-on attachment and are required to maintain KMN at kinetochores before end-on attachment. To test if Plk1 and Aurora-B activity are also required to maintain KMN at end-on attached kinetochores, we arrested in metaphase state by treatment with MG-132, and then added ZM, BI or both. We specifically visualized metaphase cells where all kinetochores should be attached in an end-on fashion. We observed ~20-25% reduction in Ndc80 levels at kinetochore upon treatment with either Aurora-B or Plk1 inhibitor alone (Fig.4-1G-I), which was similar to the nocodazole treated condition when microtubules were absent. When the metaphase arrested cells were

treated with both Plk1 and Aurora-B inhibitors we saw no further reduction of Ndc80 at kinetochores (Fig.4-1G-I). Thus, Aurora-B and Plk1 is not required to maintain most Ndc80 after end-on attachment.

It has been demonstrated that Plk1 cooperates with Mps1 to phosphorylate the MELT repeats on Knl1 (Schubert et al., 2015). Plk1 also cooperates with Aurora-B to maintain SAC arrest in absence of microtubules (O'Connor et al., 2015). However, it is unclear if phosphorylation of MELT repeats is only role of Plk1 in maintenance of the SAC arrest. Since the presence of KMN at the kinetochore is critical for maintenance of SAC arrest and our observation that the KMN maintenance in absence of microtubules requires Aurora-B and Plk1 activity, suggested that the loss of SAC arrest upon inhibition of Plk1 and Aurora-B may be due to destabilization of KMN complex itself. We first confirmed that SAC arrest in HeLa-TReX, 293-T, a DLD-1 and RPE-1 cells in absence of microtubules is indeed dependent on Plk1 and Aurora-B activity (Fig.4-2A-D). We reasoned that if the loss of SAC upon Aurora-B and Plk1 inhibition was due to reduction of KMN then restoring the KMN complex under these conditions should rescue the SAC arrest. Aurora-B phosphorylates Dsn1 on S100 and S109 to positively regulate KMN assembly (Huis in 't Veld et al., 2016; Kim and Yu, 2015; Rago et al., 2015; Yang et al., 2008). We thus tested if expression of the phospho-mimetic mutant of Dsn1 S100E and 109E can rescue the loss of SAC in absence of microtubules upon Plk1 and Aurora-B inhibition. Indeed, we saw a partial rescue of SAC arrest in cells overexpressing Dsn1 S100E and S109E (Fig.4-2E). We conclude that Aurora-B and Plk1 kinases play an independent role in maintenance of SAC arrest in absence of

microtubules by stabilizing the KMN components at the kinetochore.

Apart from Plk1, CENP-I also plays an Aurora-B independent role in maintenance of SAC arrest by stabilizing KMN components at the kinetochore (Kim and Yu, 2015; Matson and Stukenberg, 2014; Matson et al., 2012). Therefore, we determined if Plk1 regulates the CENP-I dependent branch of SAC arrest. To test this we inhibited Aurora-B or Plk1 or both in nocodazole arrested HeLa-TReX cells that are either treated with control or CENP-I siRNA and determined the percent of cells in mitosis at the end of the treatment. Cells in which either CENP-I was depleted or Plk1 was inhibited maintained SAC arrest in presence nocodazole (Fig.4-3A-B). As previously seen, CENP-I depleted cells or Plk1 inhibitor treated cells were unable to maintain SAC arrest upon treatment with Aurora-B inhibitor (Fig.4-2A-E, 3-3A-B). In contrast, cells in which CENP-I was depleted and Plk1 kinase activity was inhibited could still maintain the SAC arrest (Fig.4-3A-B). This suggests that CENP-I and Plk1 function is the same pathway for SAC maintenance that is independent from the Aurora-B dependent pathway.

CENP-I also plays a role in SAC maintenance by enabling recruitment of KMN to the kinetochore in absence of microtubules, similar to our observation with Plk1. To determine the role of Plk1 in regulating the Aurora-B independent arm of SAC arrest and KMN maintenance we tested how CENP-I and Plk1 regulate each other. We first determined if Plk1 and CENP-I regulate localization of each other to the kinetochore. As we mentioned before CENP-I recruitment was not affected upon either Plk1 or Aurora-B or both (Fig.4-1J). CENP-I is required for recruitment of CENP-U, which is one of the established Plk1 recruiter at the kinetochores (Foltz et

al., 2006; Kang et al., 2006; Okada et al., 2006). We thus tested if CENP-I is required for Plk1 localization to the kinetochore. Both Plk1 kinase localization and a *bona fide* Plk1 substrate phosphorylation (BubR1 pT680) at the kinetochore were dramatically reduced upon CENP-I depletion (Fig.4-3C-E). We therefore conclude that Plk1 functions downstream of CENP-I to maintain SAC arrest and KMN stability in absence of microtubules.

CENP-I recruits Ndc80 complex to the kinetochore either directly or indirectly through CENP-T (Kim and Yu, 2015; Matson et al., 2012). Since, Plk1 functions downstream of CENP-I in maintaining SAC arrest we tested whether Plk1 kinase regulated an interaction between Ndc80 and CENP-I. We immunoprecipitated Ndc80 from HeLa-TReX cells, that were arrested in mitosis using nocodazole. We observed an interaction between CENP-I and Ndc80 as previously reported and also found that the interaction was reduced in presence of a Plk1 inhibitor (Fig.4-4A). This suggested that Plk1 positively regulates interaction between CENP-I and Ndc80.

To test whether the interaction between CENP-I and Ndc80 was regulated by kinetochore attachment state we immunoprecipitated Ndc80 from the cells arrested in presence of 0.33uM nocodazole and then either washed and incubated the cells for two hours in 0.33uM nocodazole, representing the state before end-on attachment, or MG132, representing state of an end-on attached kinetochore. Interestingly, Ndc80-CENP-I interaction was only seen in prometaphase like condition but not in metaphase like condition, when the end-on attachments are already formed (Fig.4-4B). Normally Plk1 is removed from metaphase kinetochores.

To test if the loss of Plk1 is the reason behind reduction of the Ndc80-CENP-I interaction after kinetochores obtain end-on attachments we forced targeted Plk1 to metaphase aligned kinetochores and determined the interaction between Ndc80 and CENP-I. We exogenously targeted Plk1 to three different locations on the centromeres/kinetochores, through expressing chimeric proteins where Plk1 was fused with CENP-B DNA binding domain (CENP-B^{DBD}) or Mis12 or Nuf2; and immunoprecipitated Ndc80 from the cells that were arrested in metaphase state using the strategy describe before. The targeting of Plk1 to centromeres through CENP-B^{DBD} and to kinetochores through Mis12 was sufficient to restore Ndc80-CENP-I interaction even in metaphase like state (Fig.4-4C, D). We conclude that the Plk1 activity near the inner-kinetochore is required to allow Ndc80 recruitment through CENP-I dependent pathway before end-on attachment but not after end-on attachment.

Discussion:

Here we demonstrate that Aurora-B and Plk1 activity is required for the stabilization of the KMN kinetochore proteins before but not after the end-on attachment. We confirm that Aurora-B regulates the direct interaction between Mis12 complex and CENP-C, whereas Plk1 regulates the interaction between CENP-I and Ndc80 complex. We also show that Plk1 regulated CENP-I-Ndc80 interaction specifically occurs in prometaphase before end-on attachment and is important for maintenance of SAC arrest in absence of microtubules and Aurora-B activity. Changes in the organization of the kinetochore before and after end-on attachment

have been observed by light microscopy studies (Magidson et al., 2015; Maresca and Salmon, 2009; Wynne and Funabiki, 2015; 2016). Although, dramatic changes occur in the amount of spindle assembly checkpoint proteins or proteins that promote lateral attachment at kinetochore upon end-on attachment, the core kinetochore components like KMN are shown to change only subtly before and after end-on attachment (Magidson et al., 2015; Wynne and Funabiki, 2016). Therefore our findings are surprising as it was assumed that the KMN is recruited in early prophase where it remains until late anaphase.

From our observations it is clear that the Plk1 regulates the interaction between CENP-I and Ndc80 complex, however, the identity of Plk1 substrates that are important for this regulation is still mysterious. Given a plethora of Plk1 substrates and phosphorylation sites that have been mapped by phospho-proteome studies (Santamaria et al., 2011), there is a need for extensive careful work to identify and characterize the key substrate. Unfortunately, our initial attempts to identify the key Plk1 substrates have not yielded any positive results. However, we have enabled a number of future studies by defining a new role for Plk1 and identifying a number of new assays for Plk1 in regulating kinetochore assembly.

Our finding can explain the dependence of SAC on Aurora-B and Plk1 activity in absence of microtubules. Based on our observation we suggest that at least one key function of Plk1 and Aurora-B in the maintenance of SAC, in absence of microtubules, is to maintain kinetochore structure to allow the SAC signaling; this is different from the previously reported function of Plk1 in phosphorylating MELT repeats on Knl1. It is tempting to speculate that the KMN that is specifically

recruited to kinetochores before attachment would be more adept at SAC signaling than the KMN recruited after attachment.

Ndc80 can be a cargo of dynein and can get stripped from the kinetochores in a dynein-dependent process after the addition of azide (Silva et al., 2014). Our observation of dependence of Ndc80 localization at antipoleward kinetochore on Plk1 activity suggests that the CENP-I-Ndc80 interaction plays a crucial role in preventing dynein-dependent stripping of Ndc80 complex from the kinetochores by stabilizing the Ndc80 interaction with the inner-kinetochore. Dynein moves the whole mitotic chromosome during prometaphase but upon end-on attachment, it walks away from the kinetochores with a subset of kinetochore proteins, the molecular basis for this switch in cargo is unexplained. It is tempting to hypothesize that Aurora-B and Plk1 dependent stabilization of Ndc80 complex allows for a strong interaction between dynein recruitment module and Ndc80 complex, which allows the dynein to move the whole chromosomes. Upon end-on attachment the reduction of Plk1 and Aurora-B at the kinetochore reduces strength of interaction between Ndc80 complex and the CCAN, which allows removal of only a subset of proteins from the kinetochore. Ndc80 is not stripped because it now generates new attachments through CENP-T. The identity of Plk1 substrates will be important to test this hypothesis.

Appreciating that Plk1 controls the state of kinetochores before end-on attachment may also provide insight into why Plk1 is required to generate end-on attachments (Liu et al., 2012). Current models suggest that this is due to the phosphorylation of the KARD domain on BubR1 that recruits PP2A, but whether this is the only role of

Plk1 has not been tested (Suijkerbuijk et al., 2012). It is possible that the kinetochore state before attachment is an important intermediate that matures into an end-on attachment. For example, there may be a kinetic barrier to simply catching a microtubule end so that kinetochores require mechanisms to bind the side of a microtubule and then convert then into end-on attachment.

Finally, dramatic structural changes that occur at kinetochore have been characterized in a process called intra-kinetochore stretch by light microscopy (Maresca and Salmon, 2009; Uchida et al., 2009). This process is thought to underlie the silencing of the SAC. Plk1 may regulate the intra-kinetochore stretch by regulating the interaction between CENP-I-Ndc80 complex. In fact, targeting of Plk1 to kinetochores generates kinetochores with lower stretch suggesting that Plk1, rather than the pulling forces of microtubules, may be the central regulator of this process (Liu et al., 2012).

Materials and Methods:

Immuno-florescence, immune-precipitation and western-blotting protocols are same as described in chapter 2.

Figure 4-1. Aurora-B and Plk1 activity is required to stabilize outer kinetochore before end-on attachment but not after attachment. (A) Micrographs of HeLa-TReX cells arrested in mitosis for 1.5 hours with STLC and treated with either Plk1 inhibitor (100nM BI-2536) or DMSO for 1.5 hour and stained for Ndc80 and CENP-T. All treatments were done in presence of MG-132. (B) Box and whisker graph of Ndc80 intensity from experiment shown in A. (C) Box and whisker graph of CENP-T intensity from experiment shown in A. (D) Micrographs of HeLa-TReX cells arrested in mitosis for 1.5 hours with nocodazole (3.3uM) and treated with either Plk1 or Aurora-B (2uM ZM447439) inhibitor or both for 1.5 hour. All treatments were done in presence of MG-132. (E) Box and whisker graph of Ndc80 intensity from experiment shown in D. (F) Box and whisker graph of CENP-T intensity from experiment shown in D. (G) Micrographs of HeLa-TReX cells arrested in mitosis for 2 hours with MG-132 (10uM) and treated with either Plk1 or Aurora-B (2uM ZM447439) inhibitor or both for 1.5 hour. (H) Box and whisker graph of Ndc80 intensity from experiment shown in G. (I) Box and whisker graph of CENP-T intensity from experiment shown in G. (J) Table showing presence of indicated proteins at the kinetochore in presence of the indicated treatment. For statistical analysis, Mann Whitney test was applied and ns indicates $P > 0.5$, *** indicates $P < 0.0001$, ** indicates $P < 0.001$. Scale bar 5um.

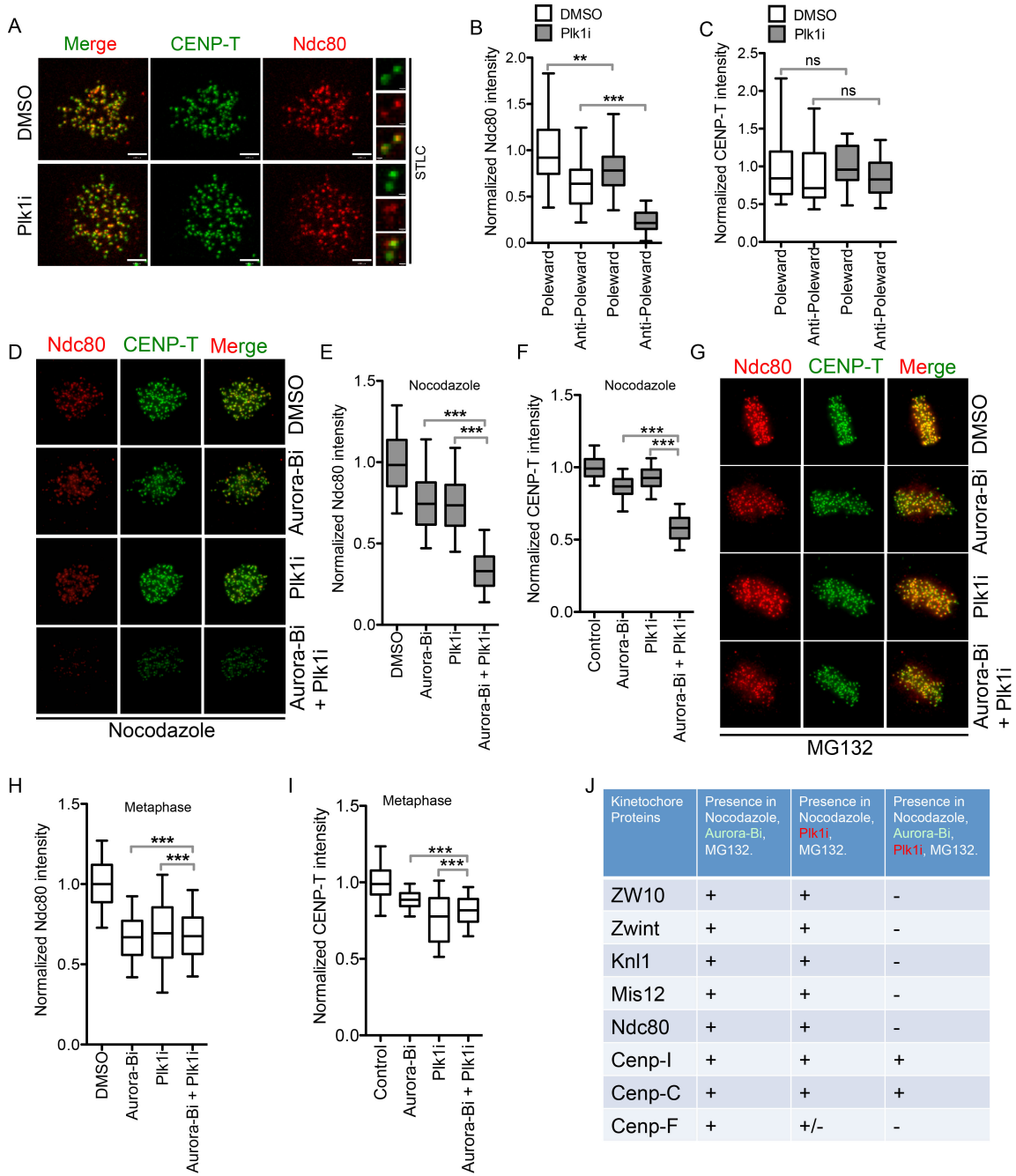


Figure.4-1

Figure 4-2. Aurora-B and Plk1 maintain SAC arrest in absence of microtubules by stabilizing outer-kinetochore. (A) Schematic of the experimental setup for B-D.

Cells were arrested in mitosis by treating with nocodazole. The cells were then treated with Plk1 and Aurora-B inhibitor as indicated. (B) Graph showing mitotic index under indicated condition from the experiments shown in A. Western blot of Cyclin-B1 from HeLa-TREX (C), RPE1 (D) and DLD1 (D) cells treated as shown in A. (E) Western blot showing Cyclin-B1 levels in nocodazole arrested cells treated as indicated. Tubulin was used as a loading control.

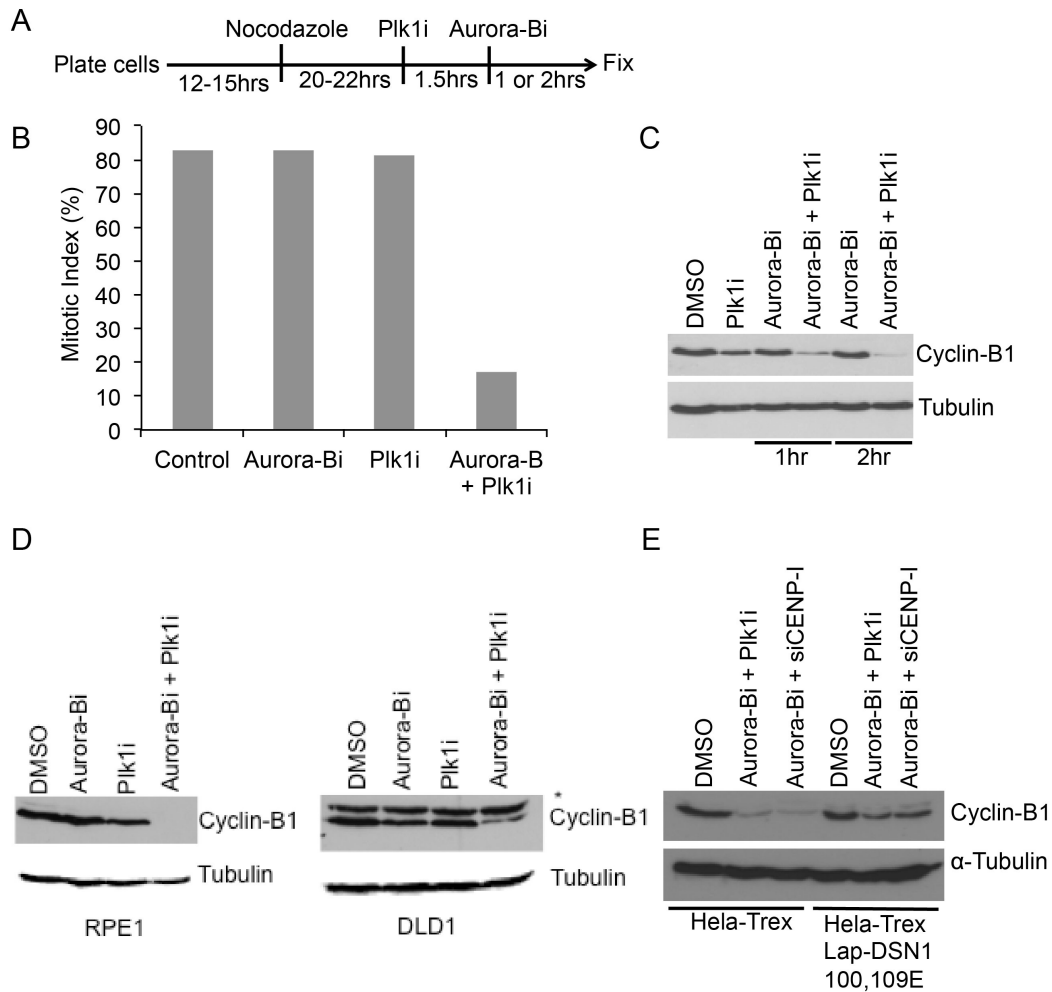


Figure. 4-2

Figure 4-3. Plk1 is in the CENP-I dependent pathway of SAC maintenance. (A) Schematic of the experimental setup for experiment shown in B. (B) Mitotic index for cells treated as in A under indicated condition. (C) Micrographs showing staining of Plk1 and ACA in HeLa-TReX cells treated with either control or CENP-I siRNA. (D) Box and whisker graph of Plk1 intensity from experiment shown in C. For statistical analysis, Mann Whitney test was applied *** indicates $P < 0.0001$. (E) Micrographs showing staining of BubR1 pT680 and ACA in HeLa-TReX cells treated with either control or CENP-I siRNA. Scale bar 5 μ m.

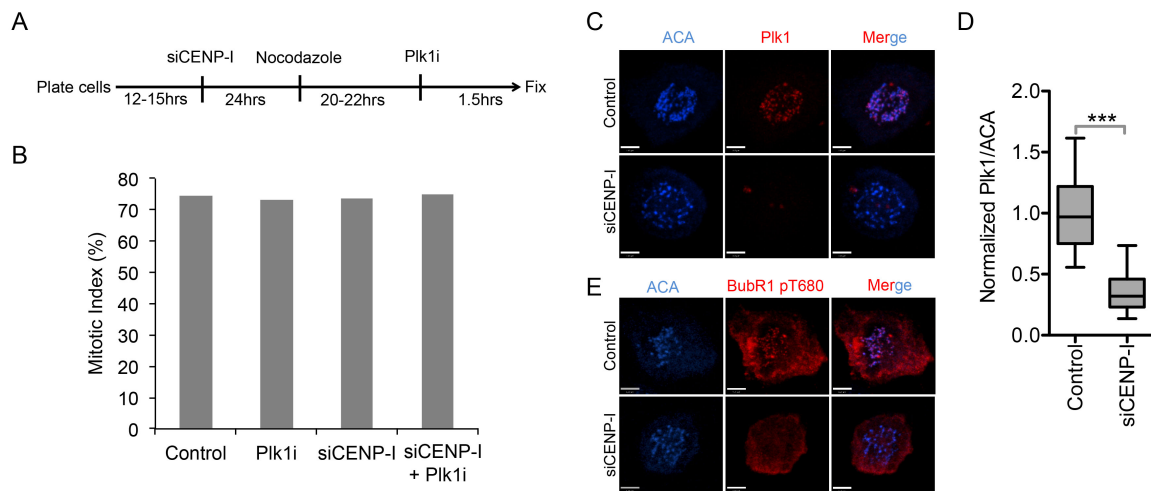


Figure. 4-3

Figure 4-4. Plk1 regulates pro-metaphase specific CENP-I-Ndc80 interaction.

(A) Western blots from the Ndc80 immuno-precipitation under indicated conditions. Cells were treated as shown in the schematic shown above. (B) Western blots from the Ndc80 immuno-precipitation experiments of the cells treated as shown in schematic above to obtain cells under prometaphase and metaphase condition. (C and D) Cells were treated as shown in the schematic above to achieve Plk1 targeting to the kinetochore. Immune-blots from Ndc80 immuno-precipitation experiments under indicated conditions are shown at the bottom.

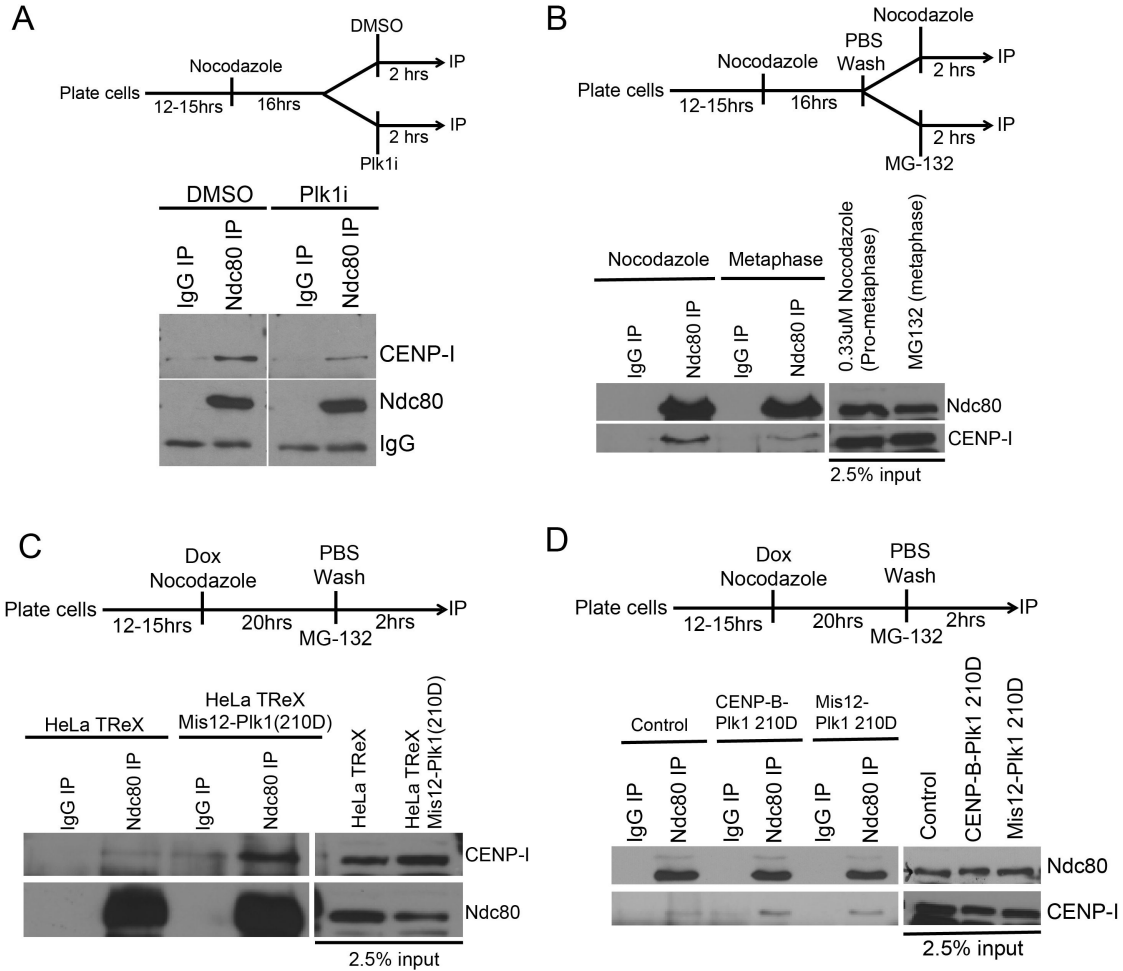


Figure.4-4

Figure 4-5. Model for KMN maintenance during mitosis. Before end-on attachment Aurora-B stabilizes KMN-CCAN interaction by phosphorylating DNS1 on S100 and S109 and allowing CENP-C-Dsn1 interaction. Plk1 on the other hand inhibits dynein dependent stripping of Ndc80 complex before end-on attachment; Plk1 also stabilizes CCAN-KMN/Ndc80 interaction by allowing CENP-I-Ndc80 interaction. Kinetochores rearrangement after end-on attachment stabilizes CCAN-KMN/Ndc80 interaction. CCAN-KMN/Ndc80 upon end-on attachments is minimally dependent on Aurora-B or Plk1 activity.

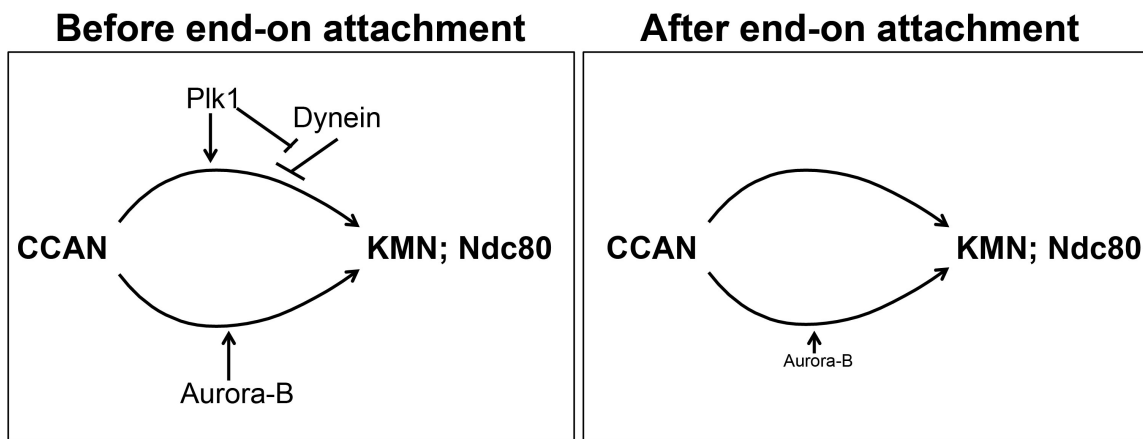


Figure. 4-5

Chapter 5
Concluding remarks and future directions.

Towards a systems level understanding of the CPC signaling:

Over the last few years the role of CPC in ensuring genomic stability has become clearer. The key substrates that the CPC regulates in order to achieve genomic stability have also become less mysterious. However, the molecular mechanisms behind these regulations remain unclear. The impediment in revealing these molecular mechanisms has been a lack of unifying model that takes in to account various observations and processes pertaining to the CPC. Another impediment has been a lack of separation of function mutants in the CPC that allow rigorous testing of these models. The impressive work done in multiple labs that revealed the centromere-signaling network (CSN) has been a major advance. The holistic view of the CPC signaling by considering the CSN as a whole has helped us come up with a framework, which has been able to explain coordination and regulation of multiple key events during mitosis (discussed in chapter 1).

The growing list of cofactors and regulators of the CPC during mitosis, such as microtubules, RNA, R-loops, DNA damage signaling kinases, various enzymes and histone modifications, have made our understanding of the CPC biology richer but also increasingly complex. In an attempt to deal with this complexity and still extract some clarity we employed an *in vitro* biochemical approach to define key separation of function mutants of the microtubule-CPC interaction and combined it with cell biological approaches to test existing models of kinetochore phosphorylation by the CPC. This approach has allowed us to come up with a clearer more plausible mechanism of kinetochore phosphorylation by the CPC and helped us reveal an important role for non-centromeric CPC in regulation of the

kinetochores. Since, the kinetochore phosphorylation by the CPC follows a non-linear dynamics our collaboration with Dr. Grishchuk has helped us get key mechanistic insights in to the role microtubules play in regulating kinetochore phosphorylation by the CPC and its effect on error correction process.

This kind of multi-disciplinary approach for multiple cofactors of the CPC can lead to a systems level understanding of the CPC biology and reveal design principles which ensure error free mitosis.

Understanding the role of microtubules in regulating kinase activity gradient:

The CPC during mitosis is localized to key sites in the cell at high concentration. This combined with the auto-phosphorylation dependent activation mechanism of the CPC gives rise to gradients of kinase activity. These gradients may have important role to play in our understanding of the spatial signaling during mitosis. For example anaphase gradient of Aurora-B activity emanating from the midzone has been shown to be important in regulating the timing and location of nuclear envelope reformation during telophase (Afonso et al., 2014). How the kinase activity gradients forms and how this long distance signaling can happen in presence of phosphatases in the cells are interesting unanswered questions. The gradients of the CPC activity emanating from the centromere to the chromosome arms has been shown to be depend on the presence of microtubules (Banerjee et al., 2014). It is tempting to hypothesize that the microtubule may act as a scaffold on which diffusible CPC molecules can bind and come close to each other, which would allow auto activation. This kind of mechanism can ensure long range signaling. The

microtubule-binding mutant of the CPC described in chapter 2 can be an ideal tool to test this hypothesis.

Control of lateral to end-on kinetochore microtubule attachment:

Premature end-on attachments can lead to improper kinetochore microtubule interaction, which can lead to chromosome instability. The kinetochores are thus thought to initially form lateral attachments with the walls of the microtubule through kinetochore localized motor proteins (Tanaka, 2012). At this stage the key kinetochore microtubule-binding protein Ndc80 is phosphorylated by the CPC, which prevents formation of end-on attachment (DeLuca et al., 2011; Shrestha et al., 2017). How the kinetochore transitions from lateral to an end-on attachment state once it reaches the end of a microtubule is unclear. The mechanism described in Chapter 2 for kinetochore phosphorylation driven by cooperation between the centromeric CPC and non-centromeric microtubule bound CPC has the potential to explain how laterally attached kinetochores can transition to an end-on attached state. When the kinetochores are attached in lateral manner, the geometry of kinetochore microtubule interaction would place the inner-centromere in close proximity to the microtubules on which the motor proteins that are bound to kinetochores are walking. This will ensure high phosphorylation of Ndc80. However, when the kinetochore reaches the end of the microtubules the leading sister kinetochore will detach from the end but the trailing sister kinetochore will still be attached at this point the distance between inner-centromere and microtubule wall will increase, as the microtubule slides away, and the CPC will no

longer be able to phosphorylate the kinetochore allowing the Ndc80 to make attachments with the end of the microtubules.

Understanding the phase separation characteristics of the CPC:

In chapter 3, I provided evidence for existence of the CPC in a phase-separated state in the inner-centromere. This observation predicts that the inner-centromere is in a liquid/gel like state and behaves like a membrane-less organelle. Thinking of the inner-centromere in terms of a liquid or gel like state has important implications for CPC biology and may explain various seemingly paradoxical observations. For example the localization of CPC through Survivin dependent H3pT3 binding is well established (Kelly et al., 2010; Wang et al., 2010; Yamagishi et al., 2010), yet it is hard to understand how can Survivin be the most dynamic member of the CPC and still be responsible for anchoring the CPC to the inner-centromere (Delacour-Larose et al., 2004). The idea proposed in chapter 3 solves this paradox by suggesting that the histone binding is only required for nucleation or early concentration of the CPC at the inner-centromere and the phase separation is what ensures its stable localization. Considering the CPC in the inner-centromere as a gel will have an important impact on understanding the force transduction by the inner-centromeric chromatin and may be an important part of the spring like behavior of this region. In order to more rigorously test the nature of the CPC in the inner-centromere there is a need to define regions of the CPC that can drive phase separation or gelation. Although, we have defined one such region on Borealin in chapter 3, I think an unbiased approach such as cross-linking mass spec would be highly suited to define

better mutants, which might help differentiate between gelation and phase-separation properties and reveal their importance to the CPC biology.

The ability of the chromatin or microtubules to induce CPC phase separation is interesting. This observation gives rise to a hypothesis that many of the proteins or co-factors responsible for the CPC localization to the inner-centromere or midzone may be inducing phase separation of the CPC by lowering the concentration of the CPC at which the phase separation occurs. If true this kind of explanation may simplify the enormous complexity that comes from numerous cofactors that play a role in CPC localization. This is especially interesting for Sgo1, which is a part of the CSN and drives recruitment of the CPC to the H2ApT120 chromatin. In conventional biochemical terms it is hard to imagine how stoichiometry of the interaction between CPC-Sgo1 would ensure localization of most of the CPC given the sub stoichiometric amounts of Sgo1 that are present in the cytoplasm compared to the amount of CPC members (Wühr et al., 2014). The hypothesis that Sgo1 might induce phase separation of the CPC can explain this discrepancy. In fact, Sgo1 has been shown to induce phase separation of HP1 α at sub-stoichiometric amounts (Larson et al., 2017). Apart from Sgo1, Mps1 is also shown to play an important role in regulating the amount of CPC in the inner-centromere through phosphorylating Borealin (Jelluma et al., 2008b). These phosphorylation sites are near the region responsible for phase separation and can thus regulate phase separation behavior of the CPC. It would be interesting to test this hypothesis in future.

Another aspect of the CPC at the inner-centromere is its ability to recruit

specific proteins to the inner-centromeres that impart unique properties to inner-centromere compared to the rest of the chromatin. I have shown that multiple *bona fide* inner-centromere components can specifically partition to the CPC phase. This observation may explain how various proteins localize to the inner-centromere in a CPC dependent manner and may underlie critical functions of the CPC at the inner-centromere such as cohesion protection.

Towards reconstitution of the inner-centromere:

Perhaps the most exciting thing from our observation of the phase separation of the CPC is the potential that this behavior of the CPC may help us capture the aspects of the complex biochemistry that occurs in the cell and recreate it *in vitro*. The obvious place to start would be look at the effect of phase separation on CPC activation. The CPC is activated by concentration dependent auto-activation thus the high local concentration of the CPC in a coacervate can have dramatic effects on kinase activation. This system would also be useful to understand chromatin independent effects of phase separation on kinase activation. Adding different agents present in the inner-centromeres, such as RNA, HP1 α etc, will allow a systematic analysis of their effect on Aurora-B kinase activation. More complex reactions such as cohesion protection can also be reconstituted in-vitro by taking advantage of the phase separation property of the CPC in the future.

Apart from kinase activation, our observation about microtubule nucleation from the ISB coacervates at the sub-critical concentration of the tubulin is interesting. It is clear that kinetochore nucleation near kinetochore occurs at the

start of mitosis (Khodjakov et al., 2003; Mishra et al., 2010; Sikirzhytski et al., 2018; Tulu et al., 2006), however the nucleator of this process is not known. The CPC has been implicated in regulating this process although indirectly thought inhibiting a microtubule depolymerase. It would be important to test if CPC can play a direct role in nucleating microtubules near kinetochores or in midzone.

The CPC has a dynamic localization throughout mitosis and thus there must be a process to breakdown CPC coacervates once formed. The Cdc48/p97-Ufd1-Npl4 seems to be an ideal candidate for this. This complex has been implicated in regulating the concentration of the CPC on the chromatin (Dobrynin et al., 2011). The extraction of the CPC from the inner-centromere in anaphase is an active process. Cdc48/p97 is an AAA+ AtPase chaperone that has an important role in breaking apart large macromolecular assemblies. It is thus tempting to hypothesize that Cdc48/p97-Ufd1-Npl4 can negatively regulate CPC phase separation by reversing it. It will be thus interesting to test if Cdc48/p97-Ufd1-Npl4 complex can play a role *in-vitro* in dissolving a CPC coacervates. If yes, manipulating Cdc48/p97-Ufd1-Npl4 in cells expressing the phase separation defective CPC would be predicted to have no effect on CPC localization.

Regulation of kinetochore structure before and after end-on attachment:

In chapter 4, I have shown that distinct pathways regulate maintenance of the outer kinetochore before and after end-on attachment. This observation provides an evidence of the dramatic change that occurs at the core kinetochore before and after end-on attachment. Our observation that Plk1 regulated CENP-I-Ndc80 interaction

is an important regulated interaction that may be the molecular basis for the rearrangement of the kinetochore that happens upon end-on attachment.

One of the most conspicuous change that occurs at kinetochore upon end-on attachment is the increase in the distance between Ndc80 N-terminus and the CENP-A chromatin. This change in the distance between Ndc80 and CENP-A is termed as intra-kinetochore stretch and is thought to be important for SAC silencing. The molecular basis for this change is unknown. Careful measurements of relative distances between different regions of the kinetochore from prometaphase to metaphase show a big change between CENP-I and Ndc80 complexes (Varma et al., 2013). Plk1 is also shown to be a regulator of the intra-kinetochore stretch (Liu et al., 2012). It is therefore possible that the Plk1 regulated Ndc80-CENP-I interaction described in chapter 4 is the mechanism behind this intra-kinetochore stretch. To test this hypothesis identity of the key Plk1 substrate is important.

One way to get to this substrate to first understand which pool of Ndc80 is regulated by the Plk1 kinase. Ectopic targeting of Lac-I fused to CENP-T (1-250aa) or CENP-C (1-100aa) or CENP-I to the lacO array, in engineered U2OS cells, can allow analysis of KMN assembly downstream of these proteins in isolation. This approach simplifies the complexity that is present at the native kinetochore due to multiple interactions. This sort of analysis combined with the Plk1 dependent phosphoroteomic data can point to the key substrate of the Plk1 that regulates CENP-I-Ndc80 interaction.

Ndc80 is more efficient in coupling the depolymerizing microtubules in an oligomeric state (Janczyk et al., 2017). Recruitment of the multiple Ndc80 by CENP-

T is thought to allow this organization of Ndc80 (Huis in 't Veld et al., 2016). The Ndc80-CENP-I interaction before end-on attachment may provide a mechanism to arrange the different Ndc80 molecule, recruited to CENP-T, so that they are in a right oligomeric state to bind kinetochores. This may explain the requirement for the Plk1 activity for establishment of end-on attachment. Interestingly, yeast homologue of CENP-I is thought to carry out a similar function (Pekgöz Altunkaya et al., 2016). Purified proteins and EM studies are needed to test this hypothesis. Ndc80-Ndc80 homo-FRET can also provide some evidence of existence of this mechanism.

Error correction of CENP-T occupancy:

CENP-T is a key regulator of the kinetochore assembly. CENP-TWSX is thought to form a nucleosome like complex and interact directly with centromeric DNA. How CENP-TWSX is specifically present only near the site adjacent to CENP-A nucleosome is unclear. Our observation that Plk1 and Aurora-B inhibition destabilize CENP-T in absence of microtubules suggest that ~50% of CENP-TWSX is not in a nucleosomal state or is in a loosely bound nucleosomal state. This observation is consistent with the FRAP studies of the CENP-TWSX complex members, which show an increased mobility from S-phase to G1 phase (Prendergast et al., 2011). The requirement for Plk1 and Aurora-B to stabilize CENP-T before end-on attachment and subsequent stabilization of the CENP-T at the centromere upon end-on attachment suggests a hypothesis where only the CENP-T that is bound to Ndc80 that yield stable microtubule attachment with the kinetochore and with

CENP-HIKM complex is retained and all other CENP-T molecules are passively lost from the chromatin due to low stability. This process will ensure the CENP-T that is retained in the next cell cycle is only the one near CENP-A nucleosomes. Testing this hypothesis would be an exciting extension of the work shown in chapter 4 and can answer some important unanswered questions.

References:

- Abrieu, A., Magnaghi-Jaulin, L., Kahana, J.A., Peter, M., Castro, A., Vigneron, S., Lorca, T., Cleveland, D.W., and Labbé, J.C. (2001). Mps1 is a kinetochore-associated kinase essential for the vertebrate mitotic checkpoint. *Cell* *106*, 83–93.
- Afonso, O., Matos, I., Pereira, A.J., Aguiar, P., Lampson, M.A., and Maiato, H. (2014). Feedback control of chromosome separation by a midzone Aurora B gradient. *Science* *345*, 332–336.
- Ainsztein, A.M., Kandels-Lewis, S.E., Mackay, A.M., and Earnshaw, W.C. (1998). INCENP centromere and spindle targeting: identification of essential conserved motifs and involvement of heterochromatin protein HP1. *J Cell Biol* *143*, 1763–1774.
- Alexander, S.P., and Rieder, C.L. (1991). Chromosome motion during attachment to the vertebrate spindle: initial saltatory-like behavior of chromosomes and quantitative analysis of force production by nascent kinetochore fibers. *J Cell Biol* *113*, 805–815.
- Amano, M., Suzuki, A., Hori, T., Backer, C., Okawa, K., Cheeseman, I.M., and Fukagawa, T. (2009). The CENP-S complex is essential for the stable assembly of outer kinetochore structure. *J Cell Biol* *186*, 173–182.
- Amaro, A.C., Samora, C.P., Holtackers, R., Wang, E., Kingston, I.J., Alonso, M., Lampson, M., McAinsh, A.D., and Meraldi, P. (2010). Molecular control of kinetochore-microtubule dynamics and chromosome oscillations. *Nat. Cell Biol.* *12*, 319–329.
- Ambadipudi, S., Biernat, J., Riedel, D., Mandelkow, E., and Zweckstetter, M. (2017). Liquid-liquid phase separation of the microtubule-binding repeats of the Alzheimer-related protein Tau. *Nat Commun* *8*, 275.
- Banani, S.F., Lee, H.O., Hyman, A.A., and Rosen, M.K. (2017). Biomolecular condensates: organizers of cellular biochemistry. *Nat. Rev. Mol. Cell Biol.* *18*, 285–298.
- Banerjee, B., Kestner, C.A., and Stukenberg, P.T. (2014). EB1 enables spindle microtubules to regulate centromeric recruitment of Aurora B. *J Cell Biol* *204*, 947–963.
- Baron, A.P., Schubert, von, C., Cubizolles, F., Siemeister, G., Hitchcock, M., Mengel, A., Schröder, J., Fernández-Montalván, A., Nussbaum, von, F., Mumberg, D., et al. (2016). Probing the catalytic functions of Bub1 kinase using the small molecule inhibitors BAY-320 and BAY-524. *Elife* *5*, 253.
- Basilico, F., Maffini, S., Weir, J.R., Prumbaum, D., Rojas, A.M., Zimniak, T., De Antoni, A., Jeganathan, S., Voss, B., van Gerwen, S., et al. (2014). The pseudo GTPase CENP-M

drives human kinetochore assembly. *Elife* 3, e02978.

Bassett, E.A., Wood, S., Salimian, K.J., Ajith, S., Foltz, D.R., and Black, B.E. (2010). Epigenetic centromere specification directs aurora B accumulation but is insufficient to efficiently correct mitotic errors. *J Cell Biol* 190, 177–185.

Bekier, M.E., Mazur, T., Rashid, M.S., and Taylor, W.R. (2015). Borealin dimerization mediates optimal CPC checkpoint function by enhancing localization to centromeres and kinetochores. *Nat Commun* 6, 6775.

Bharadwaj, R., Qi, W., and Yu, H. (2004). Identification of two novel components of the human NDC80 kinetochore complex. *J. Biol. Chem.* 279, 13076–13085.

Biggins, S., and Murray, A.W. (2001). The budding yeast protein kinase Ipl1/Aurora allows the absence of tension to activate the spindle checkpoint. *Genes Dev.* 15, 3118–3129.

Bolognesi, B., Lorenzo Gotor, N., Dhar, R., Cirillo, D., Baldrighi, M., Tartaglia, G.G., and Lehner, B. (2016). A Concentration-Dependent Liquid Phase Separation Can Cause Toxicity upon Increased Protein Expression. *Cell Rep* 16, 222–231.

Boyarchuk, Y., Salic, A., Dasso, M., and Arnaoutov, A. (2007). Bub1 is essential for assembly of the functional inner centromere. *J Cell Biol* 176, 919–928.

Buonomo, S.B., Clyne, R.K., Fuchs, J., Loidl, J., Uhlmann, F., and Nasmyth, K. (2000). Disjunction of homologous chromosomes in meiosis I depends on proteolytic cleavage of the meiotic cohesin Rec8 by separin. *Cell* 103, 387–398.

Caldas, G.V., DeLuca, K.F., and DeLuca, J.G. (2013). KNL1 facilitates phosphorylation of outer kinetochore proteins by promoting Aurora B kinase activity. *J Cell Biol* 203, 957–969.

Campbell, C.S., and Desai, A. (2013). Tension sensing by Aurora B kinase is independent of survivin-based centromere localization. *Nature* 497, 118–121.

Carmena, M., Lombardia, M.O., Ogawa, H., and Earnshaw, W.C. (2014). Polo kinase regulates the localization and activity of the chromosomal passenger complex in meiosis and mitosis in *Drosophila melanogaster*. *Open Biol* 4, 140162–140162.

Carmena, M., Pinson, X., Platani, M., Salloum, Z., Xu, Z., Clark, A., MacIsaac, F., Ogawa, H., Eggert, U., Glover, D.M., et al. (2012a). The chromosomal passenger complex activates Polo kinase at centromeres. *PLoS Biol.* 10, e1001250.

Carmena, M., Wheelock, M., Funabiki, H., and Earnshaw, W.C. (2012b). The chromosomal passenger complex (CPC): from easy rider to the godfather of mitosis. *Nat. Rev. Mol. Cell Biol.* 13, 789–803.

Carretero, M., Ruiz-Torres, M., Rodríguez-Corsino, M., Barthelemy, I., and Losada, A. (2013). Pds5B is required for cohesion establishment and Aurora B accumulation at centromeres. *Embo J.* *32*, 2938–2949.

Carroll, C.W., Silva, M.C.C., Godek, K.M., Jansen, L.E.T., and Straight, A.F. (2009). Centromere assembly requires the direct recognition of CENP-A nucleosomes by CENP-N. *Nat. Cell Biol.* *11*, 896–902.

Cheerambathur, D.K., Gassmann, R., Cook, B., Oegema, K., and Desai, A. (2013). Crosstalk between microtubule attachment complexes ensures accurate chromosome segregation. *Science* *342*, 1239–1242.

Cheeseman, I.M., Anderson, S., Jwa, M., Green, E.M., Kang, J.S., Yates, J.R., Chan, C.S.M., Drubin, D.G., and Barnes, G. (2002). Phospho-regulation of kinetochore-microtubule attachments by the Aurora kinase Ipl1p. *Cell* *111*, 163–172.

Cheeseman, I.M., Chappie, J.S., Wilson-Kubalek, E.M., and Desai, A. (2006). The conserved KMN network constitutes the core microtubule-binding site of the kinetochore. *Cell* *127*, 983–997.

Cheeseman, I.M., Hori, T., Fukagawa, T., and Desai, A. (2008). KNL1 and the CENP-H/I/K complex coordinately direct kinetochore assembly in vertebrates. *Mol. Biol. Cell* *19*, 587–594.

Cheeseman, I.M., Niessen, S., Anderson, S., Hyndman, F., Yates, J.R., Oegema, K., and Desai, A. (2004). A conserved protein network controls assembly of the outer kinetochore and its ability to sustain tension. *Genes Dev.* *18*, 2255–2268.

Cimini, D., Howell, B., Maddox, P., Khodjakov, A., Degrossi, F., and Salmon, E.D. (2001). Merotelic kinetochore orientation is a major mechanism of aneuploidy in mitotic mammalian tissue cells. *J Cell Biol* *153*, 517–527.

Cimini, D., Wan, X., Hirel, C.B., and Salmon, E.D. (2006). Aurora kinase promotes turnover of kinetochore microtubules to reduce chromosome segregation errors. *Curr. Biol.* *16*, 1711–1718.

Dai, J., Sullivan, B.A., and Higgins, J.M.G. (2006). Regulation of mitotic chromosome cohesion by Haspin and Aurora B. *Developmental Cell* *11*, 741–750.

Dai, J., Sultan, S., Taylor, S.S., and Higgins, J.M.G. (2005). The kinase haspin is required for mitotic histone H3 Thr 3 phosphorylation and normal metaphase chromosome alignment. *Genes Dev.* *19*, 472–488.

Daum, J.R., Potapova, T.A., Sivakumar, S., Daniel, J.J., Flynn, J.N., Rankin, S., and Gorbsky, G.J. (2011). Cohesion fatigue induces chromatid separation in cells delayed at metaphase. *Curr. Biol.* *21*, 1018–1024.

De Antoni, A., Maffini, S., Knapp, S., Musacchio, A., and Santaguida, S. (2012). A small-molecule inhibitor of Haspin alters the kinetochore functions of Aurora B. *J Cell Biol* *199*, 269–284.

De Antoni, A., Pearson, C.G., Cimini, D., Canman, J.C., Sala, V., Nezi, L., Mapelli, M., Sironi, L., Faretta, M., Salmon, E.D., et al. (2005). The Mad1/Mad2 complex as a template for Mad2 activation in the spindle assembly checkpoint. *Curr. Biol.* *15*, 214–225.

Delacour-Larose, M., Molla, A., Skoufias, D.A., Margolis, R.L., and Dimitrov, S. (2004). Distinct dynamics of Aurora B and Survivin during mitosis. *Cell Cycle* *3*, 1418–1426.

DeLuca, J.G., Gall, W.E., Ciferri, C., Cimini, D., Musacchio, A., and Salmon, E.D. (2006). Kinetochore microtubule dynamics and attachment stability are regulated by Hec1. *Cell* *127*, 969–982.

DeLuca, K.F., Lens, S.M.A., and DeLuca, J.G. (2011). Temporal changes in Hec1 phosphorylation control kinetochore-microtubule attachment stability during mitosis. *J. Cell. Sci.* *124*, 622–634.

DeLuca, K.F., Meppelink, A., Broad, A.J., Mick, J.E., Peersen, O.B., Pektas, S., Lens, S.M.A., and DeLuca, J.G. (2017). Aurora A kinase phosphorylates Hec1 to regulate metaphase kinetochore-microtubule dynamics. *J Cell Biol* *102*, jcb.201707160.

Desai, A., Rybina, S., Müller-Reichert, T., Shevchenko, A., Shevchenko, A., Hyman, A., and Oegema, K. (2003). KNL-1 directs assembly of the microtubule-binding interface of the kinetochore in *C. elegans*. *Genes Dev.* *17*, 2421–2435.

Ditchfield, C., Johnson, V.L., Tighe, A., Ellston, R., Haworth, C., Johnson, T., Mortlock, A., Keen, N., and Taylor, S.S. (2003). Aurora B couples chromosome alignment with anaphase by targeting BubR1, Mad2, and Cenp-E to kinetochores. *J Cell Biol* *161*, 267–280.

Dobrynin, G., Popp, O., Romer, T., Bremer, S., Schmitz, M.H.A., Gerlich, D.W., and Meyer, H. (2011). Cdc48/p97-Ufd1-Npl4 antagonizes Aurora B during chromosome segregation in HeLa cells. *J. Cell. Sci.* *124*, 1571–1580.

Dreier, M.R., Bekier, M.E., and Taylor, W.R. (2011). Regulation of sororin by Cdk1-mediated phosphorylation. *J. Cell. Sci.* *124*, 2976–2987.

Drinnenberg, I.A., Henikoff, S., and Malik, H.S. (2016). Evolutionary Turnover of Kinetochore Proteins: A Ship of Theseus? *Trends Cell Biol.* *26*, 498–510.

Du, J., Kelly, A.E., Funabiki, H., and Patel, D.J. (2012). Structural basis for recognition of H3T3ph and Smac/DIABLO N-terminal peptides by human Survivin. *Structure* *20*, 185–195.

Earnshaw, W.C., and Cooke, C.A. (1991). Analysis of the distribution of the INCENPs throughout mitosis reveals the existence of a pathway of structural changes in the chromosomes during metaphase and early events in cleavage furrow formation. *J. Cell. Sci.* *98 (Pt 4)*, 443–461.

Emanuele, M.J., Lan, W., Jwa, M., Miller, S.A., Chan, C.S.M., and Stukenberg, P.T. (2008). Aurora B kinase and protein phosphatase 1 have opposing roles in modulating kinetochore assembly. *J Cell Biol* *181*, 241–254.

Espeut, J., Lara-Gonzalez, P., Sassine, M., Shiau, A.K., Desai, A., and Abrieu, A. (2015). Natural Loss of Mps1 Kinase in Nematodes Uncovers a Role for Polo-like Kinase 1 in Spindle Checkpoint Initiation. *Cell Rep* *12*, 58–65.

Etemad, B., Kuijt, T.E.F., and Kops, G.J.P.L. (2015). Kinetochore-microtubule attachment is sufficient to satisfy the human spindle assembly checkpoint. *Nat Commun* *6*, 8987.

Fachinetti, D., Han, J.S., McMahon, M.A., Ly, P., Abdullah, A., Wong, A.J., and Cleveland, D.W. (2015). DNA Sequence-Specific Binding of CENP-B Enhances the Fidelity of Human Centromere Function. *Developmental Cell* *33*, 314–327.

Falk, S.J., Lee, J., Sekulic, N., Sennett, M.A., Lee, T.-H., and Black, B.E. (2016). CENP-C directs a structural transition of CENP-A nucleosomes mainly through sliding of DNA gyres. *Nat. Struct. Mol. Biol.* *23*, 204–208.

Famulski, J.K., and Chan, G.K. (2007). Aurora B kinase-dependent recruitment of hZW10 and hROD to tensionless kinetochores. *Curr. Biol.* *17*, 2143–2149.

Fang, G., Yu, H., and Kirschner, M.W. (1998a). Direct binding of CDC20 protein family members activates the anaphase-promoting complex in mitosis and G1. *Mol. Cell* *2*, 163–171.

Fang, G., Yu, H., and Kirschner, M.W. (1998b). The checkpoint protein MAD2 and the mitotic regulator CDC20 form a ternary complex with the anaphase-promoting complex to control anaphase initiation. *Genes Dev.* *12*, 1871–1883.

Fink, S., Turnbull, K., Desai, A., and Campbell, C.S. (2017). An engineered minimal chromosomal passenger complex reveals a role for INCENP/Sli15 spindle association in chromosome biorientation. *J Cell Biol* *216*, 911–923.

Fischle, W., Tseng, B.S., Dormann, H.L., Ueberheide, B.M., Garcia, B.A., Shabanowitz, J., Hunt, D.F., Funabiki, H., and Allis, C.D. (2005). Regulation of HP1-chromatin binding by histone H3 methylation and phosphorylation. *Nature* *438*, 1116–1122.

Foltz, D.R., Jansen, L.E.T., Black, B.E., Bailey, A.O., Yates, J.R., and Cleveland, D.W. (2006). The human CENP-A centromeric nucleosome-associated complex. *Nat. Cell Biol.* *8*, 458–469.

Fraschini, R., Beretta, A., Sironi, L., Musacchio, A., Lucchini, G., and Piatti, S. (2001). Bub3 interaction with Mad2, Mad3 and Cdc20 is mediated by WD40 repeats and does not require intact kinetochores. *Embo J.* *20*, 6648–6659.

Gandhi, R., Gillespie, P.J., and Hirano, T. (2006). Human Wapl is a cohesin-binding protein that promotes sister-chromatid resolution in mitotic prophase. *Curr. Biol.* *16*, 2406–2417.

Gascoigne, K.E., and Cheeseman, I.M. (2013). CDK-dependent phosphorylation and nuclear exclusion coordinately control kinetochore assembly state. *J Cell Biol* *201*, 23–32.

Gassmann, R., Essex, A., Hu, J.-S., Maddox, P.S., Motegi, F., Sugimoto, A., O'Rourke, S.M., Bowerman, B., McLeod, I., Yates, J.R., et al. (2008). A new mechanism controlling kinetochore-microtubule interactions revealed by comparison of two dynein-targeting components: SPDL-1 and the Rod/Zwilch/Zw10 complex. *Genes Dev.* *22*, 2385–2399.

Gassmann, R., Holland, A.J., Varma, D., Wan, X., Civril, F., Cleveland, D.W., Oegema, K., Salmon, E.D., and Desai, A. (2010). Removal of Spindly from microtubule-attached kinetochores controls spindle checkpoint silencing in human cells. *Genes Dev.* *24*, 957–971.

Ghenoiu, C., Wheelock, M.S., and Funabiki, H. (2013). Autoinhibition and Polo-dependent multisite phosphorylation restrict activity of the histone H3 kinase Haspin to mitosis. *Mol. Cell* *52*, 734–745.

Giménez-Abián, J.F., Sumara, I., Hirota, T., Hauf, S., Gerlich, D., la Torre, de, C., Ellenberg, J., and Peters, J.-M. (2004). Regulation of sister chromatid cohesion between chromosome arms. *Curr. Biol.* *14*, 1187–1193.

Glotzer, M. (2009). The 3Ms of central spindle assembly: microtubules, motors and MAPs. *Nat. Rev. Mol. Cell Biol.* *10*, 9–20.

Guo, L.Y., Allu, P.K., Zandarashvili, L., McKinley, K.L., Sekulic, N., Dawicki-McKenna, J.M., Fachinetti, D., Logsdon, G.A., Jamiolkowski, R.M., Cleveland, D.W., et al. (2017). Centromeres are maintained by fastening CENP-A to DNA and directing an arginine anchor-dependent nucleosome transition. *Nat Commun* *8*, 15775.

Guse, A., Carroll, C.W., Moree, B., Fuller, C.J., and Straight, A.F. (2011). In vitro centromere and kinetochore assembly on defined chromatin templates. *Nature* *477*, 354–358.

Haase, J., Bonner, M.K., Halas, H., and Kelly, A.E. (2017). Distinct Roles of the Chromosomal Passenger Complex in the Detection of and Response to Errors in Kinetochore-Microtubule Attachment. *Developmental Cell* *42*, 640–654.e645.

- Hagting, A., Elzen, Den, N., Vodermaier, H.C., Waizenegger, I.C., Peters, J.-M., and Pines, J. (2002). Human securin proteolysis is controlled by the spindle checkpoint and reveals when the APC/C switches from activation by Cdc20 to Cdh1. *J Cell Biol* *157*, 1125–1137.
- Hara, K., Zheng, G., Qu, Q., Liu, H., Ouyang, Z., Chen, Z., Tomchick, D.R., and Yu, H. (2014). Structure of cohesin subcomplex pinpoints direct shugoshin-Wapl antagonism in centromeric cohesion. *Nat. Struct. Mol. Biol.* *21*, 864–870.
- Hardwick, K.G., Johnston, R.C., Smith, D.L., and Murray, A.W. (2000). MAD3 encodes a novel component of the spindle checkpoint which interacts with Bub3p, Cdc20p, and Mad2p. *J Cell Biol* *148*, 871–882.
- Hasson, D., Panchenko, T., Salimian, K.J., Salman, M.U., Sekulic, N., Alonso, A., Warburton, P.E., and Black, B.E. (2013). The octamer is the major form of CENP-A nucleosomes at human centromeres. *Nat. Struct. Mol. Biol.* *20*, 687–695.
- Hauf, S., Waizenegger, I.C., and Peters, J.M. (2001). Cohesin cleavage by separase required for anaphase and cytokinesis in human cells. *Science* *293*, 1320–1323.
- Hauf, S., Cole, R.W., LaTerra, S., Zimmer, C., Schnapp, G., Walter, R., Heckel, A., van Meel, J., Rieder, C.L., and Peters, J.-M. (2003). The small molecule Hesperadin reveals a role for Aurora B in correcting kinetochore-microtubule attachment and in maintaining the spindle assembly checkpoint. *J Cell Biol* *161*, 281–294.
- Hengeveld, R.C.C., Vromans, M.J.M., Vleugel, M., Hadders, M.A., and Lens, S.M.A. (2017). Inner centromere localization of the CPC maintains centromere cohesion and allows mitotic checkpoint silencing. *Nat Commun* *8*, 15542.
- Hindriksen, S., Lens, S.M.A., and Hadders, M.A. (2017). The Ins and Outs of Aurora B Inner Centromere Localization. *Front. Cell Dev. Biol.* *5*, 65–21.
- Hirota, T., Lipp, J.J., Toh, B.-H., and Peters, J.-M. (2005). Histone H3 serine 10 phosphorylation by Aurora B causes HP1 dissociation from heterochromatin. *Nature* *438*, 1176–1180.
- Hiruma, Y., Sacristan, C., Pachis, S.T., Adamopoulos, A., Kuijt, T., Ubbink, M., Castelmur, von, E., Perrakis, A., and Kops, G.J.P.L. (2015). CELL DIVISION CYCLE. Competition between MPS1 and microtubules at kinetochores regulates spindle checkpoint signaling. *Science* *348*, 1264–1267.
- Hori, T., Amano, M., Suzuki, A., Backer, C.B., Welburn, J.P., Dong, Y., McEwen, B.F., Shang, W.-H., Suzuki, E., Okawa, K., et al. (2008). CCAN makes multiple contacts with centromeric DNA to provide distinct pathways to the outer kinetochore. *Cell* *135*, 1039–1052.
- Howell, B.J., McEwen, B.F., Canman, J.C., Hoffman, D.B., Farrar, E.M., Rieder, C.L., and

- Salmon, E.D. (2001). Cytoplasmic dynein/dynactin drives kinetochore protein transport to the spindle poles and has a role in mitotic spindle checkpoint inactivation. *J Cell Biol* 155, 1159–1172.
- Huis in 't Veld, P.J., Jeganathan, S., Petrovic, A., Singh, P., John, J., Krenn, V., Weissmann, F., Bange, T., and Musacchio, A. (2016). Molecular basis of outer kinetochore assembly on CENP-T. *Elife* 5, 576.
- Hümmer, S., and Mayer, T.U. (2009). Cdk1 negatively regulates midzone localization of the mitotic kinesin Mklp2 and the chromosomal passenger complex. *Curr. Biol.* 19, 607–612.
- Hwang, L.H., Lau, L.F., Smith, D.L., Mistrot, C.A., Hardwick, K.G., Hwang, E.S., Amon, A., and Murray, A.W. (1998). Budding yeast Cdc20: a target of the spindle checkpoint. *Science* 279, 1041–1044.
- Itoh, G., Ikeda, M., Iemura, K., Amin, M.A., Kuriyama, S., Tanaka, M., Mizuno, N., Osakada, H., Haraguchi, T., and Tanaka, K. (2018). Lateral attachment of kinetochores to microtubules is enriched in prometaphase rosette and facilitates chromosome alignment and bi-orientation establishment. *Sci Rep* 8, 3888.
- Jain, A., and Vale, R.D. (2017). RNA phase transitions in repeat expansion disorders. *Nature* 546, 243–247.
- Jambhekar, A., Emerman, A.B., Schweidenback, C.T.H., and Blower, M.D. (2014). RNA stimulates Aurora B kinase activity during mitosis. *PLoS ONE* 9, e100748.
- Janczyk, P.Ł., Skorupka, K.A., Tooley, J.G., Matson, D.R., Kestner, C.A., West, T., Pornillos, O., and Stukenberg, P.T. (2017). Mechanism of Ska Recruitment by Ndc80 Complexes to Kinetochores. *Developmental Cell* 41, 438–449.e4.
- Jelluma, N., Brenkman, A.B., McLeod, I., Yates, J.R., Cleveland, D.W., Medema, R.H., and Kops, G.J.P.L. (2008a). Chromosomal instability by inefficient Mps1 auto-activation due to a weakened mitotic checkpoint and lagging chromosomes. *PLoS ONE* 3, e2415.
- Jelluma, N., Brenkman, A.B., van den Broek, N.J.F., Cruijssen, C.W.A., van Osch, M.H.J., Lens, S.M.A., Medema, R.H., and Kops, G.J.P.L. (2008b). Mps1 phosphorylates Borealin to control Aurora B activity and chromosome alignment. *Cell* 132, 233–246.
- Jeyaprakash, A.A., Klein, U.R., Lindner, D., Ebert, J., Nigg, E.A., and Conti, E. (2007). Structure of a Survivin-Borealin-INCENP core complex reveals how chromosomal passengers travel together. *Cell* 131, 271–285.
- Ji, Z., Gao, H., and Yu, H. (2015). CELL DIVISION CYCLE. Kinetochore attachment sensed by competitive Mps1 and microtubule binding to Ndc80C. *Science* 348, 1260–1264.

- Jia, L., Li, B., and Yu, H. (2016). The Bub1-Plk1 kinase complex promotes spindle checkpoint signalling through Cdc20 phosphorylation. *Nat Commun* 7, 10818.
- Johnson, V.L., Scott, M.I.F., Holt, S.V., Hussein, D., and Taylor, S.S. (2004). Bub1 is required for kinetochore localization of BubR1, Cenp-E, Cenp-F and Mad2, and chromosome congression. *J. Cell. Sci.* 117, 1577–1589.
- Kajtez, J., Solomatina, A., Novak, M., Polak, B., Vukušić, K., Rüdiger, J., Cojoc, G., Milas, A., Šumanovac Šestak, I., Risteski, P., et al. (2016). Overlap microtubules link sister k-fibres and balance the forces on bi-oriented kinetochores. *Nat Commun* 7, 10298.
- Kallio, M.J., McClelland, M.L., Stukenberg, P.T., and Gorbsky, G.J. (2002). Inhibition of aurora B kinase blocks chromosome segregation, overrides the spindle checkpoint, and perturbs microtubule dynamics in mitosis. *Curr. Biol.* 12, 900–905.
- Kang, J., Chaudhary, J., Dong, H., Kim, S., Brautigam, C.A., and Yu, H. (2011). Mitotic centromeric targeting of HP1 and its binding to Sgo1 are dispensable for sister-chromatid cohesion in human cells. *Mol. Biol. Cell* 22, 1181–1190.
- Kang, Y.H., Park, J.-E., Yu, L.-R., Soung, N.-K., Yun, S.-M., Bang, J.K., Seong, Y.-S., Yu, H., Garfield, S., Veenstra, T.D., et al. (2006). Self-regulated Plk1 recruitment to kinetochores by the Plk1-PBIP1 interaction is critical for proper chromosome segregation. *Mol. Cell* 24, 409–422.
- Kasuboski, J.M., Bader, J.R., Vaughan, P.S., Tauhata, S.B.F., Winding, M., Morrissey, M.A., Joyce, M.V., Boggess, W., Vos, L., Chan, G.K., et al. (2011). Zwint-1 is a novel Aurora B substrate required for the assembly of a dynein-binding platform on kinetochores. *Mol. Biol. Cell* 22, 3318–3330.
- Kato, H., Jiang, J., Zhou, B.-R., Rozendaal, M., Feng, H., Ghirlando, R., Xiao, T.S., Straight, A.F., and Bai, Y. (2013). A conserved mechanism for centromeric nucleosome recognition by centromere protein CENP-C. *Science* 340, 1110–1113.
- Kawashima, S.A., Yamagishi, Y., Honda, T., Ishiguro, K.-I., and Watanabe, Y. (2010). Phosphorylation of H2A by Bub1 prevents chromosomal instability through localizing shugoshin. *Science* 327, 172–177.
- Kelly, A.E., Ghenoiu, C., Xue, J.Z., Zierhut, C., Kimura, H., and Funabiki, H. (2010). Survivin reads phosphorylated histone H3 threonine 3 to activate the mitotic kinase Aurora B. *Science* 330, 235–239.
- Khodjakov, A., Copenagle, L., Gordon, M.B., Compton, D.A., and Kapoor, T.M. (2003). Minus-end capture of preformed kinetochore fibers contributes to spindle morphogenesis. *J Cell Biol* 160, 671–683.
- Kim, S., and Yu, H. (2015). Multiple assembly mechanisms anchor the KMN spindle checkpoint platform at human mitotic kinetochores. *J Cell Biol* 208, 181–196.

- Kim, Y., Holland, A.J., Lan, W., and Cleveland, D.W. (2010). Aurora kinases and protein phosphatase 1 mediate chromosome congression through regulation of CENP-E. *Cell* 142, 444–455.
- Kirschner, M., and Mitchison, T. (1986). Beyond self-assembly: from microtubules to morphogenesis. *Cell* 45, 329–342.
- Kitajima, T.S., Sakuno, T., Ishiguro, K.-I., Iemura, S.-I., Natsume, T., Kawashima, S.A., and Watanabe, Y. (2006). Shugoshin collaborates with protein phosphatase 2A to protect cohesin. *Nature* 441, 46–52.
- Klein, U.R., Nigg, E.A., and Gruneberg, U. (2006). Centromere Targeting of the Chromosomal Passenger Complex Requires a Ternary Subcomplex of Borealin, Survivin, and the N-Terminal Domain of INCENP. *PLoS Biol* 4, 2547–2558.
- Kline, S.L., Cheeseman, I.M., Hori, T., Fukagawa, T., and Desai, A. (2006). The human Mis12 complex is required for kinetochore assembly and proper chromosome segregation. *J Cell Biol* 173, 9–17.
- Knowlton, A.L., Lan, W., and Stukenberg, P.T. (2006). Aurora B is enriched at merotelic attachment sites, where it regulates MCAK. *Curr. Biol.* 16, 1705–1710.
- Krenn, V., and Musacchio, A. (2015). The Aurora B Kinase in Chromosome Bi-Orientation and Spindle Checkpoint Signaling. *Front Oncol* 5, 225.
- Krupina, K., Kleiss, C., Metzger, T., Fournane, S., Schmucker, S., Hofmann, K., Fischer, B., Paul, N., Porter, I.M., Raffelsberger, W., et al. (2016). Ubiquitin Receptor Protein UBASH3B Drives Aurora B Recruitment to Mitotic Microtubules. *Developmental Cell* 36, 63–78.
- Kruse, T., Zhang, G., Larsen, M.S.Y., Lischetti, T., Streicher, W., Kragh Nielsen, T., Bjørn, S.P., and Nilsson, J. (2013). Direct binding between BubR1 and B56-PP2A phosphatase complexes regulate mitotic progression. *J. Cell. Sci.* 126, 1086–1092.
- Kueng, S., Hegemann, B., Peters, B.H., Lipp, J.J., Schleiffer, A., Mechtler, K., and Peters, J.-M. (2006). Wapl controls the dynamic association of cohesin with chromatin. *Cell* 127, 955–967.
- Lampson, M.A., and Grishchuk, E.L. (2017). Mechanisms to Avoid and Correct Erroneous Kinetochore-Microtubule Attachments. *Biology (Basel)* 6, 1.
- Lampson, M.A., Renduchitala, K., Khodjakov, A., and Kapoor, T.M. (2004). Correcting improper chromosome-spindle attachments during cell division. *Nat. Cell Biol.* 6, 232–237.
- Lan, W., Zhang, X., Kline-Smith, S.L., Rosasco, S.E., Barrett-Wilt, G.A., Shabanowitz, J., Hunt, D.F., Walczak, C.E., and Stukenberg, P.T. (2004). Aurora B phosphorylates

centromeric MCAK and regulates its localization and microtubule depolymerization activity. *Curr. Biol.* *14*, 273–286.

Larson, A.G., Elnatan, D., Keenen, M.M., Trnka, M.J., Johnston, J.B., Burlingame, A.L., Agard, D.A., Redding, S., and Narlikar, G.J. (2017). Liquid droplet formation by HP1 α suggests a role for phase separation in heterochromatin. *Nature* *547*, 236–240.

Lawrimore, J., Vasquez, P.A., Falvo, M.R., Taylor, R.M., Vicci, L., Yeh, E., Forest, M.G., and Bloom, K. (2015). DNA loops generate intracentromere tension in mitosis. *J Cell Biol* *210*, 553–564.

Lens, S.M.A., Rodriguez, J.A., Vader, G., Span, S.W., Giaccone, G., and Medema, H. (2006). Uncoupling the Central Spindle-associated Function of the Chromosomal Passenger Complex from Its Role at Centromeres. *17*, 1–13.

Lénárt, P., Petronczki, M., Steegmaier, M., Di Fiore, B., Lipp, J.J., Hoffmann, M., Rettig, W.J., Kraut, N., and Peters, J.-M. (2007). The small-molecule inhibitor BI 2536 reveals novel insights into mitotic roles of polo-like kinase 1. *Curr. Biol.* *17*, 304–315.

Liu, D., Davydenko, O., and Lampson, M.A. (2012). Polo-like kinase-1 regulates kinetochore-microtubule dynamics and spindle checkpoint silencing. *J Cell Biol* *198*, 491–499.

Liu, D., Vader, G., Vromans, M.J.M., Lampson, M.A., and Lens, S.M.A. (2009). Sensing chromosome bi-orientation by spatial separation of aurora B kinase from kinetochore substrates. *Science* *323*, 1350–1353.

Liu, D., Vleugel, M., Backer, C.B., Hori, T., Fukagawa, T., Cheeseman, I.M., and Lampson, M.A. (2010). Regulated targeting of protein phosphatase 1 to the outer kinetochore by KNL1 opposes Aurora B kinase. *J Cell Biol* *188*, 809–820.

Liu, H., Qu, Q., Warrington, R., Rice, A., Cheng, N., and Yu, H. (2015). Mitotic Transcription Installs Sgo1 at Centromeres to Coordinate Chromosome Segregation. *Mol. Cell* *59*, 426–436.

London, N., and Biggins, S. (2014). Mad1 kinetochore recruitment by Mps1-mediated phosphorylation of Bub1 signals the spindle checkpoint. *Genes Dev.* *28*, 140–152.

London, N., Ceto, S., Ranish, J.A., and Biggins, S. (2012). Phosphoregulation of Spc105 by Mps1 and PP1 regulates Bub1 localization to kinetochores. *Curr. Biol.* *22*, 900–906.

Luo, X., Fang, G., Coldiron, M., Lin, Y., Yu, H., Kirschner, M.W., and Wagner, G. (2000). Structure of the Mad2 spindle assembly checkpoint protein and its interaction with Cdc20. *Nat. Struct. Biol.* *7*, 224–229.

- Luo, X., Tang, Z., Rizo, J., and Yu, H. (2002). The Mad2 spindle checkpoint protein undergoes similar major conformational changes upon binding to either Mad1 or Cdc20. *Mol. Cell* 9, 59–71.
- Luo, X., Tang, Z., Xia, G., Wassmann, K., Matsumoto, T., Rizo, J., and Yu, H. (2004). The Mad2 spindle checkpoint protein has two distinct natively folded states. *Nat. Struct. Mol. Biol.* 11, 338–345.
- Magidson, V., O'Connell, C.B., Lončarek, J., Paul, R., Mogilner, A., and Khodjakov, A. (2011). The spatial arrangement of chromosomes during prometaphase facilitates spindle assembly. *Cell* 146, 555–567.
- Magidson, V., Paul, R., Yang, N., Ault, J.G., O'Connell, C.B., Tikhonenko, I., McEwen, B.F., Mogilner, A., and Khodjakov, A. (2015). Adaptive changes in the kinetochore architecture facilitate proper spindle assembly. *Nat. Cell Biol.* 17, 1134–1144.
- Mahen, R., Koch, B., Wachsmuth, M., Politi, A.Z., Perez-Gonzalez, A., Mergenthaler, J., Cai, Y., and Ellenberg, J. (2014). Comparative assessment of fluorescent transgene methods for quantitative imaging in human cells. *Mol. Biol. Cell* 25, 3610–3618.
- Maiato, H., Rieder, C.L., and Khodjakov, A. (2004). Kinetochore-driven formation of kinetochore fibers contributes to spindle assembly during animal mitosis. *J Cell Biol* 167, 831–840.
- Maldonado, M., and Kapoor, T.M. (2011). Constitutive Mad1 targeting to kinetochores uncouples checkpoint signalling from chromosome biorientation. *Nat. Cell Biol.* 13, 475–482.
- Maresca, T.J., and Salmon, E.D. (2009). Intrakinetochore stretch is associated with changes in kinetochore phosphorylation and spindle assembly checkpoint activity. *J Cell Biol* 184, 373–381.
- Masumoto, H., Masukata, H., Muro, Y., Nozaki, N., and Okazaki, T. (1989). A human centromere antigen (CENP-B) interacts with a short specific sequence in alphoid DNA, a human centromeric satellite. *J Cell Biol* 109, 1963–1973.
- Matson, D.R., and Stukenberg, P.T. (2014). CENP-I and Aurora B act as a molecular switch that ties RZZ/Mad1 recruitment to kinetochore attachment status. *J Cell Biol* 205, 541–554.
- Matson, D.R., Demirel, P.B., Stukenberg, P.T., and Burke, D.J. (2012). A conserved role for COMA/CENP-H/I/N kinetochore proteins in the spindle checkpoint. *Genes Dev.* 26, 542–547.
- McClelland, M.L., Gardner, R.D., Kallio, M.J., Daum, J.R., Gorbsky, G.J., Burke, D.J., and Stukenberg, P.T. (2003). The highly conserved Ndc80 complex is required for kinetochore assembly, chromosome congression, and spindle checkpoint activity.

Genes Dev. *17*, 101–114.

McEwen, B.F., Chan, G.K., Zubrowski, B., Savoian, M.S., Sauer, M.T., and Yen, T.J. (2001). CENP-E is essential for reliable bioriented spindle attachment, but chromosome alignment can be achieved via redundant mechanisms in mammalian cells. *Mol. Biol. Cell* *12*, 2776–2789.

McGuinness, B.E., Hirota, T., Kudo, N.R., Peters, J.-M., and Nasmyth, K. (2005). Shugoshin prevents dissociation of cohesin from centromeres during mitosis in vertebrate cells. *PLoS Biol.* *3*, e86.

McKinley, K.L., Sekulic, N., Guo, L.Y., Tsinman, T., Black, B.E., and Cheeseman, I.M. (2015). The CENP-L-N Complex Forms a Critical Node in an Integrated Meshwork of Interactions at the Centromere-Kinetochore Interface. *Mol. Cell* *60*, 886–898.

Meppelink, A., Kabeche, L., Vromans, M.J.M., Compton, D.A., and Lens, S.M.A. (2015). Shugoshin-1 balances Aurora B kinase activity via PP2A to promote chromosome bi-orientation. *Cell Rep* *11*, 508–515.

Meraldi, P., and Sorger, P.K. (2005). A dual role for Bub1 in the spindle checkpoint and chromosome congression. *Embo J.* *24*, 1621–1633.

Miller, S.A., Johnson, M.L., and Stukenberg, P.T. (2008). Kinetochore attachments require an interaction between unstructured tails on microtubules and Ndc80(Hec1). *Curr. Biol.* *18*, 1785–1791.

Mishra, R.K., Chakraborty, P., Arnautov, A., Fontoura, B.M.A., and Dasso, M. (2010). The Nup107-160 complex and gamma-TuRC regulate microtubule polymerization at kinetochores. *Nat. Cell Biol.* *12*, 164–169.

Mitchison, T.J., and Kirschner, M.W. (1985). Properties of the kinetochore in vitro. II. Microtubule capture and ATP-dependent translocation. *J Cell Biol* *101*, 766–777.

Moyle, M.W., Kim, T., Hattersley, N., Espeut, J., Cheerambathur, D.K., Oegema, K., and Desai, A. (2014). A Bub1-Mad1 interaction targets the Mad1-Mad2 complex to unattached kinetochores to initiate the spindle checkpoint. *J Cell Biol* *204*, 647–657.

Musacchio, A., and Desai, A. (2017). A Molecular View of Kinetochore Assembly and Function. *Biology (Basel)* *6*, 5.

Nagpal, H., Hori, T., Furukawa, A., Sugase, K., Osakabe, A., Kurumizaka, H., and Fukagawa, T. (2015). Dynamic changes in CCAN organization through CENP-C during cell-cycle progression. *Mol. Biol. Cell* *26*, 3768–3776.

Nasmyth, K., and Haering, C.H. (2009). Cohesin: its roles and mechanisms. *Annu. Rev. Genet.* *43*, 525–558.

Neumann, B., Walter, T., Hériché, J.-K., Bulkescher, J., Erfle, H., Conrad, C., Rogers, P., Poser, I., Held, M., Liebel, U., et al. (2010). Phenotypic profiling of the human genome by time-lapse microscopy reveals cell division genes. *Nature* *464*, 721–727.

Niedzialkowska, E., Wang, F., Porebski, P.J., Minor, W., Higgins, J.M.G., and Stukenberg, P.T. (2012). Molecular basis for phosphospecific recognition of histone H3 tails by Survivin paralogues at inner centromeres. *Mol. Biol. Cell* *23*, 1457–1466.

Nijenhuis, W., Castelmur, von, E., Littler, D., De Marco, V., Tromer, E., Vleugel, M., van Osch, M.H.J., Snel, B., Perrakis, A., and Kops, G.J.P.L. (2013). A TPR domain-containing N-terminal module of MPS1 is required for its kinetochore localization by Aurora B. *J Cell Biol* *201*, 217–231.

Nijenhuis, W., Vallardi, G., Teixeira, A., Kops, G.J.P.L., and Saurin, A.T. (2014). Negative feedback at kinetochores underlies a responsive spindle checkpoint signal. *Nat. Cell Biol.* *16*, 1257–1264.

Nishino, T., Takeuchi, K., Gascoigne, K.E., Suzuki, A., Hori, T., Oyama, T., Morikawa, K., Cheeseman, I.M., and Fukagawa, T. (2012). CENP-T-W-S-X forms a unique centromeric chromatin structure with a histone-like fold. *Cell* *148*, 487–501.

Nishiyama, T., Ladurner, R., Schmitz, J., Kreidl, E., Schleiffer, A., Bhaskara, V., Bando, M., Shirahige, K., Hyman, A.A., Mechtler, K., et al. (2010). Sororin mediates sister chromatid cohesion by antagonizing Wapl. *Cell* *143*, 737–749.

Nishiyama, T., Sykora, M.M., Huis in 't Veld, P.J., Mechtler, K., and Peters, J.-M. (2013). Aurora B and Cdk1 mediate Wapl activation and release of acetylated cohesin from chromosomes by phosphorylating Sororin. *Proc. Natl. Acad. Sci. U.S.A.* *110*, 13404–13409.

O'Connor, A., Maffini, S., Rainey, M.D., Kaczmarczyk, A., Gaboriau, D., Musacchio, A., and Santocanale, C. (2015). Requirement for PLK1 kinase activity in the maintenance of a robust spindle assembly checkpoint. *Biol Open* *5*, 11–19.

Okada, M., Cheeseman, I.M., Hori, T., Okawa, K., McLeod, I.X., Yates, J.R., Desai, A., and Fukagawa, T. (2006). The CENP-H-I complex is required for the efficient incorporation of newly synthesized CENP-A into centromeres. *Nat. Cell Biol.* *8*, 446–457.

Overlack, K., Primorac, I., Vleugel, M., Krenn, V., Maffini, S., Hoffmann, I., Kops, G.J.P.L., and Musacchio, A. (2015). A molecular basis for the differential roles of Bub1 and BubR1 in the spindle assembly checkpoint. *Elife* *4*, e05269.

Pekgöz Altunkaya, G., Malvezzi, F., Demianova, Z., Zimniak, T., Litos, G., Weissmann, F., Mechtler, K., Herzog, F., and Westermann, S. (2016). CCAN Assembly Configures Composite Binding Interfaces to Promote Cross-Linking of Ndc80 Complexes at the Kinetochore. *Curr. Biol.* *26*, 2370–2378.

Peters, J.-M., Tedeschi, A., and Schmitz, J. (2008). The cohesin complex and its roles in chromosome biology. *Genes Dev.* 22, 3089–3114.

Petrovic, A., Mosalaganti, S., Keller, J., Mattiuzzo, M., Overlack, K., Krenn, V., De Antoni, A., Wohlgemuth, S., Cecatiello, V., Pasqualato, S., et al. (2014). Modular assembly of RWD domains on the Mis12 complex underlies outer kinetochore organization. *Mol. Cell* 53, 591–605.

Prendergast, L., van Vuuren, C., Kaczmarczyk, A., Doering, V., Hellwig, D., Quinn, N., Hoischen, C., Diekmann, S., and Sullivan, K.F. (2011). Premitotic assembly of human CENPs -T and -W switches centromeric chromatin to a mitotic state. *PLoS Biol.* 9, e1001082.

Przewloka, M.R., Venkei, Z., Bolanos-Garcia, V.M., Debski, J., Dadlez, M., and Glover, D.M. (2011). CENP-C is a structural platform for kinetochore assembly. *Curr. Biol.* 21, 399–405.

Qian, J., Beullens, M., Lesage, B., and Bollen, M. (2013). Aurora B defines its own chromosomal targeting by opposing the recruitment of the phosphatase scaffold Repo-Man. *Curr. Biol.* 23, 1136–1143.

Qian, J., Lesage, B., Beullens, M., Van Eynde, A., and Bollen, M. (2011). PP1/Repo-man dephosphorylates mitotic histone H3 at T3 and regulates chromosomal aurora B targeting. *Curr. Biol.* 21, 766–773.

Rago, F., Gascoigne, K.E., and Cheeseman, I.M. (2015). Distinct organization and regulation of the outer kinetochore KMN network downstream of CENP-C and CENP-T. *Curr. Biol.* 25, 671–677.

Resnick, T.D., Satinover, D.L., MacIsaac, F., Stukenberg, P.T., Earnshaw, W.C., Orr-Weaver, T.L., and Carmena, M. (2006). INCENP and Aurora B promote meiotic sister chromatid cohesion through localization of the Shugoshin MEI-S332 in *Drosophila*. *Developmental Cell* 11, 57–68.

Ricke, R.M., Jeganathan, K.B., Malureanu, L., Harrison, A.M., and van Deursen, J.M. (2012). Bub1 kinase activity drives error correction and mitotic checkpoint control but not tumor suppression. *J Cell Biol* 199, 931–949.

Rosasco-Nitcher, S.E., Lan, W., Khorasanizadeh, S., and Stukenberg, P.T. (2008). Centromeric Aurora-B activation requires TD-60, microtubules, and substrate priming phosphorylation. *Science* 319, 469–472.

Sacristan, C., and Kops, G.J.P.L. (2015). Joined at the hip: kinetochores, microtubules, and spindle assembly checkpoint signaling. *Trends Cell Biol.* 25, 21–28.

Sacristan, C., Ahmad, M.U.D., Keller, J., Fermie, J., Groenewold, V., Tromer, E., Fish, A., Melero, R., Carazo, J.M., Klumperman, J., et al. (2018). Dynamic kinetochore size

regulation promotes microtubule capture and chromosome biorientation in mitosis. *Nat. Cell Biol.* *27*, 5.

Salimian, K.J., Ballister, E.R., Smoak, E.M., Wood, S., Panchenko, T., Lampson, M.A., and Black, B.E. (2011). Feedback control in sensing chromosome biorientation by the Aurora B kinase. *Curr. Biol.* *21*, 1158–1165.

Samejima, K., Platani, M., Wolny, M., Ogawa, H., Vargiu, G., Knight, P.J., Peckham, M., and Earnshaw, W.C. (2015). The Inner Centromere Protein (INCENP) Coil Is a Single α -Helix (SAH) Domain That Binds Directly to Microtubules and Is Important for Chromosome Passenger Complex (CPC) Localization and Function in Mitosis. *J. Biol. Chem.* *290*, 21460–21472.

Sampath, S.C., Ohi, R., Leismann, O., Salic, A., Pozniakovski, A., and Funabiki, H. (2004). The chromosomal passenger complex is required for chromatin-induced microtubule stabilization and spindle assembly. *Cell* *118*, 187–202.

Santaguida, S., and Musacchio, A. (2009). The life and miracles of kinetochores. *Embo J.* *28*, 2511–2531.

Santaguida, S., Vernieri, C., Villa, F., Ciliberto, A., and Musacchio, A. (2011). Evidence that Aurora B is implicated in spindle checkpoint signalling independently of error correction. *Embo J.* *30*, 1508–1519.

Santamaria, A., Wang, B., Elowe, S., Malik, R., Zhang, F., Bauer, M., Schmidt, A., Silljé, H.H.W., Körner, R., and Nigg, E.A. (2011). The Plk1-dependent phosphoproteome of the early mitotic spindle. *Mol. Cell Proteomics* *10*, M110.004457.

Sarangapani, K.K., Akiyoshi, B., Duggan, N.M., Biggins, S., and Asbury, C.L. (2013). Phosphoregulation promotes release of kinetochores from dynamic microtubules via multiple mechanisms. *Proc. Natl. Acad. Sci. U.S.A.* *110*, 7282–7287.

Saurin, A.T., van der Waal, M.S., Medema, R.H., Lens, S.M.A., and Kops, G.J.P.L. (2011). Aurora B potentiates Mps1 activation to ensure rapid checkpoint establishment at the onset of mitosis. *Nat Commun* *2*, 316.

Schubert, von, C., Cubizolles, F., Bracher, J.M., Sliedrecht, T., Kops, G.J.P.L., and Nigg, E.A. (2015). Plk1 and Mps1 Cooperatively Regulate the Spindle Assembly Checkpoint in Human Cells. *Cell Rep* *12*, 66–78.

Screpanti, E., De Antoni, A., Alushin, G.M., Petrovic, A., Melis, T., Nogales, E., and Musacchio, A. (2011). Direct binding of Cenp-C to the Mis12 complex joins the inner and outer kinetochore. *Curr. Biol.* *21*, 391–398.

Sessa, F., Mapelli, M., Ciferri, C., Tarricone, C., Areces, L.B., Schneider, T.R., Stukenberg, P.T., and Musacchio, A. (2005). Mechanism of Aurora B activation by INCENP and inhibition by hesperadin. *Mol. Cell* *18*, 379–391.

- Shepperd, L.A., Meadows, J.C., Sochaj, A.M., Lancaster, T.C., Zou, J., Buttrick, G.J., Rappsilber, J., Hardwick, K.G., and Millar, J.B.A. (2012). Phosphodependent recruitment of Bub1 and Bub3 to Spc7/KNL1 by Mph1 kinase maintains the spindle checkpoint. *Curr. Biol.* 22, 891–899.
- Shintomi, K., and Hirano, T. (2009). Releasing cohesin from chromosome arms in early mitosis: opposing actions of Wapl-Pds5 and Sgo1. *Genes Dev.* 23, 2224–2236.
- Shrestha, R.L., and Draviam, V.M. (2013). Lateral to end-on conversion of chromosome-microtubule attachment requires kinesins CENP-E and MCAK. *Curr. Biol.* 23, 1514–1526.
- Shrestha, R.L., Conti, D., Tamura, N., Braun, D., Ramalingam, R.A., Cieslinski, K., Ries, J., and Draviam, V.M. (2017). Aurora-B kinase pathway controls the lateral to end-on conversion of kinetochore-microtubule attachments in human cells. *Nat Commun* 8, 150.
- Sikirzhytski, V., Renda, F., Tikhonenko, I., Magidson, V., McEwen, B.F., and Khodjakov, A. (2018). Microtubules assemble near most kinetochores during early prometaphase in human cells. *J Cell Biol* 53, jcb.201710094.
- Silva, P.M.A., Reis, R.M., Bolanos-Garcia, V.M., Florindo, C., Tavares, Á.A., and Bousbaa, H. (2014). Dynein-dependent transport of spindle assembly checkpoint proteins off kinetochores toward spindle poles. *FEBS Lett.* 588, 3265–3273.
- Sivakumar, S., Janczyk, P.Ł., Qu, Q., Brautigam, C.A., Stukenberg, P.T., Yu, H., and Gorbisky, G.J. (2016). The human SKA complex drives the metaphase-anaphase cell cycle transition by recruiting protein phosphatase 1 to kinetochores. *Elife* 5, 868.
- Smith, C.A., McAinsh, A.D., and Burroughs, N.J. (2016). Human kinetochores are swivel joints that mediate microtubule attachments. *Elife* 5, 319.
- Solé, R.V., and Bascompte, J. (2012). *Self-Organization in Complex Ecosystems.* (MPB-42) (Princeton University Press).
- Strom, A.R., Emelyanov, A.V., Mir, M., Fyodorov, D.V., Darzacq, X., and Karpen, G.H. (2017). Phase separation drives heterochromatin domain formation. *Nature* 547, 241–245.
- Stukenberg, P.T., and Burke, D.J. (2015). Connecting the microtubule attachment status of each kinetochore to cell cycle arrest through the spindle assembly checkpoint. *Chromosoma* 124, 463–480.
- Stukenberg, P.T., and Foltz, D.R. (2010). Kinetochores: orchestrating the chromosomal minuet. *Curr. Biol.* 20, R522–R525.
- Sudakin, V., Chan, G.K., and Yen, T.J. (2001). Checkpoint inhibition of the APC/C in

HeLa cells is mediated by a complex of BUBR1, BUB3, CDC20, and MAD2. *J Cell Biol* 154, 925–936.

Suijkerbuijk, S.J.E., Vleugel, M., Teixeira, A., and Kops, G.J.P.L. (2012). Integration of kinase and phosphatase activities by BUBR1 ensures formation of stable kinetochore-microtubule attachments. *Developmental Cell* 23, 745–755.

Sumara, I., Vorlaufer, E., Stukenberg, P.T., Kelm, O., Redemann, N., Nigg, E.A., and Peters, J.-M. (2002). The dissociation of cohesin from chromosomes in prophase is regulated by Polo-like kinase. *Mol. Cell* 9, 515–525.

Sun, L., Gao, J., Dong, X., Liu, M., Li, D., Shi, X., Dong, J.-T., Lu, X., Liu, C., and Zhou, J. (2008). EB1 promotes Aurora-B kinase activity through blocking its inactivation by protein phosphatase 2A. *Proc. Natl. Acad. Sci. U.S.a.* 105, 7153–7158.

Suzuki, A., Badger, B.L., and Salmon, E.D. (2015). A quantitative description of Ndc80 complex linkage to human kinetochores. *Nat Commun* 6, 8161.

Takeuchi, K., Nishino, T., Mayanagi, K., Horikoshi, N., Osakabe, A., Tachiwana, H., Hori, T., Kurumizaka, H., and Fukagawa, T. (2014). The centromeric nucleosome-like CENP-T-W-S-X complex induces positive supercoils into DNA. *Nucleic Acids Res.* 42, 1644–1655.

Tanaka, K. (2012). Dynamic regulation of kinetochore-microtubule interaction during mitosis. *J. Biochem.* 152, 415–424.

Tanaka, T.U., Rachidi, N., Janke, C., Pereira, G., Galova, M., Schiebel, E., Stark, M.J.R., and Nasmyth, K. (2002). Evidence that the Ipl1-Sli15 (Aurora kinase-INCENP) complex promotes chromosome bi-orientation by altering kinetochore-spindle pole connections. *Cell* 108, 317–329.

Tang, Z., Shu, H., Qi, W., Mahmood, N.A., Mumby, M.C., and Yu, H. (2006). PP2A is required for centromeric localization of Sgo1 and proper chromosome segregation. *Developmental Cell* 10, 575–585.

Tanno, Y., Kitajima, T.S., Honda, T., Ando, Y., Ishiguro, K.-I., and Watanabe, Y. (2010). Phosphorylation of mammalian Sgo2 by Aurora B recruits PP2A and MCAK to centromeres. *Genes Dev.* 24, 2169–2179.

Thompson, S.L., and Compton, D.A. (2011). Chromosome missegregation in human cells arises through specific types of kinetochore-microtubule attachment errors. *Proc. Natl. Acad. Sci. U.S.a.* 108, 17974–17978.

Thrower, D.A., Jordan, M.A., and Wilson, L. (1996). Modulation of CENP-E organization at kinetochores by spindle microtubule attachment. *Cell Motil. Cytoskeleton* 35, 121–133.

- Tipton, A.R., Wren, J.D., Daum, J.R., Siefert, J.C., and Gorbsky, G.J. (2017). GTSE1 regulates spindle microtubule dynamics to control Aurora B kinase and Kif4A chromokinesin on chromosome arms. *J Cell Biol* 216, 3117–3132.
- Trinkle-Mulcahy, L., Andersen, J., Lam, Y.W., Moorhead, G., Mann, M., and Lamond, A.I. (2006). Repo-Man recruits PP1 gamma to chromatin and is essential for cell viability. *J Cell Biol* 172, 679–692.
- Trivedi, P., and Stukenberg, P.T. (2016). Review A Centromere-Signaling Network Underlies the Coordination among Mitotic Events. *Trends in Biochemical Sciences* 41, 160–174.
- Tseng, B.S., Tan, L., Kapoor, T.M., and Funabiki, H. (2010). Dual Detection of Chromosomes and Microtubules by the Chromosomal Passenger Complex Drives Spindle Assembly. *Developmental Cell* 18, 903–912.
- Tsukahara, T., Tanno, Y., and Watanabe, Y. (2010). Phosphorylation of the CPC by Cdk1 promotes chromosome bi-orientation. *Nature* 467, 719–723.
- Tulu, U.S., Fagerstrom, C., Ferenz, N.P., and Wadsworth, P. (2006). Molecular requirements for kinetochore-associated microtubule formation in mammalian cells. *Curr. Biol.* 16, 536–541.
- Uchida, K.S.K., Takagaki, K., Kumada, K., Hirayama, Y., Noda, T., and Hirota, T. (2009). Kinetochore stretching inactivates the spindle assembly checkpoint. *J Cell Biol* 184, 383–390.
- Uhlmann, F., Lottspeich, F., and Nasmyth, K. (1999). Sister-chromatid separation at anaphase onset is promoted by cleavage of the cohesin subunit Scc1. *Nature* 400, 37–42.
- Uhlmann, F., Wernic, D., Poupart, M.A., Koonin, E.V., and Nasmyth, K. (2000). Cleavage of cohesin by the CD clan protease separin triggers anaphase in yeast. *Cell* 103, 375–386.
- Vagnarelli, P., Hudson, D.F., Ribeiro, S.A., Trinkle-Mulcahy, L., Spence, J.M., Lai, F., Farr, C.J., Lamond, A.I., and Earnshaw, W.C. (2006). Condensin and Repo-Man-PP1 co-operate in the regulation of chromosome architecture during mitosis. *Nat. Cell Biol.* 8, 1133–1142.
- Vagnarelli, P., Ribeiro, S., Sennels, L., Sanchez-Pulido, L., de Lima Alves, F., Verheyen, T., Kelly, D.A., Ponting, C.P., Rappsilber, J., and Earnshaw, W.C. (2011). Repo-Man coordinates chromosomal reorganization with nuclear envelope reassembly during mitotic exit. *Developmental Cell* 21, 328–342.
- van der Horst, A., and Lens, S.M.A. (2014). Cell division: control of the chromosomal passenger complex in time and space. *Chromosoma* 123, 25–42.

- van der Horst, A., Vromans, M.J.M., Bouwman, K., van der Waal, M.S., Hadders, M.A., and Lens, S.M.A. (2015). Inter-domain Cooperation in INCENP Promotes Aurora B Relocation from Centromeres to Microtubules. *Cell Rep* *12*, 380–387.
- van der Waal, M.S., Saurin, A.T., Vromans, M.J.M., Vleugel, M., Wurzenberger, C., Gerlich, D.W., Medema, R.H., Kops, G.J.P.L., and Lens, S.M.A. (2012). Mps1 promotes rapid centromere accumulation of Aurora B. *EMBO Rep.* *13*, 847–854.
- Varma, D., Wan, X., Cheerambathur, D., Gassmann, R., Suzuki, A., Lawrimore, J., Desai, A., and Salmon, E.D. (2013). Spindle assembly checkpoint proteins are positioned close to core microtubule attachment sites at kinetochores. *J Cell Biol* *202*, 735–746.
- Vink, M., Simonetta, M., Transidico, P., Ferrari, K., Mapelli, M., De Antoni, A., Massimiliano, L., Ciliberto, A., Faretta, M., Salmon, E.D., et al. (2006). In vitro FRAP identifies the minimal requirements for Mad2 kinetochore dynamics. *Curr. Biol.* *16*, 755–766.
- Vleugel, M., Omerzu, M., Groenewold, V., Hadders, M.A., Lens, S.M.A., and Kops, G.J.P.L. (2015). Sequential multisite phospho-regulation of KNL1-BUB3 interfaces at mitotic kinetochores. *Mol. Cell* *57*, 824–835.
- Waizenegger, I.C., Hauf, S., Meinke, A., and Peters, J.M. (2000). Two distinct pathways remove mammalian cohesin from chromosome arms in prophase and from centromeres in anaphase. *Cell* *103*, 399–410.
- Wang, E., Ballister, E.R., and Lampson, M.A. (2011a). Aurora B dynamics at centromeres create a diffusion-based phosphorylation gradient. *J Cell Biol* *194*, 539–549.
- Wang, F., Dai, J., Daum, J.R., Niedzialkowska, E., Banerjee, B., Stukenberg, P.T., Gorbsky, G.J., and Higgins, J.M.G. (2010). Histone H3 Thr-3 phosphorylation by Haspin positions Aurora B at centromeres in mitosis. *Science* *330*, 231–235.
- Wang, F., Ulyanova, N.P., van der Waal, M.S., Patnaik, D., Lens, S.M.A., and Higgins, J.M.G. (2011b). A positive feedback loop involving Haspin and Aurora B promotes CPC accumulation at centromeres in mitosis. *Curr. Biol.* *21*, 1061–1069.
- Weir, J.R., Faesen, A.C., Klare, K., Petrovic, A., Basilico, F., Fischböck, J., Pentakota, S., Keller, J., Pesenti, M.E., Pan, D., et al. (2016). Insights from biochemical reconstitution into the architecture of human kinetochores. *Nature* *537*, 249–253.
- Welburn, J.P.I., Vleugel, M., Liu, D., Yates, J.R., Lampson, M.A., Fukagawa, T., and Cheeseman, I.M. (2010). Aurora B phosphorylates spatially distinct targets to differentially regulate the kinetochore-microtubule interface. *Mol. Cell* *38*, 383–392.
- Wendt, K.S., Yoshida, K., Itoh, T., Bando, M., Koch, B., Schirghuber, E., Tsutsumi, S., Nagae, G., Ishihara, K., Mishiro, T., et al. (2008). Cohesin mediates transcriptional

insulation by CCCTC-binding factor. *Nature* 451, 796–801.

Westhorpe, F.G., Fuller, C.J., and Straight, A.F. (2015). A cell-free CENP-A assembly system defines the chromatin requirements for centromere maintenance. *J Cell Biol* 209, 789–801.

Wheatley, S.P., Kandels-Lewis, S.E., Adams, R.R., Ainsztein, A.M., and Earnshaw, W.C. (2001). INCENP binds directly to tubulin and requires dynamic microtubules to target to the cleavage furrow. *Experimental Cell Research* 262, 122–127.

Wheelock, M.S., Wynne, D.J., Tseng, B.S., and Funabiki, H. (2017). Dual recognition of chromatin and microtubules by INCENP is important for mitotic progression. *J Cell Biol* 216, 925–941.

Williams, S.J., Abrieu, A., and Losada, A. (2017). Bub1 targeting to centromeres is sufficient for Sgo1 recruitment in the absence of kinetochores. *Chromosoma* 126, 279–286.

Woodruff, J.B., Ferreira Gomes, B., Widlund, P.O., Mahamid, J., Honigmann, A., and Hyman, A.A. (2017). The Centrosome Is a Selective Condensate that Nucleates Microtubules by Concentrating Tubulin. *Cell* 169, 1066–1077.e10.

Wühr, M., Freeman, R.M., Presler, M., Horb, M.E., Peshkin, L., Gygi, S., and Kirschner, M.W. (2014). Deep proteomics of the *Xenopus laevis* egg using an mRNA-derived reference database. *Curr. Biol.* 24, 1467–1475.

Wynne, D.J., and Funabiki, H. (2015). Kinetochores function is controlled by a phospho-dependent coexpansion of inner and outer components. *J Cell Biol* 210, 899–916.

Wynne, D.J., and Funabiki, H. (2016). Heterogeneous architecture of vertebrate kinetochores revealed by three-dimensional superresolution fluorescence microscopy. *Mol. Biol. Cell* 27, 3395–3404.

Xu, P., Raetz, E.A., Kitagawa, M., Virshup, D.M., and Lee, S.H. (2013). BUBR1 recruits PP2A via the B56 family of targeting subunits to promote chromosome congression. *Biol Open* 2, 479–486.

Yamagishi, Y., Honda, T., Tanno, Y., and Watanabe, Y. (2010). Two histone marks establish the inner centromere and chromosome bi-orientation. *Science* 330, 239–243.

Yamagishi, Y., Yang, C.-H., Tanno, Y., and Watanabe, Y. (2012). MPS1/Mph1 phosphorylates the kinetochore protein KNL1/Spc7 to recruit SAC components. *Nat. Cell Biol.* 14, 746–752.

Yang, Y., Wu, F., Ward, T., Yan, F., Wu, Q., Wang, Z., McGlothen, T., Peng, W., You, T.,

Sun, M., et al. (2008). Phosphorylation of HsMis13 by Aurora B kinase is essential for assembly of functional kinetochore. *J. Biol. Chem.* *283*, 26726–26736.

Yue, Z., Carvalho, A., Xu, Z., Yuan, X., Cardinale, S., Ribeiro, S., Lai, F., Ogawa, H., Gudmundsdottir, E., Gassmann, R., et al. (2008a). Deconstructing Survivin: comprehensive genetic analysis of Survivin function by conditional knockout in a vertebrate cell line. *J Cell Biol* *183*, 279–296.

Yue, Z., Carvalho, A., Xu, Z., Yuan, X., Cardinale, S., Ribeiro, S., Lai, F., Ogawa, H., Gudmundsdottir, E., Gassmann, R., et al. (2008b). Deconstructing Survivin: comprehensive genetic analysis of Survivin function by conditional knockout in a vertebrate cell line. *J Cell Biol* *183*, 279–296.

Zaytsev, A.V., Mick, J.E., Maslennikov, E., Nikashin, B., DeLuca, J.G., and Grishchuk, E.L. (2015). Multisite phosphorylation of the NDC80 complex gradually tunes its microtubule-binding affinity. *Mol. Biol. Cell* *26*, 1829–1844.

Zaytsev, A.V., Segura-Peña, D., Godzi, M., Calderon, A., Ballister, E.R., Stamatov, R., Mayo, A.M., Peterson, L., Black, B.E., Ataulakhanov, F.I., et al. (2016). Bistability of a coupled Aurora B kinase-phosphatase system in cell division. *Elife* *5*, e10644.

Zaytsev, A.V., Sundin, L.J.R., DeLuca, K.F., Grishchuk, E.L., and DeLuca, J.G. (2014). Accurate phosphoregulation of kinetochore-microtubule affinity requires unconstrained molecular interactions. *J Cell Biol* *206*, 45–59.

Zhou, L., Liang, C., Chen, Q., Zhang, Z., Zhang, B., Yan, H., Qi, F., Zhang, M., Yi, Q., Guan, Y., et al. (2017). The N-Terminal Non-Kinase-Domain-Mediated Binding of Haspin to Pds5B Protects Centromeric Cohesion in Mitosis. *Curr. Biol.* *27*, 992–1004.

Zhou, L., Tian, X., Zhu, C., Wang, F., and Higgins, J.M.G. (2014). Polo-like kinase-1 triggers histone phosphorylation by Haspin in mitosis. *EMBO Rep.* *15*, 273–281.